

UCLA

UCLA Electronic Theses and Dissertations

Title

Computing Maximally Supersymmetric Scattering Amplitudes

Permalink

<https://escholarship.org/uc/item/9kd1c85g>

Author

Stankowicz, James Michael

Publication Date

2016

Supplemental Material

<https://escholarship.org/uc/item/9kd1c85g#supplemental>

Peer reviewed|Thesis/dissertation

UNIVERSITY OF CALIFORNIA
Los Angeles

Computing Maximally Supersymmetric Scattering Amplitudes

A dissertation submitted in partial satisfaction
of the requirements for the degree
Doctor of Philosophy in Physics

by

James Michael Stankowicz Jr.

2016

© Copyright by
James Michael Stankowicz Jr.
2016

ABSTRACT OF THE DISSERTATION

Computing Maximally Supersymmetric Scattering Amplitudes

by

James Michael Stankowicz Jr.

Doctor of Philosophy in Physics

University of California, Los Angeles, 2016

Professor Zvi Bern, Chair

This dissertation reviews work in computing $\mathcal{N} = 4$ super-Yang–Mills (sYM) and $\mathcal{N} = 8$ maximally supersymmetric gravity (mSUGRA) scattering amplitudes in $D = 4$ spacetime dimensions in novel ways.

After a brief introduction and overview in Ch. 1, the various techniques used to construct amplitudes in the remainder of the dissertation are discussed in Ch. 2. This includes several new concepts such as $d \log$ and pure integrand bases, as well as how to construct the amplitude using exactly one kinematic point where it vanishes. Also included in this chapter is an outline of the Mathematica package `on_shell_diagrams_and_numerics.m` (`osdn`) that was developed for the computations herein. The rest of the dissertation is devoted to explicit examples.

In Ch. 3, the starting point is tree-level sYM amplitudes that have integral representations with residues that obey amplitude relations. These residues are shown to have corresponding residue numerators that allow a double copy prescription that results in mSUGRA residues.

In Ch. 4, the two-loop four-point sYM amplitude is constructed in several ways, showcasing many of the techniques of Ch. 2; this includes an example of how to use `osdn`. The two-loop five-point amplitude is also presented in a pure integrand representation with comments on how it was constructed from one homogeneous cut of the amplitude. On-going

work on the two-loop n -point amplitude is presented at the end of Ch. 4.

In Ch. 5, the three-loop four-point amplitude is presented in the d log representation and in the pure integrand representation.

In Ch. 6, there are several examples of four- through seven-loop planar diagrams that illustrate how considerations of the singularity structure of the amplitude underpin dual-conformal invariance. Taken with the previous examples, this is additional evidence that the structure known to exist in the planar sector extends to the full theory. At the end of this chapter is a proof that all mSUGRA amplitudes have a pole at infinity for ($L \geq 4$)-loops.

Finally in Ch. 7, the current status of ultraviolet divergences in the five-loop four-point mSUGRA amplitude is addressed. This includes a discussion of ongoing work aimed at resolving the mSUGRA finiteness question.

The following Mathematica scripts are submitted with this dissertation:

- `on_shell_diagrams_and_numerics.m` with dependencies:
 - `all_trees_*.m`
 - `external_kinematics*_point.m`
 - `rational_external*_point.m`

where “*” is a wild-card string of any set of characters of any length – either an integer or a number spelled out.

The dissertation of James Michael Stankowicz Jr. is approved.

Gregory Eskin

Per J Kraus

Zvi Bern, Committee Chair

University of California, Los Angeles

2016

I dedicate this work and all that went into it to my family: past, present, and future. Past: My mother Sue, my father Jim, my sister and brother Christina and Matthew. Current: My wife-to-be Sarah. Future: My in-laws-to-be, Nancy, Mike, Katie and Megan, who offered me and Sarah immeasurable support (and dog-sitting!) the last six years.

TABLE OF CONTENTS

1	Introduction	1
1.1	Background	1
1.2	$\mathcal{N} = 4$ super-Yang–Mills	3
1.3	Motivation	8
1.4	Outline	12
1.5	Definitions	12
 2	 Technology	 14
2.1	Residues and Cuts	14
2.2	Constructing Amplitudes	20
2.2.1	Numerator Ansatz	20
2.2.2	Integrand Basis	21
2.3	$d \log$ Forms	21
2.3.1	Simple Examples	21
2.3.2	$d \log$ by Ansatz	24
2.3.3	Pure Integrand Basis	27
2.4	Homogeneous Constraints	29
2.4.1	Motivation	29
2.4.2	On-shell Diagrams	30
2.5	Color-Kinematics Duality	32
2.6	<code>osdn</code> : On-shell Diagrams and Numerics	33
2.6.1	Graph Functions	34

2.6.2	Momentum and Spinor Functions	35
2.6.3	Numerical Cuts	36
2.6.4	Color Functions	37
2.6.5	Analytic Spinors	37
2.6.6	Ansatz	37
2.6.7	Cut Construction	38
2.6.8	Spinor Algebra	38
2.6.9	Miscellaneous	38
3	Tree Level Amplitudes	39
3.1	RSVW String and the Connected Prescription	39
3.2	Linear Algebra Notation	40
3.2.1	Outline of Proof	44
3.2.2	Four-Point Illustration	45
3.3	Residue Numerators	47
3.4	Six-Point Calculation	50
4	Two-loop Super-Yang–Mills Amplitudes	54
4.1	Two-loop Four-point Super-Yang–Mills Amplitude	54
4.1.1	$d\log$ Representation	55
4.1.2	Pure Integrand Representation	60
4.1.3	Matching Zeros	62
4.1.4	Example Using <code>osdn</code>	66
4.2	Two-loop Five-point Super-Yang–Mills Amplitude	79
4.3	Two-loop n -point Super-Yang–Mills Amplitude	85

5	Three-Loop Four-Point Super-Yang–Mills Amplitude	91
5.1	$d\log$ Form	91
5.1.1	Diagram Numerators	92
5.1.2	Determining the Coefficients	99
5.2	Pure Integrand Basis	105
6	Higher-loop Four-point Planar Amplitudes	111
6.1	Higher-loop Planar Super-Yang–Mills Amplitudes	111
6.1.1	Dual Conformal Invariance	112
6.1.2	Algorithm for Vanishing Integrands	113
6.1.3	Applying the Algorithm	115
6.2	Maximal Supergravity Poles	122
6.2.1	Logarithmic Singularities	122
6.2.2	Poles at Infinity	124
7	Five-loop Four-point Amplitudes	127
7.1	Motivation	127
7.2	Color-Kinematics Duality on Cuts	128
8	Conclusion	134

LIST OF FIGURES

1.1	Four-point scattering amplitude	2
1.2	Amplitude crossing symmetry	4
2.1	One-loop “two mass easy” topology	15
2.2	Jacobian from a cut	18
2.3	Sample on-shell diagrams	30
2.4	Generic Jacobi relation	33
3.1	Tree-level four-point KK to BCJ amplitude basis	46
3.2	Tree-level six-point NMHV poles	51
4.1	Two-loop four-point integrands	55
4.2	Two-loop four-point vanishing cut	62
4.3	Two-loop four-point amplitude on a cut	62
4.4	Two-loop five-point vanishing cut	81
4.5	Two-loop n -point on-shell diagram skeletons	87
4.6	Two-loop n -point dressed on-shell diagrams	88
4.7	Two-loop six-point graphs	89
4.8	Two-loop seven-point graphs	90
5.1	Three-loop four-point vanishing cut	108
6.1	Momentum twistor configurations	113
6.2	Four-loop four-point planar integrands	116
6.3	Four-loop four-point planar contact term integrands	117

6.4	Five-loop four-point sample planar graph	119
6.5	Five-loop four-point planar integrands with non-zero coefficient	120
6.6	Five-loop four-point planar integrands with zero coefficients	120
6.7	Six-loop four-point planar integrands with zero coefficient	122
6.8	Gravity residue with pole at infinity	124
7.1	Five-loop four-point example graphs	130
7.2	Five-loop four-point graph with three-point subdiagram	132

LIST OF TABLES

1.1	Status of $\mathcal{N} = 4$ SYM Amplitudes	7
4.1	Two-loop five-point integrand basis.	82
4.2	Two-loop five-point extraneous pure integrand	83
4.3	Two-loop five-point amplitude numerators	84
5.1	Three-loop four-point $d \log$ diagrams and basis	100
5.2	Three-loop four-point $d \log$ contact terms	101
5.3	Three-loop four-point $d \log$ collapsed propagator terms	101
5.4	Three-loop four-point integrand basis	109
5.5	Three-loop four-point amplitude numerators	110

ACKNOWLEDGMENTS

I would like to thank Zvi Bern for his mentorship, especially in demonstrating just how far one can go starting with an ansatz! I would like to thank Sean Litsey who made the Ph.D. process at least half as easy. I would like to thank Jaroslav Trnka and Enrico Herrmann for their energetic and exciting collaboration, and the Walter Burke Institute at Caltech for being ever willing to host (and in many instances provide lunch!).

I would like to thank the National Defense Science and Engineering Graduate Fellowship Program for funding me from 2010-2013. I would like to thank the UCLA Dissertation Year Fellowship Program for supporting me from 2015-2016. I would like to thank Department of Energy Award Number DE-SC0009937 for support in 2016.

The material in Ch. 3 is based on Ref. [1] in collaboration with Sean Litsey. The material in Secs. 4.1 and 4.2, and Chs. 2, 5, and 6 is based on Refs. [2, 3] in collaboration with Zvi Bern, Enrico Herrmann, Sean Litsey, and Jaroslav Trnka. The material in Sec. 4.3 is based on work with the collaborators listed above and Jacob Bourjaily. The material in Ch. 7 is based on ongoing work with Zvi Bern, John Joseph Carrasco, Wei-Ming Chen, Henrik Johansson, and Radu Roiban.

VITA

2006-2010	University of Florida Honors College - Bachelor of Science
2010-2011	University of California, Los Angeles - Masters of Science
2010-2013	National Defense Science and Engineering Fellow
2015-2016	University of California, Los Angeles Dissertation Year Fellowship

PUBLICATIONS

Zvi Bern, Enrico Herrmann, Sean Litsey, James Stankowicz, and Jaroslav Trnka. Evidence for a Nonplanar Amplituhedron. 2015.

Zvi Bern, Enrico Herrmann, Sean Litsey, James Stankowicz, and Jaroslav Trnka. Logarithmic Singularities and Maximally Supersymmetric Amplitudes. JHEP, 06:202, 2015.

Sean Litsey and James Stankowicz. Kinematic numerators and a double-copy formula for $\mathcal{N} = 4$ super-Yang-Mills residues. Phys. Rev., D90(2):025013, 2014.

CHAPTER 1

Introduction

1.1 Background

In particle physics, a typical quantity of interest is the scattering cross section, σ . In classical physics, scattering a marble off a much larger beach ball has $\sigma \approx \pi R_{\text{beach ball}}^2$ – the cross-sectional area of the beach ball.

This notion generalizes to particle physics, where the cross section is an effective area corresponding roughly to the sizes of the interacting particles. In quantum field theory (QFT), a cross section depends on the square of the absolute value of an amplitude,

$$\sigma \sim |\mathcal{A}|^2, \tag{1.1}$$

where \mathcal{A} is the quantum mechanical probability amplitude of the incoming particles evolving into the outgoing particles. The quantity \mathcal{A} is called the *scattering amplitude*.

One way to compute such scattering amplitudes is via a generating functional in a given QFT:

$$\mathcal{A} \sim \int \mathcal{D}\phi f[\phi] \exp\left(-\int d^D x \mathcal{L}(\phi, \partial\phi)\right), \tag{1.2}$$

where $\phi \equiv \phi(x)$ are the quantum fields representing the particles, the functional $f[\phi]$ represents an interaction of the fields, and \mathcal{L} is the Lagrangian of the theory defined in D spacetime dimensions with coordinates x . Throughout this dissertation, $D = 4$. Planck's constant \hbar is implicitly in the argument of the exponent in Eq. (1.2) such that the argument is dimension free, but $\hbar = 1$ by appropriate choice of units.

$$\begin{aligned}
\mathcal{A}_4 &\sim \left(\begin{array}{c} 2 \\ 1 \end{array} \right) \text{---} \begin{array}{c} 3 \\ 4 \end{array} + \dots \Big) + \left(\begin{array}{c} 2 \\ 1 \end{array} \begin{array}{c} 3 \\ 4 \end{array} \begin{array}{c} \text{---} \\ \text{---} \\ \text{---} \\ \text{---} \\ \text{---} \\ \text{---} \end{array} \begin{array}{c} 5 \\ 4 \end{array} + \dots \Big) + \left(\begin{array}{c} 2 \\ 1 \end{array} \begin{array}{c} 3 \\ 4 \end{array} \begin{array}{c} \text{---} \\ \text{---} \\ \text{---} \\ \text{---} \\ \text{---} \\ \text{---} \\ \text{---} \\ \text{---} \end{array} \begin{array}{c} 5 \\ 6 \\ 4 \end{array} + \dots \Big) + \dots, \\
&\begin{array}{c} 2 \\ 1 \end{array} \text{---} \begin{array}{c} 3 \\ 4 \end{array} \sim \frac{N_s(k_1, k_2, k_4)}{(k_1 + k_2)^2}, \\
&\begin{array}{c} 2 \\ 1 \end{array} \begin{array}{c} 3 \\ 4 \end{array} \begin{array}{c} \text{---} \\ \text{---} \\ \text{---} \\ \text{---} \\ \text{---} \\ \text{---} \end{array} \begin{array}{c} 5 \\ 4 \end{array} \sim \int \frac{d^4 \ell_5 N_{\text{box}}(k_1, k_2, k_4, \ell_5)}{(\ell_5)^2 (\ell_5 - k_1)^2 (\ell_5 - k_1 - k_2)^2 (\ell_5 + k_4)^2}, \\
&\begin{array}{c} 2 \\ 1 \end{array} \begin{array}{c} 3 \\ 4 \end{array} \begin{array}{c} \text{---} \\ \text{---} \\ \text{---} \\ \text{---} \\ \text{---} \\ \text{---} \\ \text{---} \\ \text{---} \end{array} \begin{array}{c} 5 \\ 6 \\ 4 \end{array} \sim \int \frac{d^4 \ell_5 d^4 \ell_6 N_{\text{double-box}}(k_1, k_2, k_4, \ell_5, \ell_6)}{(\ell_5)^2 (\ell_5 - k_1)^2 (\ell_5 - k_1 - k_2)^2 (\ell_5 - \ell_6)^2 (\ell_6 - k_1 - k_2)^2 (\ell_6 + k_4)^2}.
\end{aligned}$$

Figure 1.1: A schematic example of expanding the four-particle scattering amplitude in Feynman diagrams. The “ \sim ” indicate that various factors and other details are omitted. The N_s , N_{box} , $N_{\text{double-box}}$ are dictated by the Lagrangian. The parentheses indicate grouping by loop-order. The “ \dots ” within parentheses indicate a sum over all connected graphs at the same loop order.

Feynman rules are a standard method to perturbatively expand such generating functionals. One way of organizing the Feynman rules results in an expansion in *loop-order*; an example for four-point scattering in a theory with trivalent interactions appears in Fig. 1.1. For a given Lagrangian, the rules associate graphs to integrals in momentum space. Momentum is the four-vector Fourier-conjugate to the position four-vector $x^\mu = (ct, \vec{x})$, with dimensions such that the speed of light $c = 1$. The loop momenta coordinates are always denoted by ℓ_l in this dissertation. In this organizational scheme, the problem of computing scattering amplitudes reduces to computing the *Feynman integrals* of *graphs* or *diagrams* exemplified on the bottom of Fig. 1.1.

While Feynman rules in principle indicate how to write any generating functional to any order in perturbation theory, it is intractable to go beyond low loop-levels. In some sense, this dissertation is about bypassing Feynman rules to efficiently obtain simpler expressions for the scattering amplitude. This approach has had much recent success.

A good sandbox for testing techniques that bypass Feynman rules is the four-dimensional, maximally-supersymmetric ($\mathcal{N} = 4$) Yang-Mills theory (sYM) with gauge group $SU(N)$.

There is a brief overview of this theory in the next section. Active research, including the topics in this dissertation, is in uncovering the mathematical structure of sYM amplitudes. Some of the aims of these research programs are:

1. Uncovering structure via new techniques. This often unveils yet more structure making it possible to advance to higher loop order: a classic bootstrap approach.
2. Exploring the divergence structure of maximally supersymmetric ($\mathcal{N} = 8$) gravity (mSUGRA), as there is a very direct connection between sYM and mSUGRA amplitudes.
3. Developing techniques that apply directly or offer insight into other, more realistic theories.

Points 1 and 2 are the main focus of this dissertation.

1.2 $\mathcal{N} = 4$ super-Yang–Mills

This subsection details some of the properties of sYM theory that are useful in subsequent chapters. For a complete, modern review see Ref. [4].

It is convenient to formulate sYM theory in an on-shell superspace formalism [5]. This formalism allows any amplitude to be computed by taking derivatives with respect to a superfield multiplet. Superspace and supersymmetric Ward identities relate various amplitudes to all-gluon amplitudes such that sYM may be split into sectors based on the all-gluon scattering amplitudes.

Since gluons are massless spin-one particles, the gluon velocity is either parallel or anti-parallel to the spin. This dot product of spin and velocity is the helicity, h , of the gluon and is normalized to $h = \pm 1$.

One general property about scattering amplitudes is that they display crossing symmetry: the amplitude is related by analytic continuation under exchanging any number of incoming

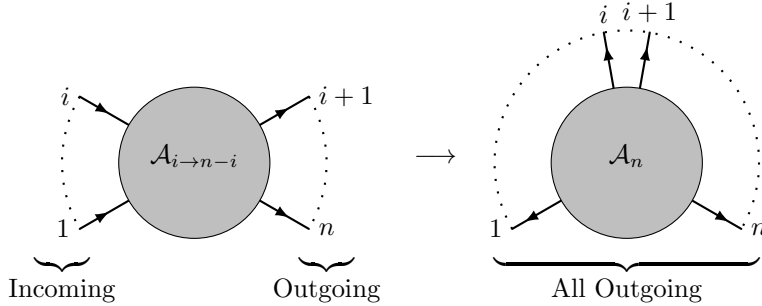


Figure 1.2: Scattering amplitudes exhibit crossing symmetry. The left figure illustrates i incoming particles scattering into $n - i$ outgoing particles with amplitude $\mathcal{A}_{i \rightarrow n-i}$. This maps into an amplitude of n outgoing particles, \mathcal{A}_n , illustrated on the right.

particles for the same number of outgoing particles with opposite helicity. This is demonstrated in Fig. 1.2. Practically, this means all amplitudes may be computed by choosing all particles as outgoing.¹

The on-shell superspace formalism also implies that the L -loop amplitude can be expanded in terms of $P_{4k}^{(L)}$, a Grassmann-valued polynomial of degree $4k$. The details of the on-shell superspace are such that $K = k + 2$, where K is the number of negative helicity gluons. The integer k is most often used in the literature to count how far from *maximally helicity violating* an amplitude is. This name comes from considering the $K = 0$ scattering cross section. By crossing symmetry, this is a $1^- 2^- \rightarrow 3^+ 4^+ 5^+ 6^+ \dots n^+$ gluon scattering process, where the integer labels the gluon and the sign its helicity. This expression manifestly violates helicity conservation, since there is helicity -2 incoming and $n - 2$ outgoing, for a “violation” of n . The $K = 0$ and $K = 1$ amplitudes can be shown to vanish, and so the $K = 2$ amplitude is maximally helicity violating. Switching to $k = K - 2$ indexes the maximally helicity violating, or MHV, amplitude by $k = 0$. Then $k = 1$ is the next-to-MHV amplitude (NMHV), $k = 2$ is the next-to-next-to-MHV amplitude (N²MHV), and so on for N ^{k} MHV amplitudes.

¹Another common convention in the literature is to choose all incoming particles.

For an n -particle amplitude, the N^{n-k} MHV amplitude is the complex conjugate of the N^k MHV amplitude. These are denoted with an overbar. For example:

$$\overline{\text{MHV}} = N^{n-2}\text{MHV}. \quad (1.3)$$

Much of the work presented here is for $n = 4$ or $n = 5$ external particles. For $n = 4$, the only non-vanishing amplitude is the MHV amplitude, and for $n = 5$, the NMHV amplitude is the conjugate of the MHV amplitude, and this again is the only non-vanishing amplitude.

Since the gluons are massless and all equations are in $D = 4$ dimensions, the amplitude can be written as a function of spinor helicity variables. These variables result from mapping Lorentz four-vectors into 2×2 matrices via the Pauli matrices:

$$p_{a\dot{b}} = p_\mu(\sigma^\mu)_{a\dot{b}}, \quad p^{\dot{a}b} = p_\mu(\bar{\sigma}^\mu)^{\dot{a}b}, \quad (1.4)$$

$$\sigma^\mu_{a\dot{b}} = (\sigma^0, \sigma^i)_{a\dot{b}}, \quad (\bar{\sigma}^\mu)^{\dot{a}b} = (\sigma^0, -\sigma^i)^{\dot{a}b}, \quad (1.5)$$

$$\sigma^0 = \begin{pmatrix} 1 & 0 \\ 0 & 1 \end{pmatrix}, \quad \sigma^1 = \begin{pmatrix} 0 & 1 \\ 1 & 0 \end{pmatrix}, \quad \sigma^2 = \begin{pmatrix} 0 & -i \\ i & 0 \end{pmatrix}, \quad \sigma^3 = \begin{pmatrix} 1 & 0 \\ 0 & -1 \end{pmatrix}. \quad (1.6)$$

For massive momentum this results in $-p^\mu p_\mu = \det(p_{a\dot{b}}) = m^2$. For massless gluons, the determinant vanishes and so the momenta can be written as the outer product of vectors:

$$p_{a\dot{b}} \equiv \lambda_a \tilde{\lambda}_{\dot{b}} \equiv |p\rangle [p], \quad p^{\dot{a}b} \equiv \tilde{\lambda}^{\dot{a}} \lambda^b \equiv [p] \langle p|. \quad (1.7)$$

These λ 's and $\tilde{\lambda}$'s are the spinor helicity variables; they are indiscriminately exchanged for the “bra-ket” notation in this dissertation and in the literature. When the spinor is labeled by its external particle index i , the bra-ket notation is:

$$(\lambda_i)_a \leftrightarrow |i\rangle, \quad (\tilde{\lambda}_i)_{\dot{a}} \leftrightarrow [\dot{i}], \quad (1.8)$$

$$(\lambda_i)^a \leftrightarrow \langle i|, \quad (\tilde{\lambda}_i)^{\dot{a}} \leftrightarrow [\dot{i}]. \quad (1.9)$$

Indices are raised and lowered by the anti-symmetric tensor

$$\varepsilon^{ab} = \varepsilon^{\dot{a}\dot{b}} = \begin{pmatrix} 0 & 1 \\ -1 & 0 \end{pmatrix} = -\varepsilon_{ab} = -\varepsilon_{\dot{a}\dot{b}}. \quad (1.10)$$

In the bra-ket notation, contractions allow a compact notation:

$$\epsilon^{ab}(\lambda_i)_a(\lambda_j)_b \equiv \langle ij \rangle = -\langle ji \rangle \equiv \epsilon^{ba}(\lambda_i)_b(\lambda_j)_a, \quad (1.11)$$

$$\epsilon^{\dot{a}\dot{b}}(\tilde{\lambda}_i)_{\dot{a}}(\tilde{\lambda}_j)_{\dot{b}} \equiv [ij] = -[ji] \equiv \epsilon^{\dot{b}\dot{a}}(\tilde{\lambda}_i)_{\dot{b}}(\tilde{\lambda}_j)_{\dot{a}}. \quad (1.12)$$

There are additional contractions and notation that are natural extensions of this. See for example Appendix A of Ref. [4]. Complex conjugation is exchanging $\lambda \leftrightarrow \tilde{\lambda}$.

Amalgamating all these facts, the n -point sYM amplitude is a function of the momenta or spinor helicity variables of the external massless gluons, k_i , $i = 1, 2, \dots, n$, and the helicity of the gluons, $h_i = \pm 1$, $i = 1, 2, \dots, n$. The L -loop amplitude is the contribution to this amplitude at loop order L . For MHV amplitudes, it does not matter which of the gluons are negative helicity, so the amplitude may be written in terms of its contributions at different loop levels as

$$\mathcal{A}_{n,k} = \sum_{L=1}^{\infty} \mathcal{A}_{n,k}^{(L)} \quad (1.13)$$

when $k+2$ of the gluons are negative helicity. It is conventional to also call $\mathcal{A}_{n,k}^{(L)}$ an amplitude. If it matters which of the gluons are negative, then the convention is to abbreviate the external momentum k_j as just the integer j with the helicity as a superscript:

$$\mathcal{A}_n \equiv \mathcal{A}(1^{h_1}, 2^{h_2}, \dots, n^{h_n}) \quad (1.14)$$

$$= \sum_{L=1}^{\infty} \mathcal{A}^{(L)}(1^{h_1}, 2^{h_2}, \dots, n^{h_n}). \quad (1.15)$$

One of the reasons for so much interest in these sYM amplitudes is that the amplitudes exhibit symmetries beyond those present in the Lagrangian of the theory. In particular

Status of $\mathcal{N} = 4$ Amplitudes		
	Planar	Full
Integrand	Many results	This dissertation
Integrated	Some results	Few results

Table 1.1: Current status of scattering amplitudes in SYM. This dissertation address integrands of the full theory.

the planar sYM amplitudes obey an infinite dimensional Yangian symmetry that was only recently discovered [6], despite the fact that Yang and Mills [7] could in principle have identified it. The “planar” sYM theory corresponds to a large- N limit of the full theory and the amplitude integrands of the theory are simpler to study than the full theory as a result of the infinite dimensional symmetry. Some of the “many results” for the planar integrand indicated in Tab. 1.1 are listed at the beginning of the next section. Included in this is a discussion of the amplituhedron which was a large motivating factor for much of the work in this dissertation. It is an open question, partially addressed in this dissertation, which of the novel properties appearing in the planar theory have generalizations in the full theory. This is indicated in Tab. 1.1.

Actually obtaining integrated results is a related area of research, but is not done by directly integrating the integrands. In the planar integrated sector (the bottom left cell of Tab. 1.1), there are techniques for computing, for example, the six-point NMHV amplitude through four-loops [8–10] that rely heavily on various features of the planar integrand. These results and techniques hint at a connection [11] between the generalized polylogarithms [12–15] that result from integration and the $d \log$ forms presented in this dissertation, although the question of how to map between the two remains an open one [16]. In particular, understanding how to integrate the nonplanar integrands presented here would open the door to computing more nonplanar amplitudes, where there are currently only two-loop four-point [17] and partial three-loop four-point [18] results.

Aside from uncovering unexpected structure of sYM amplitudes, another reason to study

these amplitudes is that they are very closely related to the scattering amplitudes of mSUGRA. The relation was made very precise by Bern-Carrasco-Johannson (BCJ) in Ref. [19] as outlined in Sec. 2.5. It is an open question if the terms in the mSUGRA expansion of the amplitude are finite in $D = 4$ dimensions. The current calculational limit is five-loops for the four-point amplitude, and explicit calculation has continued to hint that mSUGRA and sYM amplitudes have similar divergences meaning that mSUGRA is better behaved than traditional techniques predict.

1.3 Motivation

As briefly mentioned above, there are two main aims in this dissertation for computing sYM scattering amplitudes in novel ways: uncovering unexpected structure and addressing the mSUGRA finiteness question. This section addresses the motivation for suspecting hidden structure in nonplanar sYM - a theme that unites the calculations in Chs. 4-6. For a discussion of mSUGRA finiteness, see Ch. 7.

In planar sYM theory much hidden structure has been recently uncovered: Yangian symmetry [6], dual conformal symmetry [20–22], integrability [23, 24], a duality between Wilson loops and planar amplitudes [25–30], chromodynamic flux-tube integrability for finite-coupling expansions of the amplitude [31–33], hexagon bootstrap [8–10], and symbols and cluster polylogarithmics [12–15]. More recently, scattering amplitudes were reformulated using on-shell diagrams and the positive Grassmannian [34–40], with related work in Refs. [41–44]. This reformulation fits nicely into the geometric concept of the amplituhedron [45] (see also Refs. [46–52]), and makes connections to active areas of research in algebraic geometry and combinatorics (see e.g. Ref. [53–58]).

The calculations in this dissertation of the two-loop four- and five-point amplitudes (Ch. 4) and the three-loop four-point amplitude (Ch. 5) explicitly probe how some properties of the planar sector carry to the nonplanar sector. A basic difficulty in the nonplanar sector is that there are no global variables with which to describe a nonplanar integrand. This labeling

ambiguity obscures structures that might be hiding in the amplitude. In addition many of the features of the previous paragraph have no obvious generalization. There is no Yangian symmetry with its associated integrability constraints in the full theory. The connection between nonplanar amplitudes and Wilson loops is also murky. There is also no known way to construct nonplanar amplitudes using on-shell diagrams, the positive Grassmannian and the amplituhedron, though there has been some recent progress [59, 60].

Despite these apparent obstructions, there are reasons to suspect that many features of the planar theory can be extended to the full nonplanar theory. In particular, the conjectured duality between color and kinematics [19, 61] suggests that nonplanar integrands are directly related to planar ones, and hence properties of the nonplanar theory should be related to properties of the planar sector. However, it is not a priori obvious which features can be carried over.

The dual formulation of planar sYM scattering amplitudes using on-shell diagrams and the positive Grassmannian makes manifest that the integrand has only logarithmic singularities, and can be written as a *d log form*. Furthermore, the integrand has no poles at infinity as a consequence of dual conformal symmetry. Recently Ref. [62] conjectured the same singularity properties hold to all loop orders for all MHV amplitudes in the nonplanar sector as well. This is confirmed explicitly in Sec. 5.1 for the full three-loop four-point sYM integrand by finding a basis of diagram integrands where each term manifests these properties. In Ref. [2], we also conjectured:

Logarithmic singularities and absence of poles at infinity imply dual conformal invariance
of local integrand forms to all loop orders in the planar sector.

Evidence for this is provided from studies of the four-, five-, and six-loop amplitudes in Ch. 6. Taken all together, the results of Chs. 4-6 serve as concrete evidence that the analytic structure of amplitudes carry properties of the planar sector into the nonplanar sector.

In Ref. [3], we showed that in the planar case dual conformal invariance is equivalent to integrands with (i) no poles at infinity, and (ii) special values of leading singularities. In the

MHV sector, property (ii) and superconformal invariance imply that leading singularities are necessarily ± 1 times the usual Parke-Taylor factor [63, 64]. Moreover, the existence of a dual formulation using on-shell diagrams and the positive Grassmannian implies that (iii) integrands have only logarithmic singularities. While (i) and (iii) can be directly conjectured also for nonplanar amplitudes, property (ii) must be modified. As proven in Ref. [65] for both planar and nonplanar cases, the leading singularities are linear combinations of Parke-Taylor factors with different orderings and with coefficients ± 1 . This set of conditions was first conjectured in Ref. [2], and in Ref. [3] we gave a more detailed argument as to why the content of dual conformal symmetry is exhausted by this set of conditions. In this dissertation there is direct nontrivial evidence showing these properties hold for the two-loop five-point amplitude (Sec. 4.2) and the three-loop four-point (Sec. 5.1) amplitude.

The main purpose of the pure integrand constructions in this dissertation is to present evidence for the amplituhedron concept [45] beyond the planar limit. The amplituhedron is defined in momentum twistor variables which intrinsically require cyclic ordering of amplitudes, making direct nonplanar tests in these variables impossible. However, we can test specific implications even for nonplanar amplitudes. In Ref. [49], those authors argued that the existence of the “dual” amplituhedron implies certain positivity conditions of amplitude integrands. Indeed, these conditions were proven analytically for some simple cases and numerically in a large number of examples. Interestingly, these conditions appear to hold even in integrated results [49]. The dual amplituhedron can be interpreted as a geometric region of which the amplitude is literally a volume, in contrast to the original definition where the amplitude is a form with logarithmic singularities on the boundaries of the amplituhedron space. This implies a very interesting property when the integrand is combined into a single rational function: its numerator represents a codimension one surface which lies outside the dual amplituhedron space. The surface is simply described as a polynomial in momentum twistor variables and therefore can be fully determined by the zeros of the polynomial, which correspond to points violating positivity conditions defining the amplituhedron. A nontrivial statement implied by the amplituhedron geometry is that *all* these zeros can be interpreted

as cuts where the amplitude vanishes.

This leads to a concrete feature that can be tested even in a diagrammatic representation of a nonplanar amplitude:

The integrand should be determined entirely from homogeneous conditions,
up to an overall normalization.

Concretely, “homogeneous conditions” means the conditions of no poles at infinity, only logarithmic singularities, and also unitarity cuts that vanish. That is, in the unitarity method, the only required cut equations are the ones where one side of the equation is zero, as opposed to a nontrivial kinematical function. These zeros occur either because the amplitude vanishes on a particular branch of the cut solutions or because the cut is spurious². This conjecture has exciting implications because this feature is closely related to the underlying geometry in the planar sector, suggesting that the nonplanar contributions to amplitudes admit a similar structure.

In this dissertation, this conjecture is verified for the nonplanar two-loop four-point sYM amplitude both analytically (Sec. 4.1.2) and numerically by the Mathematica package `osdn` (Sec. 4.1.4). The conjecture also passes the nontrivial checks of the nonplanar three-loop four-point (Sec. 5.2) and two-loop five-point (Sec. 4.2) amplitudes. A key assumption is that the desired properties can all be made manifest diagram-by-diagram [2]. While it is unknown if this assumption holds for all amplitudes at all loop orders, the results at relatively low loop order presented here confirm that this is a good hypothesis. The three-loop four-point integrand was first obtained in Ref. [66], while the two-loop five-point integrand was first calculated in Ref. [67] in a format that makes the duality between color and kinematics manifest. The constructions here are different representations that make manifest that the amplitudes have only logarithmic singularities and no poles at infinity. These representations are then compatible with the notion that there exists a nonplanar analog of dual conformal

²A spurious cut is one that exposes a non-physical singularity, i.e. a singularity that is not present in the full amplitude.

symmetry and a geometric formulation of nonplanar amplitudes. The amplitudes are organized in terms of basis integrands that have only ± 1 leading singularities (Sec. 2.3.3). The coefficient of these integrals in the amplitudes are then simply sums of Parke-Taylor factors, as proved in Ref. [65]. This dissertation also shows by example that homogeneous conditions are sufficient to determine both amplitudes up to an overall factor, as expected if a nonplanar analog of the amplituhedron were to exist.

1.4 Outline

The remainder of this dissertation is organized as follows. In Ch. 2 are the various techniques used to compute and uncover properties of sYM amplitudes. In the chapters following that, the techniques are applied to compute various amplitudes. The chapters are arranged by loop-order. Most amplitudes are four-point amplitudes, except to the two-loop five-point amplitude and the two-loop n -point amplitude.

1.5 Definitions

The following abbreviations and conventions are used throughout this dissertation:

- All particles are outgoing.
- *Quantum field theory* is abbreviated QFT
- $\mathcal{N} = 4$ *super Yang-Mills* is abbreviated sYM
- $\mathcal{N} = 8$ *supergravity* is abbreviated mSUGRA
- The word *amplitude* always means the integrand of a scattering amplitude. The loop order and the theory (sYM or mSUGRA) will be clear from context.
- The symbol \mathcal{A} is reserved for sYM amplitudes and \mathcal{M} for mSUGRA amplitudes.
- All equations are in $D = 4$ dimensions.

- The words *diagram*, *graph*, and *integrand* are all used interchangeably and always refer to a Feynman integral.
- For n -point massless external gluons $s_{i,j} \equiv (k_i + k_j)^2 = 2k_i \cdot k_j$.
- For four massless external gluons, $s \equiv 2k_1 \cdot k_2$, $t \equiv 2k_2 \cdot k_3$, $u \equiv 2k_1 \cdot k_3$.
- The spacetime metric used to lower and raise Lorentz indices is $\eta^{\mu\nu} = \text{diag}(-1, 1, 1, 1)$. This sign choice as well as choices associated to signs and notation in the spinor helicity formalism may differ from some of the references.

CHAPTER 2

Technology

The sections of this chapter discuss the various techniques used to construct amplitudes in the remainder of this dissertation.

Some of the sections outline new contributions to the field while other sections are summaries of previously-known techniques that we used when constructing amplitudes in new ways. The content of Sec. 2.1, though not itself new, describes the connection between residues and cuts; this connection forms the backbone of many of the subsequent calculations. New concepts form the content of Sec. 2.2, Sec. 2.3, and Sec. 2.4. The content of Sec. 2.5 summarizes previously-existing technology for converting sYM amplitudes to mSUGRA amplitudes. The final section, Sec. 2.6, summarizes the various Mathematica functions I wrote or updated. These functions form the backbone of the computations in the later chapters.

2.1 Residues and Cuts

The main property of the integrand we considered in Refs. [2, 3] was its pole structure after taking sequential residues. In this section the connection between residues and unitarity cuts [68] is detailed. The analysis performed here in an example case is the main tool used in subsequent calculations.

The simplest way to illustrate how a sequence of residues corresponds to unitarity cuts

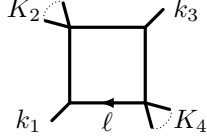


Figure 2.1: The one-loop “two mass easy” box integrand. The corresponding expression is Eq. (2.1).

is by example. In particular, consider the two-mass box integrand

$$dI = \frac{d^4\ell}{\ell^2 (\ell - k_1)^2 (\ell - k_1 - K_2)^2 (\ell + K_4)^2}, \quad (2.1)$$

where K_2 and K_4 are massive and k_1 and k_3 are massless. The corresponding diagram is in Fig. 2.1. To find poles of this expression, a first useful step is to change coordinates from the components of four-momentum ℓ^μ since they are quadratic in Eq. (2.1). Spinor helicity variables are linear coordinates in this integrand. Choosing to decompose ℓ as

$$\ell = z_{11} |1\rangle [1 + z_{13} |1\rangle [3 + z_{31} |3\rangle [1 + z_{33} |3\rangle [3], \quad (2.2)$$

the integrand is multi-linear in the new z_{ij} coordinates:

$$dI = \left| \frac{\partial\ell}{\partial z_{ij}} \right| \frac{d^4 z_{ij}}{\underbrace{(z_{13}z_{31}s_{13} + z_{11}z_{33}s_{13})}_{\ell^2} \times (q_1^2 q_2^2 q_3^2)}, \quad (2.3)$$

where

$$q_1^2 q_2^2 q_3^2 = (\ell - k_1)^2 (\ell - k_1 - K_2)^2 (\ell + K_4)^2. \quad (2.4)$$

The Jacobian is a constant $\left| \frac{\partial\ell}{\partial z_{ij}} \right| = s_{13}^2$ and can be ignored without changing the following discussion.

Performing a unitarity cut on a propagator means “solve for a component of the loop momentum such that the inverse propagator becomes zero, remove the propagator from the integrand, and multiply by a Jacobian.” This is equivalent to taking one residue around the

point

$$z_{13}z_{31} + z_{11}z_{33} = 0 \quad (2.5)$$

in a \mathbb{C}^4 complex space.

There are four different ways to take such a residue. To illustrate some of the subtleties, consider two such, by rewriting the ℓ^2 factor in the denominator of Eq. (2.3) in two ways:

$$\ell^2 = s_{13} \times \begin{cases} z_{31} (z_{13} - (-z_{11}z_{33}/z_{31})) & \text{(I)} \\ z_{13} (z_{31} - (-z_{11}z_{33}/z_{13})) & \text{(II)} \end{cases}, \quad (2.6)$$

where the factor of s_{13} can again be ignored hereafter. The first expression, Eq. (2.6)(I), produces a Jacobian of $1/z_{31}$:

$$dI_{13} \equiv \text{Res}_{\substack{\ell^2=0 \\ z_{13}}} dI = \frac{d^3 z_{ij}}{z_{31} \times (q_1^2 q_2^2 q_3^2)|_{z_{13}^*}}, \quad z_{13}^* = -z_{11}z_{33}/z_{31}. \quad (2.7)$$

The second expression, Eq. (2.6)(II), produces a Jacobian of $1/z_{13}$

$$dI_{31} \equiv \text{Res}_{\substack{\ell^2=0 \\ z_{31}}} dI = \frac{d^3 z_{ij}}{z_{13} \times (q_1^2 q_2^2 q_3^2)|_{z_{31}^*}}, \quad z_{31}^* = -z_{11}z_{33}/z_{13}. \quad (2.8)$$

Both of these expressions correspond to the unitarity cut $\ell^2 = 0$, with the Jacobians z_{31} and z_{13} respectively. Both expressions also leave three degrees of freedom of ℓ unfixed.

A *leading singularity* is the residue that results from localizing all degrees of freedom by iterations of residues.

In the preceding example, a maximal cut corresponds to using each remaining propagator to localize exactly one remaining degree of freedom. The resulting z_{ij}^* substituted into the expansion for the loop momentum, Eq. (2.2), yields an ℓ^* that satisfies

$$0 = (\ell^*)^2 = (\ell^* - k_1)^2 = (\ell^* - k_1 - K_2)^2 = (\ell^* + K_4)^2. \quad (2.9)$$

For this two-mass box example, it turns out not to matter in which order the residues are computed, as the max-cut leading singularity always takes the same value:

$$\begin{aligned} \text{LS}_{\text{max-cut}}(dI) &= \frac{1}{(k_1 + K_2)^2 (k_1 + K_4)^2 - K_2^2 K_4^2} \\ &= \frac{1}{\langle 1|K_2|3\rangle \langle 3|K_2|1\rangle}. \end{aligned} \tag{2.10}$$

A *composite cut* corresponds to localizing a component of the loop momentum via any residue that does not come directly from a propagator.

An example of a composite cut is taking a second residue of dI_{13} in Eq. (2.7) at the pole $z_{31} = 0$, or a second residue of dI_{31} in Eq. (2.8) at the pole $z_{13} = 0$. Proceeding to localize the remaining degrees of freedom in either integrand results in a composite leading singularity. The physics literature on the structure that results from residue theorems and dependence on the ordering of residues is in its infancy.

When constructing the $d\log$ integrands defined in Sec. 2.3.2, the goal is to guarantee that none of the rational functions in variables analogous to the z 's of this example ever have double poles or poles at infinity. Similarly, the pure integrand basis of Sec. 2.3.3 is constructed so that *any* leading singularity is either ± 1 or 0.

As an example, for the max-cut unit leading singularity, Eq. (2.10), a new integrand with leading singularity could be defined by

$$dI_{\pm 1} \equiv \pm \langle 1|K_2|3\rangle \langle 3|K_2|1\rangle dI \tag{2.11}$$

so that the overall factor in the leading singularity of Eq. (2.10) cancels. In some of the cases we encountered for the two-loop five-point amplitude in Sec. 4.2, instead of normalizing the integrand, we redefined integrands so that leading singularities vanished. There have been no careful studies of how the choice between ± 1 or 0 affects the integrand basis, and that may prove to be a fruitful endeavor in the future.

As illustrated by the two-mass box leading singularity example, it is not necessary to

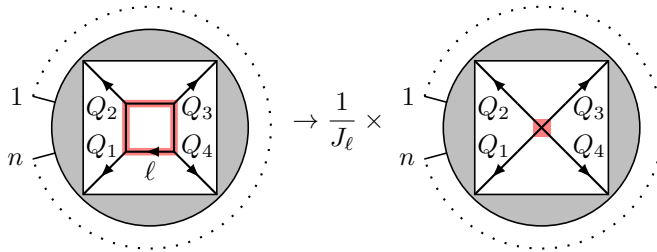


Figure 2.2: The left diagram is a generic L -loop contribution to the sYM amplitude. The external dots represent n generic external particles. The gray band represents any generic external or loop trivalent graph structure. The red (thick) highlighting indicates propagators replaced by on-shell conditions. After this replacement, the highlighted propagators leave behind the simplified diagram on the right multiplied by an inverse Jacobian, Eq. (2.14). The four momenta Q_1 , Q_2 , Q_3 and Q_4 can be either external legs or propagators of the higher-loop diagram.

compute every residue of the integrand when seeking double poles. In particular, cutting a box subdiagram from a higher loop diagram, as on the left in Fig. 2.2, can only increase the order of remaining poles in the integrand. Consider computing the four residues that correspond to cutting the four highlighted propagators in Fig. 2.2,

$$\ell^2 = (\ell - K_1)^2 = (\ell - K_1 - K_2)^2 = (\ell + K_4)^2 = 0, \quad (2.12)$$

where again K_i indicates a massive external particle. Instead of changing variables and formally computing co-dimension residues as in the preceding discussion, this residue can be computed as the Jacobian obtained by replacing the box propagator with on-shell delta functions. This Jacobian is then

$$J_\ell = |\partial P_i / \partial \ell^\mu|, \quad (2.13)$$

where the P_i 's are the four inverse propagators placed on shell in Eq. (2.12). See, for example, Ref. [69] for more details. This Jacobian also matches the rational factors appearing in front of the box integrals of appendix I of Ref. [70].

For the generic four-mass case J_ℓ , contains square roots making it difficult to work with. In special cases it simplifies. For example for $K_1 = k_1$ massless, the three-mass normalization

is

$$J_\ell = (k_1 + K_2)^2(K_4 + k_1)^2 - K_2^2 K_4^2. \quad (2.14)$$

If in addition $K_3 = k_3$ is massless, the so called “two-mass-easy” case, the Jacobian J_ℓ factorizes into a product of two factors as in Eq. (2.10); this factorized expression is useful in many calculations. Both $K_1 = k_1$ and $K_2 = k_2$ massless results in the “two-mass-hard” normalization

$$J_\ell = (k_1 + k_2)^2(K_3 + k_2)^2. \quad (2.15)$$

These formulas are useful at higher loops, where the K_i depend on other loop momenta.

These Jacobians go into the denominator of an integrand after a box-cut is applied to the integrand. Box-cuts therefore can only raise the order of the remaining poles in the integrand. The basic search for double poles is to cut embedded box subdiagrams from diagrams of interest and update the integrand by dividing by the resulting Jacobian (2.13). The numerator must cancel any resulting double pole in the integrand.

A compact notation that simplifies discussion of such cuts in subsequent sections is:

$$\text{cut} = \{ \dots, (\ell - K_i)^2, \dots, B(\ell), \dots, B(\ell', (\ell' - Q)), \dots \}. \quad (2.16)$$

Here:

- Cuts are applied in the order listed.
- A propagator listed by itself, as $(\ell - K_i)^2$ is, means: “Cut just this propagator.”
- $B(\ell)$ means: “Cut the four propagators that depend on ℓ .” This exactly corresponds to cutting the box propagators as in Eq. (2.12) and Fig. 2.2.
- $B(\ell', (\ell' - Q))$ means: “Cut the three standard propagators depending on ℓ' , as well as a fourth $1/(\ell' - Q)^2$ resulting from a previously obtained Jacobian.” The momentum Q depends on other momenta besides ℓ' . The four cut propagators form a box.

2.2 Constructing Amplitudes

The previous section outlined the main analytic tool that will be used in subsequent sections. This section turns towards the main aim: constructing amplitudes at a fixed loop order. Two different procedures for doing so are described in the following two subsections.

2.2.1 Numerator Ansatz

One expression for the amplitude is an expansion of the numerator in terms of only trivalent graphs:

$$\mathcal{A}_{n,k}^{(L)} = \sum_{\mathcal{S}_n} \sum_{(x)} \int d^{4L} \ell \frac{N^{(x)} c^{(x)}}{p^{(x)}}. \quad (2.17)$$

where:

- The sum in \mathcal{S}_n is over all permutations of n external legs.
- The sum in (x) is over all trivalent graphs at loop order L .
- The kinematic numerators are a function of all external and loop momenta: $N^{(x)} = N^{(x)}(\{k\}, \{l\})$.
- The color factors $c^{(x)}$ can be read off from the trivalent graph, as sums over the structure constants of $SU(N)$.
- The denominators, $p^{(x)} = \prod_{i=1}^{N_{int}} (q_i)^2$, are the standard products of Feynman propagators, where N_{int} is the number of internal edges of the trivalent graph, and q_i are the linear combinations of loop and external momenta imposed on each edge by momentum conservation.

Writing the amplitude in this way reduces the problem of finding the amplitude to the problem of finding the correct numerators. One way of finding these numerators is to write down ansätze for the numerators, and then constrain the ansätze such that they obey the desired properties. This is the starting point for the d log construction outlined in Sec. 2.3.2.

2.2.2 Integrand Basis

Another expression for the amplitude is an expansion of the numerator in an integrand basis:

$$\mathcal{A}_{n,k}^{(L)} = \sum_{(x)} a^{(x)} \mathcal{I}^{(x)}, \quad \mathcal{I}^{(x)} \equiv \int d\mathcal{I}^{(x)}. \quad (2.18)$$

where:

- The sum in (x) is over a basis of integrands that must be determined.
- The integrands $d\mathcal{I}^{(x)} = d\mathcal{I}^{(x)}(\{k\}, \{l\})$ depend on the external and loop momenta.
- The $a^{(x)}$ may depend on color factors and on external momenta.

The advantage of this approach to constructing the amplitude is that it is possible to tailor integrands in the basis to match certain physically-mandated poles of the amplitude. For MHV amplitudes, it is also possible to constrain the form of the $a^{(x)}$ [65]. This is the starting point for the pure integrand basis – which is also a $d \log$ basis – in Sec. 2.3.3

2.3 $d \log$ Forms

Following definitions and simple examples of $d \log$ forms in Sec. 2.3.1, Sec. 2.3.2 outlines how to construct $d \log$ forms by ansatz (see Sec. 2.2.1) and Sec. 2.3.3 outlines how to construct $d \log$ forms starting with an integrand basis (see Sec. 2.2.2).

2.3.1 Simple Examples

It is natural to define an integrand form $\Omega(x_1, \dots, x_m)$ of the integral F by stripping off the integration symbol

$$F = \int \Omega(x_1, \dots, x_m), \quad (2.19)$$

and to study its singularity structure. A form has only *logarithmic singularities* if near any pole $x_i \rightarrow a$ it behaves as

$$\Omega(x_1, \dots, x_m) \rightarrow \frac{dx_i}{x_i - a} \wedge \hat{\Omega}(x_1, \dots, \hat{x}_i, \dots, x_m), \quad (2.20)$$

where $\hat{\Omega}(x_1, \dots, \hat{x}_i, \dots, x_m)$ is an $(m - 1)$ -form¹ in all variables except \hat{x}_i . An equivalent terminology is that there are only simple poles. Under the change of variables $x_i \rightarrow g_i(x_j)$, such forms may be written

$$\Omega = d \log g_1 \wedge d \log g_2 \wedge \dots \wedge d \log g_m, \quad (2.21)$$

where

$$d \log x \equiv \frac{dx}{x}. \quad (2.22)$$

The form Ω is a *d log form*.

A simple example of such a form is $\Omega(x) = dx/x \equiv d \log x$, while $\Omega(x) = dx$ or $\Omega(x) = dx/x^2$ are examples of forms which do not have this property. A trivial two-form with logarithmic singularities is $\Omega(x, y) = dx \wedge dy/(xy) = d \log x \wedge d \log y$. A less trivial example of a *d log form* is

$$\Omega(x, y) = \frac{dx \wedge dy}{xy(x + y + 1)} = d \log \frac{x}{x + y + 1} \wedge d \log \frac{y}{x + y + 1}. \quad (2.23)$$

In this case, the property of only logarithmic singularities is not obvious from the first expression, but a change of variables resulting in the second expression makes the fact that Ω is a *d log form* manifest. This may be contrasted with the form

$$\Omega(x, y) = \frac{dx \wedge dy}{xy(x + y)}, \quad (2.24)$$

¹The signs from the wedge products will not play a role since unitarity cuts fix overall normalization in the amplitude.

which is not logarithmic because near the pole $x = 0$ it behaves as dy/y^2 ; this form cannot be written as a $d\log$ form. In general, the nontrivial changes of variables required can make it difficult to find explicit $d\log$ forms even where they exist.

For further clarification, consider the behavior of a form near $x = 0$. If the integrand scales as dx/x^m for integer m , there are two different regimes where integrands can fail to have logarithmic singularities. The first is when $m \geq 2$, which results in double or higher poles at $x = 0$. The second is when $m \leq 0$, which results in a pole at infinity. Avoiding unwanted singularities, either at finite or infinite values of x , leads to tight constraints on the integrand of each diagram. Since the denominators associated to a given diagram are the standard Feynman propagators, the only available freedom in the amplitude is to adjust the kinematic numerators. As an example, consider the form

$$\Omega(x, y) = \frac{dx \wedge dy N(x, y)}{xy(x + y)}. \quad (2.25)$$

As noted above, for a constant numerator $N(x, y) = 1$ the form develops a double pole at $x = 0$. Similarly, for $N(x, y) = x^2 + y^2$ the form behaves like dy for $x = 0$ and again it is not logarithmic. There is only one class of numerators that make the form logarithmic near $x = 0$ and $y = 0$: $N(x, y) = a_1x + a_2y$ for arbitrary a_1 and a_2 .

A discussion of loop integrands is similar: constant numerators² are dangerous for they may allow double or higher poles located at finite values of loop momenta, while a numerator with too many powers of loop momentum can develop higher poles at infinity. It turns out that the first case is generally the problem in sYM, whereas the second case usually arises in mSUGRA, where the power counting of numerators is higher than in sYM. For sYM integrands, the numerators can be carefully tuned so that only logarithmic singularities are present. The desired numerators live exactly on the boundary between too many and too few powers of loop momenta.

²Here and after “constant numerators” means “numerators independent of loop momentum”.

2.3.2 $d\log$ by Ansatz

In Ref. [62], the sYM two-loop four-point amplitude was rewritten in a form with no logarithmic singularities and no poles at infinity. This section outlines how to do the same at higher loop orders. The general procedure has four steps:

1. Define a set of parent diagrams whose propagators are the standard Feynman ones. The parent diagrams are defined to have only cubic vertices and loop momentum flowing through all propagators.
2. Construct $d\log$ numerators. These are a basis set of numerators constructed so that each diagram has only logarithmic singularities and no poles at infinity. These numerators also respect diagram symmetries, including color signs. Each $d\log$ numerator, together with the diagram propagators, forms a basis diagram.
3. Use simple unitarity cuts to determine the linear combination of basis diagrams that gives the amplitude.
4. Use the method of maximal cuts [71] to confirm that the amplitude so constructed is correct and complete.

There is no a priori guarantee that this will succeed. In principle, requiring $d\log$ numerators could be incompatible with expanding the amplitude in terms of independent diagrams with Feynman propagators. Indeed, at sufficiently high loop order there is no reason to expect that it is possible to find a covariant diagrammatic representation manifesting the desired properties; in such circumstances unphysical singularities have to cancel between diagrams. The proof that such a representation of the amplitude exists is by construction, followed by confirming that all cuts of the amplitude are correct.

Following the normalization conventions of Ref. [72], the amplitude is

$$\mathcal{A}_{4,k}^{(L)} = g^{2+2L} \frac{i^L \mathcal{K}}{(2\pi)^{DL}} \sum_{\mathcal{S}_4} \sum_{(x)} \frac{1}{S^{(x)}} c^{(x)} \int d\mathcal{I}^{(x)}(\ell_5, \dots, \ell_{4+L}), \quad (2.26)$$

where $d\mathcal{I}^{(x)}$ is the integrand form defined in Eq. (2.31). The number of spacetime dimensions D is made explicit to distinguish it from $n = 4$. In Eq. (2.26) the sum labeled by x runs over the set of distinct, non-isomorphic diagrams with only cubic vertices, and the sum over \mathcal{S}_4 is over all $4!$ permutations of external legs. The symmetry factor $S^{(x)}$ then removes overcounting that arises from automorphisms of the diagrams. The color factor $c^{(x)}$ of diagram (x) is given by dressing every three-vertex with a group-theory $SU(N)$ structure constant, $\tilde{f}^{abc} = i\sqrt{2}f^{abc}$. In the sum over permutations in Eq. (2.26), any given $d\mathcal{I}^{(x')}$ is a momentum relabeling of $d\mathcal{I}^{(x)}$ in Eq. (2.31). The expression Eq. (2.26) is straightforwardly a rearrangement of Eq. (2.17) by splitting the $N^{(x)}$ there into various factors.

The prefactor \mathcal{K} is proportional to the color-ordered tree amplitude,

$$\mathcal{K} = stA_4^{\text{tree}}(1, 2, 3, 4). \quad (2.27)$$

Furthermore, \mathcal{K} has a crossing symmetry so it can also be expressed in terms of the tree amplitude with different color orderings,

$$\mathcal{K} = suA_4^{\text{tree}}(1, 2, 4, 3) = tuA_4^{\text{tree}}(1, 3, 2, 4). \quad (2.28)$$

The explicit values of the tree amplitudes are

$$A_4^{\text{tree}}(1, 2, 3, 4) = i \frac{\delta^8(\mathcal{Q})}{\langle 12 \rangle \langle 23 \rangle \langle 34 \rangle \langle 41 \rangle}, \quad (2.29)$$

where $\delta^8(\mathcal{Q})$ is a supermomentum conserving delta function, the explicit expression of which is unimportant here.

In each parent diagram, the L independent loop momenta are labelled as $\ell_5, \dots, \ell_{4+L}$. By conserving momentum at each vertex, all other propagators have sums of the loop and external momenta flowing in them. The L -loop *integrand*, $\mathcal{I}^{(x)}$, is defined to be

$$\mathcal{I}^{(x)} \equiv \frac{N^{(x)}}{\prod_{\alpha^{(x)}} p_{\alpha^{(x)}}^2}. \quad (2.30)$$

where (x) labels the diagram, $N^{(x)}$ is the kinematic numerator, and $\prod_{\alpha(x)} p_{\alpha(x)}^2$ the Feynman propagators of the diagram. From this follows the definition of the *integrand form*

$$d\mathcal{I}^{(x)} \equiv \prod_{l=5}^{4+L} d^4 \ell_l \mathcal{I}^{(x)}. \quad (2.31)$$

This integrand form is a $4L$ form in the L independent loop momenta $\ell_5, \dots, \ell_{4+L}$, where each ℓ_l is a four-vector.

The numerator can be expanded in terms of the $d \log$ numerators $N_i^{(x)}$:

$$N^{(x)} = \sum_i a_i^{(x)} N_i^{(x)}. \quad (2.32)$$

The coefficients $a_i^{(x)}$ can be obtained by matching an expansion of the amplitude in $d \log$ numerators to unitarity cuts or other physical constraints, such as leading singularities.

The numerators $N_i^{(x)}$ are constrained as follows:

Overall dimension. The numerators $N_i^{(x)}$ are local polynomials of momentum invariants (i.e. $k_a \cdot k_b$, $k_a \cdot \ell_b$, or $\ell_a \cdot \ell_b$) with dimensionality $N_i^{(x)} \sim (p^2)^K$, where $K = P - 2L - 2$, P is the number of propagators in the integrand and p represents a momentum dimension. Numerators with $K < 0$ are forbidden.

Asymptotic scaling. For each loop momentum ℓ_l , require integrands behave asymptotically as boxes, pentagons, etc..., up to maximum power counting in all possible automorphism labellings. Mathematically this is:

$$\lim_{\ell_l \rightarrow \infty} \mathcal{I}^{(x)} = \frac{\ell^n}{(\ell_l^2)^4} \quad n \geq 0. \quad (2.33)$$

No double/higher poles. The integrand $\mathcal{I}^{(x)}$ must be free of poles of order two or more in all kinematic regions - see Eq. (2.20).

No poles at infinity. The integrand $\mathcal{I}^{(x)}$ must be free of poles of any order at infinity in

all kinematic regions:

$$(\text{Res} \cdots \underset{\ell \rightarrow \infty}{\text{Res}} \cdots \text{Res}) \mathcal{I}^{(x)} = 0, \quad (2.34)$$

where the iterated residue procedure is clarified in Sec. 2.1.

The overall dimensionality and asymptotic scaling gives power counting constraints on the subdiagrams. In practice, these two constraints dictate the initial form of an ansatz for the numerator, while the last two conditions of no higher degree poles and no poles at infinity constrain that ansatz to select $d \log$ numerators. The constraint on overall dimensionality is the requirement that the overall mass dimension of the integrand is $-4L-4$.³ The asymptotic scaling constraint includes a generalization of the absence of bubble and triangle integrals at one-loop order in sYM and mSUGRA [73, 74]. This constraint is a necessary, but not a sufficient, condition for having only logarithmic singularities and no poles at infinity.

This construction is implemented in detail for the two-loop four-point amplitude in Sec. 4.1.1. Explicit $d \log$ forms for the three-loop four-point amplitude are listed in Sec. 5.1

2.3.3 Pure Integrand Basis

In Ref. [3] we conjectured that it is possible to write all sYM MHV amplitudes as

$$\mathcal{A}_{n,\text{MHV}}^{(L)} = \sum_{\mathcal{S}_n} \sum_{k,\sigma,j} a_{\sigma,k,j} c_k \text{PT}_\sigma \int d\mathcal{I}^j. \quad (2.35)$$

In this expression, the sum over \mathcal{S}_n is a sum over all permutations of the external labels. The $a_{\sigma,k,j}$ are numerical rational coefficients; these absorb the symmetry factors with respect to Eq. (2.26). The PT_σ are generalizations of the tree amplitude of Eq. (2.29) and are defined by

$$\text{PT}_\sigma \equiv \text{PT}(\sigma_1 \sigma_2 \sigma_3 \dots \sigma_n) = \frac{\delta^8(\mathcal{Q})}{\langle \sigma_1 \sigma_2 \rangle \langle \sigma_2 \sigma_3 \rangle \dots \langle \sigma_n \sigma_1 \rangle}. \quad (2.36)$$

³This matches the dimensionality of sYM amplitude integrands in $D = 4$. The -4 term in the mass dimension originates from factoring out a dimensionful quantity from the final amplitude in Eq. (2.26).

The $d\mathcal{I}^j$ are *pure integrands*. By definition, $d\mathcal{I}$ is a pure integrand if:

- $d\mathcal{I}$ has all unit leading singularities: $\text{LS}(d\mathcal{I}) = -1, 0, \text{ or } 1$.
- $d\mathcal{I}$ has no poles at infinity.

See Sec. 2.1 for additional details on leading singularities.

The c_k in Eq. (2.35) are color factors. For pure integrands that are trivalent graphs, the unique color factors can be read off directly from the corresponding diagrams. Contact term contributions may have multiple contributing color factors.

The $a_{\sigma,k,j}$ coefficients in Eq. (2.35) are such that, up to sums of Parke-Taylor factors, the leading singularities of the amplitude are normalized to be $(\pm 1, 0)$, reflecting a known property of the amplitude [65]. This way of writing the amplitude is a straightforward rearrangement of Eq. (2.18).

The motivation for writing the amplitude as in Eq. (2.35) followed from several observed properties for nonplanar amplitudes:

- (i) The integrand has only logarithmic singularities.
- (ii) The integrand has no poles at infinity.
- (iii) The leading singularities of the integrand all take on special values.

As discussed in detail in Ref. [3], the presence of only logarithmic singularities (i) is a preliminary indication of a “volume” interpretation of nonplanar amplitudes. Demonstrating properties (ii) and (iii) provides nontrivial evidence for the existence of an analog of dual conformal symmetry for full sYM amplitudes. Since there are no nonplanar momentum twistor variables⁴, it is not possible to formulate an analogous symmetry directly, yet the basic constraints of properties (ii) and (iii) on nonplanar amplitudes would be identical to the constraints of dual conformal symmetry on planar amplitudes.

⁴Momentum twistor variables are not used in this dissertation, but they are a straightforward change of variables from spinor helicity variables.

The two-loop four-point, two-loop five-point, and three-loop four-point amplitudes are written in this pure integrand representation in Secs. 4.1, 4.2 and 5.2, respectively.

2.4 Homogeneous Constraints

This section outlines how to determine the amplitude using only conditions on where the amplitude must vanish. In Sec. 2.4.1 is the motivation for using this technique. Practical aspects to this technique are addressed in Sec. 2.4.2, where on-shell diagrams are defined and put into this context.

2.4.1 Motivation

In Ref. [3], we conjectured:

The amplitude should be determined entirely from homogeneous conditions,
up to an overall normalization.

The motivation for this conjecture is the amplituhedron [45], which is a self-consistent geometric definition of the planar amplitude. In the planar case it is possible to write the amplitude over a common denominator:

$$\mathcal{A} = \frac{N}{\prod (\text{local poles})}, \quad (2.37)$$

where N is a polynomial in momentum twistor loop variables. This means N must be completely fixed by its zeros (roots). There is evidence [49] that the zeros of N either correspond to forbidden cuts generated by the denominator or cancel higher poles in the denominator to ensure that all singularities are logarithmic. The content of the conjecture at the beginning of this section is that, in the full nonplanar theory, the MHV amplitude can be fixed by requiring the nonplanar analog of N to vanish on forbidden cuts. There are two types of forbidden cut solutions for MHV amplitudes:

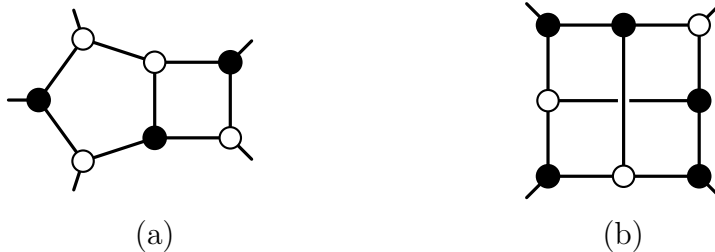


Figure 2.3: Sample planar (a) and nonplanar (b) on-shell diagrams. The black and white dots respectively represent MHV and $\overline{\text{MHV}}$ three-point amplitudes. Black lines are on-shell particles.

Unphysical cut solutions on which amplitudes of any helicity vanish. In the on-shell diagram representation (Sec. 2.4.2) this means no on-shell diagram exists.

Non-MHV cut solutions on which only MHV amplitudes vanish while other helicity amplitudes can be non-zero. In the on-shell diagram representation (Sec. 2.4.2), this means the corresponding on-shell diagram has $k \neq 2$. See Sec. 2.4.2.

These physical constraints on the amplitude serve as zero conditions for fixing the nonplanar amplitude, in lieu of the geometric constraints used to define the planar amplitude in the amplituhedron story. Successfully constructing the full amplitude from homogeneous conditions implies that there might be an amplituhedron-like construction of the full theory where these homogeneous conditions come from a geometric interpretation. We discuss this in much more detail in Ref. [3].

2.4.2 On-shell Diagrams

On-shell diagrams are graphs with decorated black or white vertices, as exemplified by Fig. 2.3. Black vertices represent MHV three-point amplitudes, white vertices $\overline{\text{MHV}}$ three-point amplitudes, and all lines, both internal and external, represent on-shell particles. There are two indices associated with any on-shell diagram: the number of external legs n and the

helicity index k . The k -index is defined from the graph

$$k = \sum_V k_V - P, \tag{2.38}$$

where the sum is over all vertices V , k_V is the k -count of the tree-level amplitude in a given vertex, and P is the number of on-shell internal propagators. Black and white vertices have $k_B = 2$ and $k_W = 1$, respectively. As examples, the on-shell diagram Fig. 2.3(a) has $k = 3 \times 2 + 4 \times 1 - 8 = 2$ and the on-shell diagram Fig. 2.3(b) has $k = 5 \times 2 + 3 \times 1 - 10 = 3$. This k corresponds to the total number of external negative helicity gluons.

There are rules that assign kinematic functions to on-shell diagrams. In the planar limit of sYM, there is a prescription for recursively combining such functions to compute the amplitude. On-shell diagrams also appear in mathematics literature in computing cells of the positive Grassmannian. These points are covered in Ref. [40].

The diagrams have another interpretation that is relevant for determining the unphysical cuts of the amplitude. In this interpretation, the diagrams encode solutions to cut equations. To convert a cut solution into an on-shell diagram:

- Draw the integrand topology being cut
- Conserve momentum at every vertex
- Decorate a trivalent vertex white when $\lambda_i \propto \lambda_j \propto \lambda_k$
- Decorate a trivalent vertex black when $\tilde{\lambda}_i \propto \tilde{\lambda}_j \propto \tilde{\lambda}_k$

This means two on-shell diagrams that represent different solutions to the same cut equations have the same edges and nodes, but the nodes are decorated differently.

An MHV amplitude must vanish on cuts where the corresponding on-shell diagrams have a number of black and white vertices and edges such that $k \neq 2$. As examples, the two-loop five-point amplitude does not have to vanish on the residue encoded on Fig. 2.3(a), since there $k = 2$. In contrast, the three-loop four-point amplitude is non-vanishing only on

residues for which $k = 2$, and so the amplitude must vanish on the residue corresponding to Fig. 2.3(b) since there $k = 3$. There are examples in the following chapters at two-loop four-point (Fig. 4.2), two-loop five-point (Fig. 4.4), and three-loop four-point (Fig. 5.1).

In practice, it is straightforward to solve all cut equations numerically then construct all corresponding on-shell diagrams with `osdn` (see Sec. 2.6). This separates the $k = 2$ from the $k \neq 2$ cut solutions, and from there the amplitude can be constrained to vanish on the $k \neq 2$ solutions. This process is done in detail for the two-loop four-point amplitude in Sec. 4.1.3, and is also discussed briefly for the two-loop five-point and three-loop four-point amplitudes in Sec. 4.2 and Sec. 5.2 respectively. There is an example of numerically generating the on-shell diagrams via `osdn` in Sec. 4.1.4.

2.5 Color-Kinematics Duality

In Ref. [61], Bern, Carrasco, and Johansson (BCJ) conjectured a duality between color and kinematics.

The conjecture is: if a sYM amplitude can be written in a trivalent graph expansion as in Eq. (2.17), with the additional constraint that the numerators obey the same relations as the color factors

$$c^{(s)} + c^{(t)} + c^{(u)} = 0 \Rightarrow N^{(s)} + N^{(t)} + N^{(u)} = 0, \quad (2.39)$$

then the mSUGRA amplitude can be written as

$$\mathcal{M}_{n,k}^{(L)} = \sum_{\mathcal{S}_n} \sum_{(x)} \int d^{4L} \ell \frac{N^{(x)} \tilde{N}^{(x)}}{p^{(x)}}, \quad (2.40)$$

where the \tilde{N} can be any representation of the sYM amplitude. In Eq. (2.39), the superscript notation indicates three different graphs related by applying a Jacobi relation to any propagator within the graph. This is illustrated in Fig. 2.4. The numerators that satisfy Eq. (2.39) are called *BCJ numerators*.

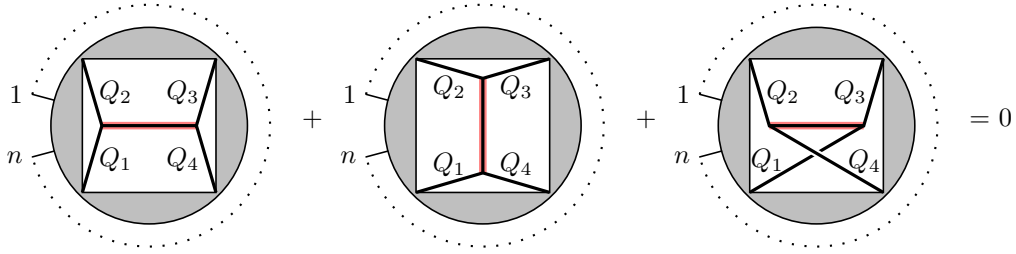


Figure 2.4: A schematic representation of a Jacobi relation between three different graphs. The external dots represent n generic external particles. The gray band represents any generic external or loop trivalent graph structure. The red propagator is the propagator on which the Jacobi identity is applied. The four momenta Q_1 , Q_2 , Q_3 and Q_4 can be either external legs or propagators of the higher-loop diagram. The first diagram is termed the s -channel, the second the t -channel, and the third the u channel in analogy to the four-point tree-level amplitude.

The color-kinematics duality conjecture has held through four-loops for the four-point amplitude in sYM and mSUGRA [72]. The current state of affairs for the five-loop four-point amplitude is covered in Ch. 7. In addition, the color-kinematics duality is used to obtain tree-level mSUGRA amplitudes in Sec. 3.3, and it is used to analyze poles at infinity of three-loop four-point mSUGRA amplitudes in Sec. 6.2.

Aside from the relationship between sYM and mSUGRA amplitudes, the BCJ numerators also reduce the complexity of sYM tree-level amplitudes. The tree-level amplitudes can be written in terms of color-stripped *partial amplitudes*. The relations implied by the BCJ numerators reduce the number of independent partial amplitudes from $(n-2)!$ to $(n-3)!$. See further discussion in Ch. 3.

2.6 osdn : On-shell Diagrams and Numerics

This section contains a description of the Mathematica package I compiled and wrote: `on_shell_diagrams_and_numerics.m` (osdn). The package is a collection of functions I used to generate ansätze, construct cuts of amplitudes, confirm properties of various integrands, and in essence generate or verify everything that appeared in our publications. Some of the

functions in `osdn` are based to varying degrees on other functions written by Zvi Bern, John Joseph Carrasco, Scott Davies, Tristan Dennen, Josh Nohle, Henrik Johansson, and Radu Roiban - in those cases who originally wrote what was not documented.

For lack of any better organizational principle, what follows is the name of functions and what they do. The Mathematica notebooks containing these functions is uploaded with this dissertation. As an example of how these functions are used, see Sec. 4.1.4; that section contains sample code for fixing the two-loop four-point amplitude by one homogeneous constraint.

2.6.1 Graph Functions

Subdiagrams

`tadpoleQ` : True if graph contains a tadpole subdiagram.

`bubbleQ` : True if graph contains a bubble subdiagram.

`triangleQ` : True if graph contains a triangle subdiagram.

`dangTreeQ` : True if graph contains a dangling tree.

`multiPropQ` : True if graph has two or more identical propagators.

`lFreePropsQ` : True if graph has internal edges independent of loop momentum.

`minimalCycles` : Returns minimal cycles of a graph.

`findSubGons` : Find subgraphs with n sides.

On-shell Diagrams

`generateSolWBList` : Determines coloring of vertices of an on-shell diagram.

`osdGraph` : Generates on-shell diagram from graph and black and white vertices.

`checkSpSolColor` : Check colorings of on-shell diagram from analytic solution.

`osdSolutionTable` : Generate table of on-shell diagram, black/white vertices, and numerical solution to cut equations.

Collapse Propagators

`blowUpVert` : Expand multi-point vertex and relabel appropriately.

`blowUpGraph` : Generate all graphs from blowing up collapsed vertices.

`collapsePropagators` : Collapse propagators in a diagram.

`numberOfGraphs` : Returns number of graphs in the blow-up.

Isomorphisms

`isomorphismQ` : True if there is an isomorphism between two graphs.

`isomorphismRule` : Generate rules for relabelling one graph to another.

`automorphismRules` : Generate rules for relabelling graph to automorphism.

`autoMomRules` : Generate rules for mapping one numerator to another.

`isoData` : Returns useful information about relabelling graphs.

2.6.2 Momentum and Spinor Functions

`getkMax` : Returns the number of external particles .

`momConsGraph` : Momentum conservation from graph.

`clean` : Momentum algebra cleaning functions.

`dComp` : Minkowski inner product in vector components.

`compClean` : Clean and convert to components of four-vector.

`toNumerical` : Convert invariants to numerical values.

`toComponents` : Convert invariants to components of four-vectors.

`spClean` : Algebraically simplify spinor products.

`spW` : Check spinor weight of an expression.

`momW` : Check momentum dimension of an expression.

2.6.3 Numerical Cuts

`genLValues` : Generate random (real) independent loop momenta.

`genExtNumerics` : Generate random external kinematics.

`loadKinematics` : Load external kinematics.

`loadRatKin` : Load rational external kinematics.

`toNumRat` : Convert expression to rational external kinematics.

`indepL` : Determine which loop momenta are independent.

`solveForL` : Determine which loop momentum components to solve for in cuts.

`allPropLabels` : List of which labels are propagators.

`allProps` : A list of all propagators of a graph.

`solveCutSols` : Setup and numerically solve the equations produced by `cutSols`.

`cutSols` : Generate cut equations.

`coeffEqns` : Gathers coefficients of parameters into equations.

`analyticCutSols` : Solve cut conditions in terms of Mandelstam invariants.

2.6.4 Color Functions

`colorDiag` : Generates f's from graph.

`colorSimplifyF` : Convert the color factors to a trace basis.

`colorSign` : Find the sign of a diagram with respect to its parent.

`colorToDiag` : Convert product of f's to graph notation.

`getCTRLList` : Generate list of ctr's appearing in expression.

`getNList` : Generate list of powers of N appearing in expression.

`getAllId` : Generate list of Mandelstam invariants appearing in expression.

`buildJacobis` : Determine relations among color factor elements.

`colorElim` : Eliminate linearly dependent color basis elements.

`jacobiIdentity` : Determine signs of Jacobi relation from one four-vertex graph.

`kinematicJacobi` : Determine kinematic color numerator relation.

2.6.5 Analytic Spinors

`asOp` : Analytic spinor outer product.

`solFromOSD` : Construct an analytic solution from an on-shell diagram.

`genSpBasis` : Generate replacement rules to change to basis of spinor invariants.

`spBasis` : Map an expression to a basis of spinors.

2.6.6 Ansatz

`relColorSign` : Return the relative color sign of two isomorphic trivalent graphs.

`imposeSymOfGraph` : Return $\text{expr} - \text{sign}^*(\text{autmorphism of expr})$.

`symmetrizeOnGraph` : Symmetrize expression from the automorphisms of graph.

2.6.7 Cut Construction

`determineParent` : Find graph in list of parent graphs.

`constructCut` : Construct cut contributions corresponding to cut graph.

`constructLPCut` : Like `constructCut` but allows non-trivalent vertices.

`relabelNum` : Match a diagram to a parent and return relabelled numerator.

`indepCuts` : Determine set of independent cuts modulo automorphisms.

`maxFromLP` : Returns trivalent graphs that result from input graph blow-up.

2.6.8 Spinor Algebra

`spAlg` : Implements spinor helicity algebra.

`spA` : Apply spinor solutions to expressions.

`spConventions` : Prints spinor conventions.

`spRep` : Go to an independent spinor basis.

`lSolProps` : Load properties of `lSol[...]` syntax.

`opExp` : Expand a loop momentum in terms of four spinor outer products.

2.6.9 Miscellaneous

`niceP` : Nicely print expression.

CHAPTER 3

Tree Level Amplitudes

This chapter focuses on tree-level sYM and mSUGRA amplitudes. Sec. 3.1 contains the tree-level twistor-string expressions for the sYM and mSUGRA amplitudes. In Sec. 3.2 is a linear algebra treatment of the color-kinematic duality. Residue numerators are defined in Sec. 3.3. A complete example of how to construct residue numerators for $n = 6$ external particles is outlined in Sec. 3.4.

3.1 RSVW String and the Connected Prescription

The Roiban, Spradlin, Volovich, and Witten (RSVW) [75–79] twistor string formula expresses the tree level sYM amplitude as an integral over a moduli space of curves in $\mathbb{CP}^{3|4}$ supertwistor space. This effectively reduces the amplitude calculation to solving an algebraic system of equations.

The RSVW formula that gives all tree level partial amplitudes is

$$\begin{aligned} \mathcal{A}_{n,k}^{(0)} &= \int \frac{d^{2n}\sigma}{\text{vol } GL(2)} \frac{1}{(12)(23)\cdots(n1)} \prod_{\alpha=1}^k \delta^2(C_{\alpha a} \tilde{\lambda}_a) \delta^{0|4}(C_{\alpha a} \tilde{\eta}_a) \\ &\quad \times \int d^2\rho_\alpha \prod_{b=1}^n \delta^2(\rho_\beta C_{\beta b} - \lambda_b), \end{aligned} \tag{3.1}$$

where the $C_{\alpha a}$ are $k \times n$ matrices parametrized by σ , as discussed in the Grassmannian formulations of Refs. [34, 37, 40], for particles in the R -charge sector given by k . The minors (12), (23), etc. are minors of $C_{\alpha a}$, and are thus functions of the σ . The delta functions enforce the conditions that the spinor helicity variables λ , $\tilde{\lambda}$, and Grassmann coordinate $\tilde{\eta}$

are appropriately orthogonal, and thus that overall supermomentum is conserved. This is also referred to as the “connected prescription” of the amplitude.

The method of determining tree-level amplitudes as integrals in $\mathbb{CP}^{3|4}$ was extended to mSUGRA [80–86]. Like the RSVW formula, the integrals for mSUGRA can be interpreted as contour integrals, and hence as sums of residues. The Cachazo-Geyer formula for gravitational amplitudes, as proposed in Ref. [83], is

$$\mathcal{M}_{n,k}^{(0)} = \int \frac{d^{2n}\sigma}{\text{vol } GL(2)} \frac{H_n}{J_n} \prod_{\alpha=1}^k \delta^2(C_{\alpha a} \tilde{\lambda}_a) \delta^{0|8}(C_{\alpha a} \tilde{\eta}_a) \int d^2\rho_\alpha \prod_{b=1}^n \delta^2(\rho_\beta C_{\beta b} - \lambda_b), \quad (3.2)$$

which is identical to the sYM formula Eq. (3.1) except for four additional supersymmetries and the replacement in the integrand of the inverse minor factor with H_n/J_n . The exact definition of H_n/J_n is not important for what follows, but it is also a function of the minors of $C_{\alpha a}$.

For the remainder of this chapter, let $\mathcal{A}_n \equiv \mathcal{A}_{n,k}^{(0)}$ and $\mathcal{M}_n \equiv \mathcal{M}_{n,k}^{(0)}$. After some set-up of notation in the following section, the numerators of the residues of \mathcal{M}_n are shown to be color-kinematic dual to the numerators of the residues of \mathcal{A}_n in Sec. 3.3.

3.2 Linear Algebra Notation

A convenient way of structuring discussions of kinematic numerators is the linear algebra approach pioneered in Ref. [87] and extended in Ref. [88]. This formalism makes generalized gauge invariance manifest, and also reinterprets the BCJ amplitude identities¹ as algebraic consistency conditions.

The sYM amplitude can be written in a so-called Del Duca-Dixon-Maltoni (DDM) de-

¹The BCJ amplitude identities are the relations that partial amplitudes obey as a result of writing the amplitude in a BCJ representation.

composition [89]. In this form, the full n -particle amplitude at tree level is

$$\mathcal{A}_n = g^{n-2} \sum_{\tau \in S_{n-2}} c_\tau A_n(1, \tau_2, \dots, \tau_{n-1}, n), \quad (3.3)$$

where the coupling constant is g , the notation $\tau \in S_{n-2}$ indicates that the sum runs over permutations τ of the particle labels $2, \dots, n-1$, the A_n are color-ordered partial amplitudes, and the c_τ are color factors² of cubic diagrams. Cubic diagrams are diagrams with only trivalent vertices, which conserve color and momentum at each vertex. Any diagrams containing higher-point contact terms are absorbed into cubic diagrams with the same color factor, with missing propagators P introduced by multiplying by $1 = \frac{P}{P}$. While there is no known Lagrangian from which this decomposition can be directly generated by Feynman rules, these trivalent diagrams are a useful way of reorganizing the usual sum over Feynman diagrams.

The partial amplitude A obey several identities; see Ref. [4], for example. Two important relations for later discussion are the Kleiss-Kuijf (KK) relations [90] and the Kawai-Lewellen-Tye (KLT) relations [91]. The KK relations are between partial amplitudes of different gluon orderings. Without going into unnecessary detail, combining the KK relations with all partial amplitude relations allows the amplitude to be expressed in a basis of $(n-2)!$ partial amplitudes. The KLT relations express tree-level mSUGRA amplitudes in terms of products of tree-level sYM amplitudes. This is made more explicit in Sec. 3.3.

Another decomposition of the tree level amplitude is

$$\mathcal{A}_n = g^{n-2} \sum_{i=1}^{(2n-5)!!} \frac{c_i n_i}{D_i}, \quad (3.4)$$

where the sum is now over the unique set of $(2n-5)!!$ cubic diagrams, with color factors c_i , products of propagators D_i , and so-called *kinematic numerators* n_i . These last objects are

²These are a product of group-theory structure constants; see Ref. [89] for details.

functions only of the external momenta and helicities, and are not uniquely defined. This is because a generalized gauge transformation $n_i \mapsto n_i + \Delta_i$, for functions Δ_i that obey

$$\sum_{i=1}^{(2n-5)!!} \frac{c_i \Delta_i}{D_i} = 0, \quad (3.5)$$

will leave the BCJ decomposition Eq. (3.4) invariant.

The notion of such a generalized gauge transformation has a natural interpretation in the linear algebra formalism. To see this interpretation, relate the DDM and BCJ decompositions. It was shown in Ref. [89] that the $(n-2)!$ color factors c_τ form a basis of the space of color factors of cubic diagrams. This is possible because the Jacobi relations of the structure constants induce linear relations among the color factors. In other words, any of the $(2n-5)!!$ color factors c_i that appear in the decomposition Eq. (3.4) can be written as

$$c_i = \sum_{\tau \in S_{n-2}} W_{i\tau} c_\tau \quad (3.6)$$

where $W_{i\tau}$ is a $(2n-5)!! \times (n-2)!$ matrix that encodes the Jacobi relations among the color factors. In this notation, sums over permutations are contractions of τ and ω , and sums over cubic diagrams are contractions of Latin indices i, j .

The color-kinematic duality is that there exists a set of color-dual numerators n_i that obey the exact same Jacobi relations as the color factors c_i . In other words, for the same matrix $W_{i\tau}$ defined above in Eq. (3.6):

$$n_i = \sum_{\tau \in S_{n-2}} W_{i\tau} n_\tau \quad (3.7)$$

for some set of $(n-2)!$ numerators n_τ . Substituting Eq. (3.6) and Eq. (3.7) into the BCJ

decomposition:

$$\begin{aligned}
\mathcal{A}_n &= g^{n-2} \sum_{i=1}^{(2n-5)!!} \sum_{\tau, \omega \in S_{n-2}} \frac{c_\tau n_\omega}{D_i} W_{i\tau} W_{i\omega} \\
&= g^{n-2} \sum_{\tau, \omega \in S_{n-2}} c_\tau n_\omega F_{\tau\omega},
\end{aligned} \tag{3.8}$$

where $F_{\tau\omega}$ is an $(n-2)! \times (n-2)!$ symmetric matrix with products of inverse propagators as entries:

$$F_{\tau\omega} \equiv \sum_{i=1}^{(2n-5)!!} \frac{W_{i\tau} W_{i\omega}}{D_i}. \tag{3.9}$$

The matrix $F_{\tau\omega}$ is a convenient way of simultaneously encoding both the color and numerator Jacobi relations in the basis of partial amplitudes.

Equating Eq. (3.8) to the DDM decomposition and matching coefficients of the c_τ yields

$$A_n(1, \tau_2, \dots, \tau_{n-1}, n) = \sum_{\omega \in S_{n-2}} F_{\tau\omega} n_\omega. \tag{3.10}$$

In matrix notation, this is a system of linear equations

$$FN = A \tag{3.11}$$

in the $(n-2)!$ -dimensional space of partial amplitudes spanned by KK basis amplitudes and indexed by $\tau \in S_{n-2}$, and where N is a column vector of numerators. Inverting this formula would result in an expression for the numerators in terms of the partial amplitudes, but inversion is impossible because F is singular. This is no surprise: the invariance of the full amplitude under generalized gauge transformations Eq. (3.5) ensures that the numerators are not unique, so F cannot be invertible.

Since F is not invertible, it has a nontrivial kernel. In an attempt to invert F despite this obstacle, Ref. [88] suggested using the machinery of *generalized inverses* or *pseudoinverses*. A generalized inverse is a matrix F^+ satisfying $FF^+F = F$, and it can be shown that such an

F^+ always exists, but is not unique. Generalized inverses are useful because of the following theorem [92]: a solution to $FN = A$ exists if and only if the consistency condition

$$FF^+A = A \tag{3.12}$$

holds for some generalized inverse F^+ . The general solution is then given by

$$N = F^+A + (I - F^+F)v \tag{3.13}$$

for an arbitrary vector v that parametrizes the kernel of F .

Notice that $I - F^+F$ is a projection operator onto the kernel of F , since, by the definition of F^+ ,

$$F(I - F^+F) = F - FF^+F = 0. \tag{3.14}$$

The consistency condition Eq. (3.12) has been conjectured to be equivalent to the BCJ amplitude identities [88], and this we proved in Ref. [1]. Note that since the existence of color-dual numerators is proven at tree level [93, 94], the consistency condition is satisfied thanks to the “if and only if” logic.

Rather than reproducing the proof what follows is an outline of the proof in Sec. 3.2.1 and then a graphical illustration of the main idea of the proof for $n = 4$ external particles in Sec. 3.2.2.

3.2.1 Outline of Proof

The goal is to show that $FF^+A = A$ is the same as the BCJ amplitude identities. The BCJ identities can be written as $\mathcal{S}A = 0$, where \mathcal{S} is a matrix that forms the linear combination of amplitudes appearing in the BCJ identities³. The proof proceeds via a

³A particular choice of \mathcal{S} is the momentum kernel, detailed in Ref. [94], for example.

dimension counting argument that allows writing

$$Q (FF^+ - I) = \mathcal{S} \tag{3.15}$$

for some $Q \in GL((n-3)!)$ embedded in an $(n-2)! \times (n-2)!$ matrix with all other entries zero, and I the $(n-2)! \times (n-2)!$ identity matrix. The result, Eq. (3.15), is exactly the target expression $FF^+A = A \iff \mathcal{S}A = 0$ up to linear transformations in Q that amount to choosing a different basis of partial amplitudes.

3.2.2 Four-Point Illustration

The proof may be illustrated graphically, as in Fig. 3.1, for $n = 4$.

If the BCJ amplitudes form the true minimal basis of color-ordered amplitudes, then the larger space spanned by amplitudes independent under KK relations must be constrained to the smaller space spanned by the BCJ amplitudes.

In this simplest example, there are $(4-2)! = 2$ amplitudes in the KK basis, and $(4-3)! = 1$ amplitude in the BCJ basis. If the KK basis were minimal, then the vector

$$A = (A(1, 2, 3, 4), A(1, 3, 2, 4)) \tag{3.16}$$

in the plane⁴ \mathbb{C}^2 would fully determine all partial amplitudes. The four-point BCJ basis linearly relates the two elements of the vector A by

$$A(1, 3, 2, 4) = \frac{u}{s} A(1, 2, 3, 4) \quad \text{or} \quad A(1, 2, 3, 4) = \frac{s}{u} A(1, 3, 2, 4) \tag{3.17}$$

where either equation is valid, and amounts to choosing either $A(1, 2, 3, 4)$ or $A(1, 3, 2, 4)$ as the BCJ basis amplitude. This is equivalent to projecting to one axis or the other in Fig. 3.1. Since the vectors A describe physically valid partial amplitudes, they cannot lie at

⁴The words “plane” for \mathbb{C}^2 and “line” for \mathbb{C} are used to highlight the geometry.

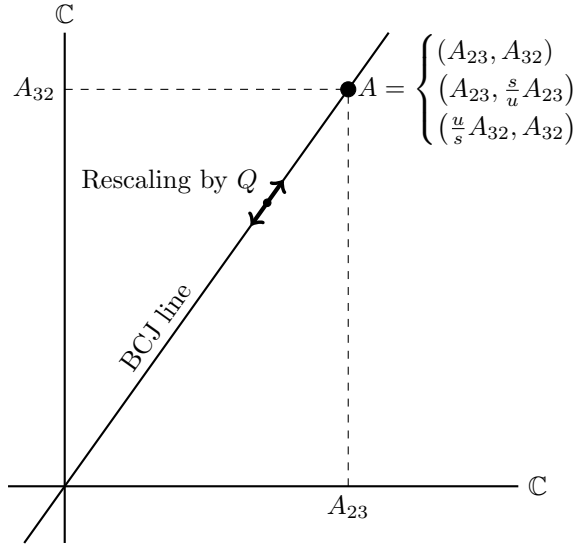


Figure 3.1: Reduction of the KK amplitude basis to the BCJ amplitude basis for $n = 4$. In the figure, $A(1, 2, 3, 4) \equiv A_{23}$ and $A(1, 3, 2, 4) \equiv A_{32}$. Because the BCJ basis is the minimal basis, any Kleiss-Kuijf amplitude vector actually lies on the “BCJ line”. Both A_{23} and A_{32} are complex numbers, indicated by the \mathbb{C} labels on the axes. The “rescaling by Q ” arrows indicate the $GL(1)$ freedom that rescales the point A along the BCJ line.

an arbitrary point in the plane, but must instead lie on the *BCJ line*.

For the four-point case, both operators FF^+ and $\mathcal{S} + I$ are rank one, and act on the KK vector of amplitudes. This means both operators necessarily map to a point along the BCJ line. The linear transformation $Q \in GL((4 - 3)!)$ in this case is just a constant that translates a point along the BCJ line, but such movement does not alter the relation between the amplitudes.

The next-highest-point case, $n = 5$, has $(5 - 2)! = 6$ amplitudes in the KK basis and $(5 - 3)! = 2$ amplitudes in the BCJ basis; geometrically the $n = 5$ case corresponds to a \mathbb{C}^6 hyperplane for the KK basis with all points actually lying on the \mathbb{C}^2 plane spanned by the BCJ basis amplitudes.

This same line of geometric reasoning supports the rank-counting argument of Ref. [1] for all n .

3.3 Residue Numerators

The goal now is to use the linear algebra formalism to examine how residues of the connected prescription sYM amplitude (3.1) double copy into the analogous mSUGRA residues of Eq. (3.2).

Since the delta functions in both formulas Eqs. (3.1) and (3.2) are the same, the residues occur at the same points, and the contours of integration are the same. This allows the sYM residues to be written in one-to-one correspondence with the mSUGRA residues:

$$A_n = \sum_r R_r, \quad \mathcal{M}_n = \sum_r R_r^G, \quad (3.18)$$

where the index r labels the same pole in either integrand.

In Ref. [1], we showed that the residues of the sYM amplitude obey the generalized inverse consistency condition:

$$FF^+R_r = 0. \quad (3.19)$$

This guarantees the existence of residue numerators defined through the generalized inverse theorem:

$$N_r \equiv F^+R_r + (I - F^+F)v. \quad (3.20)$$

By definition, these residue numerators act as kinematic numerators for the residues of the amplitude:

$$R_r = FN_r \quad (3.21)$$

The mSUGRA amplitude \mathcal{M}_n can be written in terms of sYM partial amplitudes using KLT relations. In the linear algebra notation established earlier, this is

$$\mathcal{M}_n = \left(\frac{\kappa}{2}\right)^{n-2} A^T F^+ \tilde{A}, \quad (3.22)$$

where A and \tilde{A} are the sYM partial amplitudes.

Now the main question: in the equations that yield a mSUGRA amplitude in terms of sYM amplitudes, is it possible to replace all amplitudes by residues of the amplitude, and retain the same set of equations? More precisely:

$$R_r^G \stackrel{?}{=} \left(\frac{\kappa}{2}\right)^{n-2} R_r^T F^+ \tilde{R}_r. \quad (3.23)$$

Substituting Eq. (3.18) for \mathcal{M}_n and A_n as sums of residues into the KLT relations Eq. (3.22) and separating cross terms yields

$$\begin{aligned} \sum_r R_r^G &= \sum_{r, \tilde{r}} R_r^T F^+ \tilde{R}_{\tilde{r}} \\ &= \sum_r R_r^T F^+ \tilde{R}_r + \sum_{r \neq \tilde{r}} R_r^T F^+ \tilde{R}_{\tilde{r}}, \end{aligned} \quad (3.24)$$

The KLT orthogonality conjecture

$$\sum_{r \neq \tilde{r}} R_r^T F^+ \tilde{R}_{\tilde{r}} = 0. \quad (3.25)$$

is proven in Ref. [95]. We further argue in Ref. [1] that this orthogonality means not only

$$\sum_r R_r^G = \left(\frac{\kappa}{2}\right)^{n-2} \sum_r R_r^T F^+ \tilde{R}_r. \quad (3.26)$$

but also that the two sides match in the summand:

$$R_r^G = \left(\frac{\kappa}{2}\right)^{n-2} R_r^T F^+ \tilde{R}_r. \quad (3.27)$$

Recasting this in terms of residue numerators:

$$\begin{aligned}
R_r^G &= \left(\frac{\kappa}{2}\right)^{n-2} R_r^T F^+ \tilde{R}_r \\
&= \left(\frac{\kappa}{2}\right)^{n-2} R_r^T F^+ F F^+ \tilde{R}_r \\
&= \left(\frac{\kappa}{2}\right)^{n-2} \left((F^+)^T R_r\right)^T F F^+ \tilde{R}_r \\
&= \left(\frac{\kappa}{2}\right)^{n-2} N_r^T F \tilde{N}_r.
\end{aligned} \tag{3.28}$$

The second line uses the fact that the residues obey the consistency condition $\tilde{R}_r = F F^+ \tilde{R}_r$. The last line uses the fact that for F symmetric, $(F^+)^T$ is also a generalized inverse⁵. The final line is the double-copy formula with ordinary kinematic numerators replaced by residue numerators, and the gravitational amplitude replaced by the corresponding gravitational residue. This positively answers the question of Eq. (3.23).

This argument also holds in reverse. Assuming a double-copy formula for residue numerators:

$$R_r^G = \sum_i \frac{n_{r,i} \tilde{n}_{r,i}}{D_i} \tag{3.29}$$

and reversing the logic in the equations leading to Eq. (3.28) results in the KLT relations for sYM residues. This course of argument uses “residue numerator orthogonality”

$$\sum_{\tilde{r} \neq r} N_r^T F \tilde{N}_{\tilde{r}} = 0, \tag{3.30}$$

to prove KLT orthogonality. As a simple consistency check, this was checked numerically at six points as outlined in the next section.

⁵Since $(F^+)^T$ may be different than F^+ , the resulting numerators may differ from those generated by F^+ by a generalized gauge transformation, but this is irrelevant here.

3.4 Six-Point Calculation

This section outlines one way of defining residue numerators for $n = 6$ scattering particles.

The six-point NMHV amplitude is the first case where residue numerators appear. An amplitude of any helicity may be written as an integral in $(k - 2) \times (n - k - 2)$ integration variables c_i [79]:

$$A_n = \int d^{(k-2)(n-k-2)} c_i a_n(c_i), \quad (3.31)$$

where k is the number of negative-helicity gluons in the scattering process. The function $a_n(c_i)$ in Eq. (3.31) is unimportant for the current explanation. These complex integrals produce residues and corresponding residue numerators. Since $k \leq 2$ results in no integration according to Eq. (3.31), the simplest case is $k = 3$. To select only one integration parameter:

$$(k - 2)(n - k - 2) = 1 \Rightarrow n = 6. \quad (3.32)$$

Thus $n = 6$, $k = 3$ amplitudes – colloquially six-point NMHV amplitudes – offer the first, simplest opportunity for the appearance of residue numerators.

The expression Eq. (3.31) for $n = 6$, $k = 3$ becomes

$$A_6(L, h) = \int dc a(L, h, c), \quad (3.33)$$

for a momentum label configuration $L \in \mathcal{P}(\{1, 2, \dots, n\})$ and helicity configuration $h = \{h_1, h_2, \dots, h_n\}$; the L and h were suppressed in Eq. (3.31). For general n and k , $a_n(c_i)$ contains delta functions in c_i . In the case $n = 6$, $k = 3$, the argument of the delta function is quartic in the complex variable c , and so the integral may be re-expressed as a contour integral enclosing exactly the four roots of the argument of the delta function. More explicitly if

$$a_6(L, h, c) = H_6(L, h, c) \delta(S_6(c)), \quad (3.34)$$

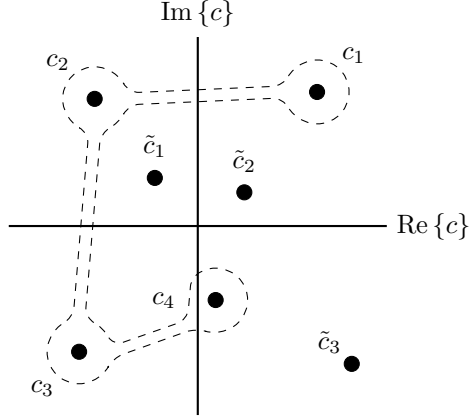


Figure 3.2: The integral for the tree-level, $n = 6$, $k = 3$ SYM amplitude may be calculated as a standard contour integral of a complex variable $c \in \mathbb{C}$. The four poles c_1 , c_2 , c_3 , and c_4 correspond to the four roots of $S(c)$, and the three remaining poles \tilde{c}_1 , \tilde{c}_2 , and \tilde{c}_3 correspond to the poles of the function $H_6(L, h, c)$ in Eq. (3.34). This figure is meant only as a guide; the locations of the poles change for different external momenta.

then

$$S_6(c) = \kappa (c - c_1)(c - c_2)(c - c_3)(c - c_4) \quad (3.35)$$

for an overall constant κ . Converting the amplitude into a complex integral and ignoring factors of $2\pi i$ which cancel in the final result:

$$\begin{aligned} A_n(L, h) &= \oint_{S_6(c)} dc \frac{H_6(L, h, c)}{S_6(c)} \\ &= \sum_{i=1}^4 \operatorname{Res}_{c=c_i} \left(\frac{H_6(L, h, c)}{S_6(c)} \right) \\ &\equiv \sum_{r=1}^4 R_r. \end{aligned} \quad (3.36)$$

A sample contour of integration for $n = 6$ appears in Fig. 3.2.

The residue numerators are now defined by expressing color-dual numerators in terms of amplitudes, replacing each amplitude with a residue of that amplitude, and indexing the

resulting residue numerator accordingly. Schematically:

$$n = f(A) \implies n_r = f(R_r), \quad A = \sum_r R_r. \quad (3.37)$$

In the $n = 3, k = 6$ case, it is straightforward to obtain $n = f(A)$ by comparing two different expressions for the gravity amplitudes. The first is the KLT expression:

$$\begin{aligned} \mathcal{M}(1, 2, 3, 4, 5, 6) = & -i \left(\frac{\kappa}{2}\right)^{6-2} \sum_{\tau \in S_3} s_{1\tau_2} s_{\tau_4 5} \tilde{A}(1, \tau_2, \tau_3, \tau_4, 5, 6) \times \\ & (s_{\tau_3 5} A(\tau_2, 1, 5, \tau_3, \tau_4, 6) + \\ & + (s_{\tau_3 \tau_4} + s_{\tau_3 5}) A(\tau_2, 1, 5, \tau_4, \tau_3, 6)), \end{aligned} \quad (3.38)$$

where S_3 is the set of all permutations of $\{2, 3, 4\}$. The second is the numerator decomposition of the gravity amplitude [96]:

$$\mathcal{M}(1, 2, 3, 4, 5, 6) = i\kappa^{6-2} \sum_{\tau \in S_4} n(1, \tau_2, \tau_3, \tau_4, \tau_5, 6) \tilde{A}(1, \tau_2, \tau_3, \tau_4, \tau_5, 6), \quad (3.39)$$

where S_4 is the set of all permutations of $\{2, 3, 4, 5\}$. Equating the two expressions for $\mathcal{M}(1, 2, 3, 4, 5, 6)$ between Eq. (3.38) and Eq. (3.39) yields expressions for the $(n-2)!$ numerators $n(1, \tau_2, \tau_3, \tau_4, \tau_5, 6)$:

$$\begin{aligned} n(1, \tau_2, \tau_3, \tau_4, 5, 6) = & -2^{-4} s_{1\tau_2} s_{\tau_4 5} (s_{\tau_3 5} A(\tau_2, 1, 5, \tau_3, \tau_4, 6) \\ & + (s_{\tau_3 \tau_4} + s_{\tau_3 5}) A(\tau_2, 1, 5, \tau_4, \tau_3, 6)), \end{aligned} \quad (3.40)$$

$$n(1, \tau_2, \tau_3, \tau_4, \tau_5, 6) = 0 \quad (\text{for } \tau_5 \neq 5). \quad (3.41)$$

The residue numerators are then constructed by replacing

$$A(\tau_1, \tau_2, \tau_3, \tau_4, \tau_5, \tau_6) \rightarrow R_r(\tau_1, \tau_2, \tau_3, \tau_4, \tau_5, \tau_6), \quad (3.42)$$

where $A_6 = \sum_r R_r$ holds. Explicitly:

$$\begin{aligned}
n_r(1, \tau_2, \tau_3, \tau_4, 5, 6) &= -2^{-4} s_{1\tau_2} s_{\tau_4 5} (s_{\tau_3 5} R_r(\tau_2, 1, 5, \tau_3, \tau_4, 6) \\
&\quad + (s_{\tau_3 \tau_4} + s_{\tau_3 5}) R_r(\tau_2, 1, 5, \tau_4, \tau_3, 6)). \tag{3.43}
\end{aligned}$$

This approach appears tautological because the residues define the residue numerators. In the end, however, the residue numerators are nothing more than complex numbers $n_r(1, \tau_2, \tau_3, \tau_4, \tau_5, 6) \in \mathbb{C}$ that serve as the numerators for the residues of amplitudes. Since this exercise is only a consistency check, the manner of determining those complex numbers is not important.

CHAPTER 4

Two-loop Super-Yang–Mills Amplitudes

In this chapter, three different two-loop amplitudes are discussed. In Sec. 4.1, is the two-loop four-point amplitude. The two-loop five-point amplitude is in Sec. 4.2. Preliminary work on the two-loop n -point amplitude is in Sec. 4.3

4.1 Two-loop Four-point Super-Yang–Mills Amplitude

The two-loop four-point amplitude is a convenient amplitude for testing and demonstrating new ideas because there are only two diagrams contributing to it, and the numerators of those diagrams are at most a few terms. For that reason, this section contains several constructions of the amplitude, illustrating the various techniques discussed in Ch. 2.

First the d log representation of the amplitude is constructed in Sec. 4.1.1, in line with the discussion in Sec. 2.3.2. Then in Sec. 4.1.2, the d log representation is rewritten in the pure integrand basis, as discussed Sec. 2.3.3. In Sec. 4.1.3, the pure integrand representation of the amplitude is constructed from the pure integrand basis by matching only one homogeneous cut of the amplitude, demonstrating the technique outlined in Sec. 2.4. Finally, in Sec. 4.1.4, there is an example of how the functions in `osdn` listed in Sec. 2.6 are used to constrain the two-loop four-point amplitude by the condition that it vanishes on a specific cut.

These sections contain considerable detail so as to highlight how the various techniques work. Details will be more sparse when more complicated amplitudes are constructed in later chapters.

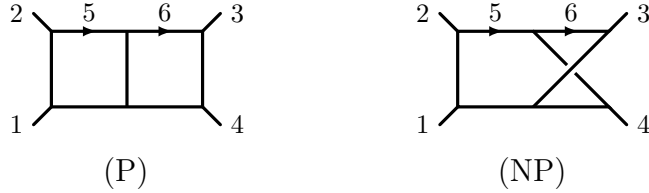


Figure 4.1: The integrals appearing in the two-loop four-point amplitude of SYM theory.

4.1.1 $d\log$ Representation

This section demonstrates how to construct the $d\log$ numerator, starting from an ansatz, as outlined in Sec. 2.3.2. The asymptotic scaling constraint implies that only the planar and nonplanar double box diagrams in Fig. 4.1 appear, since the constraints of Sec. 2.3.2 forbid triangle or bubble subdiagrams. The goal is to construct the numerators $N^{(P)}$ and $N^{(NP)}$ for the planar (Fig. 4.1(P)) and nonplanar (Fig. 4.1(NP)) diagrams respectively.

For the planar diagram, Fig. 4.1(P), only four propagators contain either loop momentum ℓ_5 or ℓ_6 . By the asymptotic scaling constraint, the numerator must be independent of both loop momenta: $N^{(P)} \sim \mathcal{O}((\ell_5)^0, (\ell_6)^0)$. Since overall dimensionality restricts $N^{(P)}$ to be quadratic in momentum, there are two independent numerator basis elements:

$$N_1^{(P)} = s, \quad N_2^{(P)} = t. \quad (4.1)$$

The resulting numerator is then a linear combination of these two basis elements:

$$N^{(P)} = a_1^{(P)}s + a_2^{(P)}t, \quad (4.2)$$

where the $a_j^{(P)}$ are constants, labeled as discussed after Eq. (2.32). There are no hidden double poles or poles at infinity from which nontrivial constraints could arise.

The nonplanar two-loop integrand $\mathcal{I}^{(NP)}$ (Fig. 4.1(NP)) is the first instance where nontrivial constraints result from requiring logarithmic singularities and the absence of poles at infinity. The choice of labels in Fig. 4.1(NP) results in five propagators with momentum ℓ_5 but only four with momentum ℓ_6 , so $N^{(NP)}$ is at most quadratic in ℓ_5 and independent of

ℓ_6 : $N^{(NP)} \sim \mathcal{O}((\ell_5)^2, (\ell_6)^0)$. Overall dimensionality again restricts $N^{(NP)}$ to be quadratic in momentum. This dictates the form of the numerator to be

$$N^{(NP)} = c_1 \ell_5^2 + c_2 (\ell_5 \cdot Q) + c_3 s + c_4 t, \quad (4.3)$$

where Q is some vector and the c_i are coefficients independent of loop momenta.

Now search the integrand

$$\mathcal{I}^{(NP)} = \frac{c_1 \ell_5^2 + c_2 (\ell_5 \cdot Q) + c_3 s + c_4 t}{\ell_5^2 (\ell_5 + k_1)^2 (\ell_5 - k_3 - k_4)^2 \ell_6^2 (\ell_5 + \ell_6)^2 (\ell_5 + \ell_6 - k_4)^2 (\ell_6 + k_3)^2} \quad (4.4)$$

for double poles as well as poles at infinity, and impose conditions on the c_i and Q such that any such poles vanish. For the nonplanar double box, cutting the four propagators carrying momentum ℓ_6 ,

$$\ell_6^2 = (\ell_5 + \ell_6)^2 = (\ell_5 + \ell_6 - k_4)^2 = (\ell_6 + k_3)^2 = 0, \quad (4.5)$$

will eventually yield double poles. To see this, first find the Jacobian for this cut:

$$J_6 = (\ell_5 - k_3)^2 (\ell_5 - k_4)^2 - (\ell_5 - k_3 - k_4)^2 \ell_5^2 = (\ell_5 \cdot q)(\ell_5 \cdot \bar{q}), \quad (4.6)$$

where $q = \lambda_3 \tilde{\lambda}_4$, $\bar{q} = \lambda_4 \tilde{\lambda}_3$.

After imposing the quadruple cut conditions in Eq. (4.5), the remaining integrand, including the Jacobian (4.6), is

$$\text{Res}_{\ell_6\text{-cut}} [\mathcal{I}^{(NP)}] \equiv \tilde{\mathcal{I}}^{(NP)} = \frac{c_1 \ell_5^2 + c_2 (\ell_5 \cdot Q) + c_3 s + c_4 t}{\ell_5^2 (\ell_5 + k_1)^2 (\ell_5 - k_3 - k_4)^2 (\ell_5 \cdot q)(\ell_5 \cdot \bar{q})}, \quad (4.7)$$

where the integrand evaluated on the cut is denoted by a new symbol $\tilde{\mathcal{I}}^{(NP)}$ for brevity.

To make the potentially problematic singularities visible, parametrize the four-dimensional part of the remaining loop momentum as

$$\ell_5 = \alpha \lambda_3 \tilde{\lambda}_3 + \beta \lambda_4 \tilde{\lambda}_4 + \gamma \lambda_3 \tilde{\lambda}_4 + \delta \lambda_4 \tilde{\lambda}_3. \quad (4.8)$$

This gives

$$\begin{aligned}
\tilde{\mathcal{I}}^{(\text{NP})} = & \left(c_1(\alpha\beta - \gamma\delta)s + c_2 [\alpha(Q \cdot k_3) + \beta(Q \cdot k_4) + \gamma\langle 3|Q|4 \rangle + \delta\langle 4|Q|3 \rangle] \right. \\
& \left. + c_3s + c_4t \right) \\
& \times \left[s^2(\alpha\beta - \gamma\delta)(\alpha\beta - \gamma\delta - \alpha - \beta + 1) \right. \\
& \left. \times \left((\alpha\beta - \gamma\delta)s + \alpha u + \beta t - \gamma\langle 13 \rangle[14] - \delta\langle 14 \rangle[13] \right) \gamma\delta \right]^{-1}, \quad (4.9)
\end{aligned}$$

with the convention $2k_i \cdot k_j = \langle ij \rangle [ij]$ and $\langle i|k_m|j \rangle \equiv \langle im \rangle [mj]$. To expose double- or higher-order poles, take residues in a certain order. For example, taking consecutive residues at $\gamma = 0$ and $\delta = 0$ followed by $\beta = 0$ gives

$$\text{Res}_{\substack{\gamma=\delta=0 \\ \beta=0}} \left[\tilde{\mathcal{I}}^{(\text{NP})} \right] = \frac{c_2\alpha(Q \cdot k_3) + c_3s + c_4t}{s^2u\alpha^2(1-\alpha)}. \quad (4.10)$$

Similarly taking consecutive residues first at $\gamma = \delta = 0$ followed by $\beta = 1$:

$$\text{Res}_{\substack{\gamma=\delta=0 \\ \beta=1}} \left[\tilde{\mathcal{I}}^{(\text{NP})} \right] = -\frac{c_1\alpha s + c_2 [\alpha(Q \cdot k_3) + (Q \cdot k_4)] + c_3s + c_4t}{s^2t\alpha(1-\alpha)^2}. \quad (4.11)$$

In both cases there are double poles in α . To eliminate the double poles, choose the c_i in the numerator such that the integrand reduces to at most a single pole in α . Canceling the double pole at $\alpha = 0$ in Eq. (4.10) requires $c_3 = c_4 = 0$. Similarly, the second residue in Eq. (4.11) enforces $c_1s + c_2(Q \cdot (k_3 + k_4)) = 0$ to cancel the double pole at $\alpha = 1$. The solution that ensures $N^{(\text{NP})}$ is a $d \log$ numerator is

$$N^{(\text{NP})} = \frac{c_1}{s} [\ell_5^2(Q \cdot (k_3 + k_4)) - (k_3 + k_4)^2(\ell_5 \cdot Q)]. \quad (4.12)$$

The integrand is now free of the uncovered double poles, but not of poles at infinity. If any of the parameters α , β , γ or δ grow large, the loop momentum ℓ_5 Eq. (4.8) also becomes large. Indeed, such a pole can be accessed by first taking the residue at $\delta = 0$, followed by

taking the residues at $\alpha = 0$ and $\beta = 0$:

$$\operatorname{Res}_{\substack{\delta=0 \\ \alpha=\beta=0}} \left[\tilde{\mathcal{I}}^{(\text{NP})} \right] = \frac{\langle 3|Q|4 \rangle}{\gamma s^2 \langle 13 \rangle [14]}. \quad (4.13)$$

The resulting form $d\gamma/\gamma$ has a pole for $\gamma \rightarrow \infty$. Similarly, taking a residue at $\gamma = 0$, followed by residues at $\alpha = 0$ and $\beta = 0$ results in a single pole for $\delta \rightarrow \infty$. To prevent such poles at infinity from appearing requires $\langle 3|Q|4 \rangle = \langle 4|Q|3 \rangle = 0$, which in turn requires that $Q = \sigma_1 k_3 + \sigma_2 k_4$ with the σ_i arbitrary constants. This is enough to determine the numerator, up to two arbitrary coefficients.

To illustrate a second approach, consider the same cut sequence Eq. (4.5) which is $\{B(\ell_6)\}$ in the notation defined at the end of Sec. 2.1. The resulting Jacobian is again Eq. (4.6). The two terms $(\ell_5 - k_3 - k_4)^2 \ell_5^2$ in the Jacobian already appear as propagators in the integrand. So to avoid double poles, the $d\log$ numerator must scale as $N^{(\text{NP})} \sim (\ell_5 - k_3 - k_4)^2 \ell_5^2$ in the kinematic regions where $(\ell_5 - k_4)^2 (\ell_5 - k_3)^2 = 0$. This constraint is sufficient to fix the ansatz for $N^{(\text{NP})}$, Eq. (4.3).

In both approaches, the constraints of having only logarithmic singularities and no poles at infinity results in a numerator for the nonplanar double box of the form,

$$N^{(\text{NP})} = a_1^{(\text{NP})} (\ell_5 - k_3)^2 + a_2^{(\text{NP})} (\ell_5 - k_4)^2, \quad (4.14)$$

where $a_1^{(\text{NP})}$ and $a_2^{(\text{NP})}$ are rational coefficients.

Imposing that the numerator respects the symmetries of the diagram, $k_3 \leftrightarrow k_4$, forces $a_2^{(\text{NP})} = a_1^{(\text{NP})}$, and results in a unique numerator up to an overall constant

$$N_1^{(\text{NP})} = (\ell_5 - k_3)^2 + (\ell_5 - k_4)^2. \quad (4.15)$$

In Ref. [2], we list explicit integrand forms that are manifestly $d\log$.

The final step is to fix coefficients such that the new $d\log$ representation matches the

amplitude. A simple method for doing so is to use previously constructed representations of the amplitude as reference data, rather than sew together lower-loop amplitudes directly.

A previously constructed representation [97] of the two-loop four-point amplitude is Eqs. (2.26) and (2.32) with numerators

$$N_{\text{old}}^{(\text{P})} = s, \quad N_{\text{old}}^{(\text{NP})} = s. \quad (4.16)$$

Demanding that the numerators are linear combinations of the basis elements constructed in Eqs. (4.2) and (4.14) results in:

$$N^{(\text{P})} = a_1^{(\text{P})} s + a_2^{(\text{P})} t, \quad N^{(\text{NP})} = a^{(\text{NP})} ((\ell_5 - k_3)^2 + (\ell_5 - k_4)^2), \quad (4.17)$$

where, for comparison to $N_{\text{old}}^{(\text{NP})}$, it is useful to rewrite the nonplanar numerator as

$$N^{(\text{NP})} = a^{(\text{NP})} (-s + (\ell_5 - k_3 - k_4)^2 + \ell_5^2). \quad (4.18)$$

The coefficients can be determined by comparing the new and old expressions on the maximal cuts. Replacing all propagators with on-shell conditions, $p_{\alpha(x)}^2 = 0$, defined in Eq. (2.30). The planar double-box numerator is unchanged on the maximal cut, since it is independent of all loop momenta. Comparing the two expressions in Eqs. (4.16) and (4.17) gives

$$a_1^{(\text{P})} = 1, \quad a_2^{(\text{P})} = 0. \quad (4.19)$$

For the nonplanar numerator, note that under the maximal cut conditions $\ell_5^2 = (\ell_5 - k_3 - k_4)^2 = 0$. Comparing the two forms of the nonplanar numerator in Eqs. (4.16) and (4.18) after imposing these conditions means

$$a_1^{(\text{NP})} = -1, \quad (4.20)$$

so that the final numerators are

$$N^{(\text{P})} = s, \quad N^{(\text{NP})} = -((\ell_5 - k_3)^2 + (\ell_5 - k_4)^2). \quad (4.21)$$

Although this fixes all coefficients in the basis, it does not prove that the $d\log$ construction gives the correct sYM amplitude. At two loops this was already proven in Ref. [62], where the difference between amplitudes in the old and the new representation was shown to vanish via the color Jacobi identity. More generally the method of maximal cuts offers a systematic and complete means of ensuring that the constructed amplitudes are correct.

4.1.2 Pure Integrand Representation

Elements of the pure integrands basis are closely related to the $d\log$ integrands of the previous section.

Renaming the $d\log$ numerators

$$\tilde{N}^{(\text{P})} = s, \quad \tilde{N}^{(\text{NP})} = (\ell_5 - k_3)^2 + (\ell_5 - k_4)^2, \quad (4.22)$$

the integrand with numerator $\tilde{N}^{(\text{P})}$ is already a pure integrand. The integrand $d\mathcal{I}^{(\text{NP})}$ with numerator $\tilde{N}^{(\text{NP})}$ has logarithmic singularities and no poles at infinity, but it is not a pure integrand. The leading singularities are not all ± 1 but also contain ratios of the form, $\pm u/t$.

The aim now is to decompose the \tilde{N} numerators so that the resulting integrands $d\mathcal{I}^j$ are pure, and then to express the amplitude in terms of the resulting pure integrand basis. In practice, this is done by retaining in Eq. (2.26) the permutation invariant function $\mathcal{K} = st\text{PT}(1234) = su\text{PT}(1243)$ – defined in Eq. (2.27) – and by requiring each basis integrand to have correct mass dimension — six in this case — and unit leading singularities ± 1 . This results in three basis elements:

$$N^{(\text{P})} = s^2 t, \quad N_1^{(\text{NP})} = su(\ell_5 - k_3)^2, \quad N_2^{(\text{NP})} = st(\ell_5 - k_4)^2. \quad (4.23)$$

The two nonplanar basis integrals are related by the symmetry of the diagram, but to maintain unit leading singularities the terms are treated as distinct. The corresponding pure integrand forms $d\mathcal{I}^{(P)}$, $d\mathcal{I}_1^{(\text{NP})}$, $d\mathcal{I}_2^{(\text{NP})}$ are obtained by including the integration measure and the appropriate propagators that can be read off from Fig. 4.1

Using these basis integrals, the full two-loop four-point amplitude can be written as a linear combination dressed with the appropriate color and Parke-Taylor factors,

$$\mathcal{A}_4^{(2)} = \frac{1}{4} \sum_{\mathcal{S}_4} \left[c_{1234}^{(P)} a^{(P)} \text{PT}(1234) \int d\mathcal{I}^{(P)} \right. \\ \left. + c_{1234}^{(\text{NP})} \left(a_1^{(\text{NP})} \text{PT}(1243) \int d\mathcal{I}_1^{(\text{NP})} + a_2^{(\text{NP})} \text{PT}(1234) \int d\mathcal{I}_2^{(\text{NP})} \right) \right], \quad (4.24)$$

where the sum in \mathcal{S}_4 is over all 24 permutations of the external legs. The overall $1/4$ divides out the symmetry factor for each diagram to remove the over-count from the permutation sum. The planar and nonplanar double-box color factors are

$$c_{1234}^{(P)} = \tilde{f}^{a_1 a_7 a_9} \tilde{f}^{a_2 a_5 a_7} \tilde{f}^{a_5 a_6 a_8} \tilde{f}^{a_9 a_8 a_{10}} \tilde{f}^{a_3 a_{11} a_6} \tilde{f}^{a_4 a_{10} a_{11}}, \\ c_{1234}^{(\text{NP})} = \tilde{f}^{a_1 a_7 a_8} \tilde{f}^{a_2 a_5 a_7} \tilde{f}^{a_5 a_{11} a_6} \tilde{f}^{a_8 a_9 a_{10}} \tilde{f}^{a_3 a_6 a_9} \tilde{f}^{a_4 a_{10} a_{11}}, \quad (4.25)$$

where the $\tilde{f}^{abc} = i\sqrt{2}f^{abc}$ are appropriately normalized color structure constants of $\text{SU}(N)$.

Matching the amplitude on unitarity cuts determines the coefficients to be

$$a^{(P)} = 1, \quad a_1^{(\text{NP})} = -1, \quad a_2^{(\text{NP})} = -1, \quad (4.26)$$

so that the amplitude in Eq. (4.24) is equivalent to the one presented in Eq. (4.21). The trivial difference is that the two pieces $d\mathcal{I}_1^{(\text{NP})}$ and $d\mathcal{I}_2^{(\text{NP})}$ are combined into one numerator in Eq. (4.21).

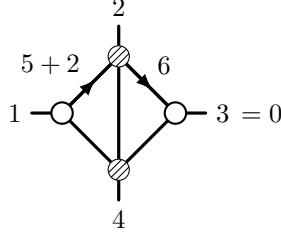


Figure 4.2: The two-loop four-point MHV amplitude vanishes on this cut. The four-point trees in the diagram have $k = 2$, so the overall helicity counting is $k = 1$.

$$\begin{aligned}
\mathcal{A}_4^{(2)} \Big|_{\text{cut}} = & N_{1234}^{(P)} c_{1234}^{(P)} \begin{array}{c} 2 \\ \text{---} \\ 1 \end{array} \begin{array}{c} \text{---} \\ 3 \\ \text{---} \\ 4 \end{array} + N_{4123}^{(P)} c_{4123}^{(P)} \begin{array}{c} 1 \\ \text{---} \\ 4 \end{array} \begin{array}{c} \text{---} \\ 2 \\ \text{---} \\ 3 \end{array} \\
& + N_{1234}^{(\text{NP})} c_{1234}^{(\text{NP})} \begin{array}{c} 2 \\ \text{---} \\ 1 \end{array} \begin{array}{c} \text{---} \\ 3 \\ \text{---} \\ 4 \end{array} + N_{4123}^{(\text{NP})} c_{4123}^{(\text{NP})} \begin{array}{c} 1 \\ \text{---} \\ 4 \end{array} \begin{array}{c} \text{---} \\ 2 \\ \text{---} \\ 3 \end{array} \\
& + N_{3214}^{(\text{NP})} c_{3214}^{(\text{NP})} \begin{array}{c} 2 \\ \text{---} \\ 3 \end{array} \begin{array}{c} \text{---} \\ 1 \\ \text{---} \\ 4 \end{array} + N_{3412}^{(\text{NP})} c_{3412}^{(\text{NP})} \begin{array}{c} 4 \\ \text{---} \\ 3 \end{array} \begin{array}{c} \text{---} \\ 1 \\ \text{---} \\ 2 \end{array} \\
& + N_{4213}^{(\text{NP})} c_{4213}^{(\text{NP})} \begin{array}{c} 2 \\ \text{---} \\ 4 \end{array} \begin{array}{c} \text{---} \\ 1 \\ \text{---} \\ 3 \end{array}
\end{aligned}$$

Figure 4.3: The two-loop four-point amplitude evaluated on the cut of Fig. 4.2. In each diagram the two shaded propagators are uncut, and every other propagator is cut. Eq. (4.33) gives the value of the cut.

4.1.3 Matching Zeros

This section implements the algorithm outlined in Sec. 2.4 of constructing the amplitude by requiring the amplitude to vanish on a cut with nonphysical k -count. In particular, the only required condition to determine the unknown coefficients $a^{(P)}$, $a_1^{(\text{NP})}$, $a_2^{(\text{NP})}$ from Eq. (4.24) is that the amplitude vanish on the cut represented in Fig. 4.2. The following argument holds with minor alterations if both white vertices in Fig. 4.2 are replaced by black vertices.

In the full amplitude, there are contributions from the planar and nonplanar double boxes

in Fig. 4.1 and their permutations of external legs. All permutations of diagrams that contribute to the cut in Fig. 4.2 are shown in Fig. 4.3, along with their numerators and color factors. There are only seven diagrams rather than nine because two of the nine diagrams have triangle subdiagrams, and so have vanishing numerators in sYM.

For the cut in Fig. 4.2, five propagators are on-shell so that the cut solution depends on α , γ , and δ , three unfixed parameters of the loop momenta. Explicitly, the cut solution is

$$\begin{aligned}\ell_5^* + k_2 &= \lambda_1 \left[\alpha \tilde{\lambda}_1 + \frac{1}{\delta \langle 13 \rangle [23]} (\delta t - \alpha(s + \delta u + \gamma \langle 13 \rangle [12])) \tilde{\lambda}_2 \right], \\ \ell_6^* &= \lambda_3 \left[\delta \tilde{\lambda}_3 + \gamma \tilde{\lambda}_2 \right].\end{aligned}\tag{4.27}$$

This solution maps to Fig. 4.2 under the rules outlined in Sec. 2.4.2 to convert a cut solution to an on-shell diagram. On this $k = 1$ cut, the MHV amplitude vanishes for any values of α , γ , δ . By cutting the Jacobian

$$J = \gamma(\delta t - \alpha(s + \delta u + \gamma \langle 13 \rangle [12])),\tag{4.28}$$

the amplitude remains zero, and this condition simplifies. Specifically the amplitude remains zero after localizing $\ell_5 + k_2$ to be collinear with k_1 and localizing ℓ_6 to be collinear with k_3 . This is equivalent to taking further residues of the already-cut integrand at $\gamma = 0$, $\alpha = \delta t / (s + \delta u)$. On this cut, the solution for the loop momenta simplifies,

$$\ell_5^* + k_2 = \frac{\delta t}{s + \delta u} \lambda_1 \tilde{\lambda}_1, \quad \ell_6^* = \delta \lambda_3 \tilde{\lambda}_3,\tag{4.29}$$

with the overall Jacobian $J' = s + u\delta$. Even in this simplified setting with one parameter δ left, the single zero cut condition Fig. 4.2 is sufficient to fix the integrand up to an overall constant.

The pure integrand numerators, using the labels in Fig. 4.1, are listed in Eq. (4.23).

Including labels for the external legs to help track relabelings, these are

$$N_{1234}^{(P,1)} = s^2 t, \quad N_{1234}^{(NP,1)} = su(\ell_5 - k_3)^2, \quad N_{1234}^{(NP,2)} = st(\ell_5 - k_4)^2. \quad (4.30)$$

As noted near Eq. (5.38) there are only two Parke-Taylor factors independent under relations for four-particle scattering, namely $PT_1 = PT(1234)$ and $PT_2 = PT(1243)$. Therefore the numerator ansatz for the planar diagram is

$$N_{1234}^{(P)} = \left(a_{1,1}^{(P)} PT_1 + a_{1,2}^{(P)} PT_2 \right) N_{1234}^{(P,1)}. \quad (4.31)$$

For the nonplanar diagram, there are two pure integrands, each of which gets decorated with the two independent Parke-Taylor factors, so that the ansatz takes the form

$$N_{1234}^{(NP)} = \left[\left(a_{1,1}^{(NP)} PT_1 + a_{1,2}^{(NP)} PT_2 \right) N_{1234}^{(NP,1)} + \left(a_{2,1}^{(NP)} PT_1 + a_{2,2}^{(NP)} PT_2 \right) N_{1234}^{(NP,2)} \right], \quad (4.32)$$

and both numerators are then decorated with corresponding color factors $c_{1234}^{(P)}$, $c_{1234}^{(NP)}$ and propagators. The $a_{i,j}^{(x)}$ coefficients are determined by demanding the integrand vanishes on the cut solution in Eq. (4.29).

Explicitly, the zero condition from the cut corresponding to Fig. 4.3 is:

$$0 = \left(\frac{c_{1234}^{(P)} N_{1234}^{(P)}}{\ell_5^2 (\ell_6 - k_3 - k_4)^2} + \frac{c_{4123}^{(P)} N_{4123}^{(P)}}{(\ell_5 - k_3)^2 (\ell_6 + k_2)^2} + \frac{c_{1234}^{(NP)} N_{1234}^{(NP)}}{\ell_5^2 (\ell_5 - \ell_6 - k_4)^2} + \frac{c_{4123}^{(NP)} N_{4123}^{(NP)}}{(\ell_5 - k_3)^2 (\ell_5 - \ell_6 + k_2)^2} + \frac{c_{3214}^{(NP)} N_{3214}^{(NP)}}{(\ell_6 + k_2)^2 (\ell_5 - \ell_6 - k_4)^2} + \frac{c_{3412}^{(NP)} N_{3412}^{(NP)}}{(\ell_6 - k_3 - k_4)^2 (\ell_5 - \ell_6 + k_2)^2} + \frac{c_{4213}^{(NP)} N_{4213}^{(NP)}}{(\ell_5 - \ell_6 + k_2)^2 (\ell_5 - \ell_6 - k_4)^2} \right) \Big|_{\ell_5^*, \ell_6^*}. \quad (4.33)$$

The sum runs over the seven contributing diagrams, following the order displayed in Fig. 4.3. The denominators are the two propagators that are left uncut in each diagram when per-

forming this cut. One of the terms in the cut equation, for example, is

$$\begin{aligned}
& \frac{c_{3214}^{(\text{NP})} N_{3214}^{(\text{NP})}}{(\ell_6 + k_2)^2 (\ell_5 - \ell_6 - k_4)^2} \\
&= \frac{c_{3214}^{(\text{NP})}}{(\ell_6 + k_2)^2 (\ell_5 - \ell_6 - k_4)^2} \\
& \quad \times \left[\left(a_{1,1}^{(\text{NP})} \text{PT}(3214) + a_{1,2}^{(\text{NP})} \text{PT}(4213) \right) tu (\ell_6 + k_1 + k_2)^2 \right. \\
& \quad \left. + \left(a_{2,1}^{(\text{NP})} \text{PT}(3214) + a_{2,2}^{(\text{NP})} \text{PT}(4213) \right) st (\ell_6 + k_2 + k_4)^2 \right].
\end{aligned} \tag{4.34}$$

This has been relabeled from the master labels of Eq. (4.30) to the labels of the third nonplanar diagram in Fig. 4.3, including the two uncut propagators. Specifically $\ell_5 \mapsto -\ell_6 - k_2$ and $\ell_6 \mapsto -\ell_5 - k_1$ is the relabeling for this diagram. A key simplifying feature is that crossing symmetry requires that the $a_{i,j}^{(x)}$ coefficients do not change under this relabeling; the result is that the same four coefficients contribute to all five of the nonplanar double boxes that appear in the cut. The Parke-Taylor factors that appear in Eq. (4.35) do not necessarily need to be in the chosen basis, although here $\text{PT}(3214) = \text{PT}_1$ and $\text{PT}(4213) = \text{PT}_2$.

The single zero condition Eq. (4.33) determines five of the six $a_{i,j}^{(x)}$ parameters. This is, consistent with the conjecture in Sec. 2.4, the maximum amount of information that can be extracted from all zero conditions. To do so in this example, reduce to the two-member Parke-Taylor basis mentioned before, and also use Jacobi identities to reduce the seven contributing color factors to a basis of four. Since the remaining Parke-Taylor and color factors are independent, setting the coefficients of $\text{PT} \cdot c$ to zero yields eight potentially

independent equations for the six coefficients. It turns out only five are independent:

$$0 = a_{1,2}^{(P)} \tag{4.35}$$

$$0 = a_{1,1}^{(P)} + 3a_{1,1}^{(NP)} + a_{2,1}^{(NP)} \tag{4.36}$$

$$0 = a_{1,1}^{(P)} + a_{1,1}^{(NP)} + a_{2,1}^{(NP)} \tag{4.37}$$

$$0 = a_{1,2}^{(P)} - a_{1,1}^{(NP)} + a_{1,2}^{(NP)} - a_{2,1}^{(NP)} + a_{2,2}^{(NP)} \tag{4.38}$$

$$0 = a_{1,2}^{(P)} + a_{1,1}^{(NP)} + a_{1,2}^{(NP)} - a_{2,1}^{(NP)} + 3a_{2,2}^{(NP)}. \tag{4.39}$$

The solution for this system is

$$a_{1,2}^{(P)} = a_{1,1}^{(NP)} = a_{2,2}^{(NP)} = 0, \quad a_{1,2}^{(NP)} = a_{2,1}^{(NP)} = -a_{1,1}^{(P)}, \tag{4.40}$$

and any of one the three $a_{1,2}^{(NP)}$, $a_{2,1}^{(NP)}$, or $a_{1,1}^{(P)}$ is the overall undetermined parameter. This matches the result in Eq. (4.26), if $a_{1,1}^{(P)} = 1$. This last condition is exactly the overall scale that the zero conditions cannot determine.

4.1.4 Example Using `osdn`

The purpose of this section is to illustrate how the code `osdn` outlined in Sec. 2.6 can be used to constrain the two-loop four-point amplitude on exactly one vanishing cut. The computation largely mirrors the previous section with some slight variation for illustrative purposes.

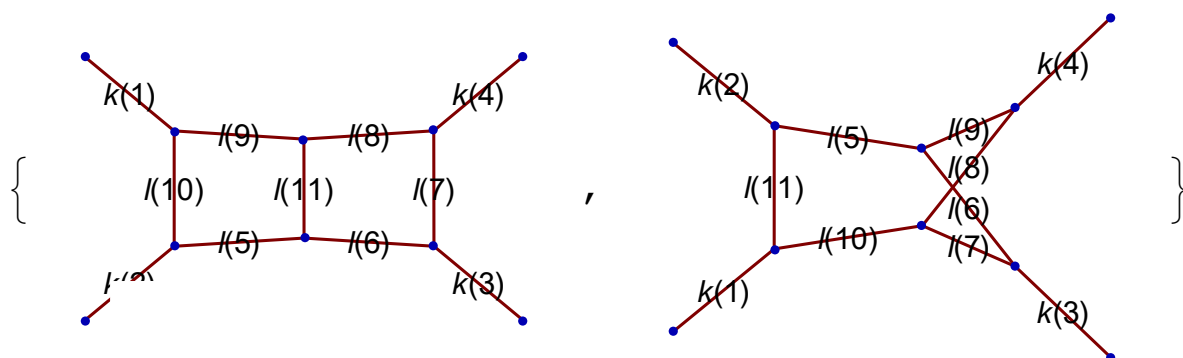
All built-in Mathematica functions start with a capital letter (`Expand`, `Simplify`, etc...), while all `osdn` functions and variables start with a lower case letter (`diag`, `constructCut`, etc...).

The two-loop four-point graphs are input as a list of trivalent vertices. The loop momentum flows from the positive to the negative vertex. The external momenta are single integers. Using these conventions, the graphs are:

Input:

```
diag[1] =  
  {  
    {-1}, {-2}, {-3}, {-4},  
    {2, 5, -10}, {6, 11, -5}, {3, 7, -6},  
    {4, 8, -7}, {9, -11, -8}, {1, 10, -9}  
  };  
diag[2] =  
  {  
    {-1}, {-2}, {-3}, {-4},  
    {2, 5, -11}, {6, -9, -5},  
    {3, 7, -6}, {10, 8, -7},  
    {4, 9, -8}, {1, 11, -10}  
  };  
allDiags = diag /@ {1, 2};  
displayGraph /@ allDiags
```

Output:



In the subsequent examples, there will be sample outputs of numerical values. These

values are generated from pseudo-random external kinematic values. The most complete implementation of external kinematics in `osdn` assigns random rational numbers to some components of the external momenta, then imposes massless conditions and momentum conservation to determine the remaining components. As an example:

Input:

```
loadKinematics[4, 1];  
kValues // N // TableForm
```

Output:

```
{  
k[1, 0] -> 3.41656 + 2.33902 I,  
k[1, 1] -> 1.64 + 0.07 I,  
k[1, 2] -> -2.02 - 1.37 I,  
k[1, 3] -> 2.41 + 2.12 I,  
k[2, 0] -> 3.81267 + 2.921 I,  
k[2, 1] -> -2.8 + 2.59 I,  
k[2, 2] -> -3.68 + 4.73 I,  
k[2, 3] -> 6.58 + 5.44 I,  
k[3, 0] -> 11.0317 - 1.37034 I,  
k[3, 1] -> 3.14 + 3.33 I,  
k[3, 2] -> 5.55 + 5.34 I,  
k[3, 3] -> 11.8517 - 4.65843 I  
}
```

where the three-digit precision numbers are rational, and the six-digit precision numbers are truncated from 200-digit-precision for legibility in the output. The `loadKinematics` function takes the number of external particles as its first argument, and the pseudo-random number seed as its second; it stores the components of momentum in `kValues` which can

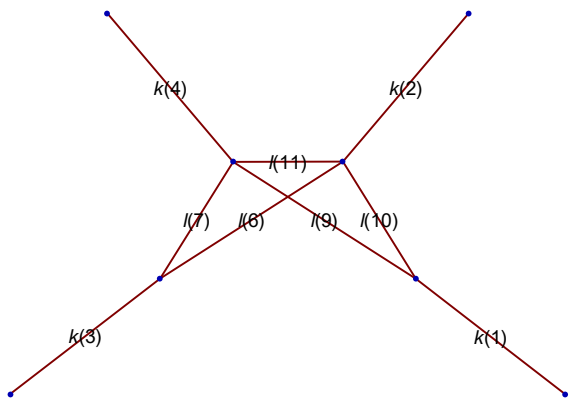
then convert an expression that is a function of the components of momenta into a numerical expression. For this numerical implementation, momentum conservation is done analytically so only the components up to k_3 are necessary in `kValues`.

Turning now to computing a cut of the amplitude, the first step is to define the desired cut:

Input:

```
cg = collapsePropagators[allDiags[[1]], {5, 8}];
displayGraph[cg]
```

Output:



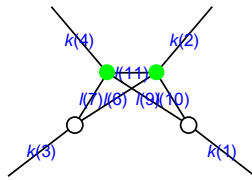
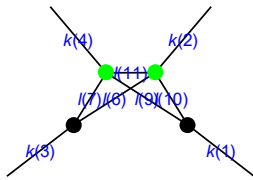
This takes the original planar double box, and collapses propagators 5 and 8 of that graph; the topology is exactly Fig. 4.2.

In the syntax of `osdn`, such graphs encode cuts. Graphs that go into cut functions have the interpretation that all visible propagators are on-shell. In this example, `cg` represents a next-to-next-to-max cut, since all but two propagators are on-shell. With this graphical definition of the cut, it is quick and painless to numerically solve cut equations corresponding to the above graph, thereby generating all on-shell diagrams:

Input:

```
loadKinematics[4, 1]
osdtab = osdSolutionTable[cg, cutSols[cg, 1]];
(* Output 1 *)
osdtab[[{1}]] /. {(1[a_] -> n_) :> 1[a] -> N[n]} // TableForm
(* Output 2 *)
osdtab[[{2}]] /. {(1[a_] -> n_) :> 1[a] -> N[n]} // TableForm
```

Output 1:



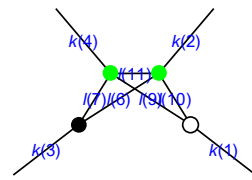
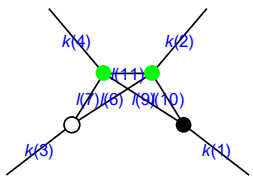
$$\begin{matrix} 3 & 1 \\ 7 & 10 \\ -6 & -9 \end{matrix}$$

1[6, 0]	→ 9.28552 - 8.2417 i
1[6, 1]	→ 19.8743 - 1.73231 i
1[6, 2]	→ 4.8 - 18.21 i
1[6, 3]	→ -4.82 - 9.4 i
1[9, 0]	→ 18.1219 - 24.1842 i
1[9, 1]	→ 30.1508 - 107.162 i
1[9, 2]	→ -99.6763 - 29.9837 i
1[9, 3]	→ -36.21 + 5.41 i

$$\begin{matrix} 3 & 1 \\ 7 & 10 \\ -6 & -9 \end{matrix}$$

1[6, 0]	→ 2.03694 - 17.4565 i
1[6, 1]	→ -8.58447 - 0.762101 i
1[6, 2]	→ 4.8 - 18.21 i
1[6, 3]	→ -4.82 - 9.4 i
1[9, 0]	→ 1.04088 - 2.1587 i
1[9, 1]	→ 17.9562 + 41.6482 i
1[9, 2]	→ -24.9227 + 22.2365 i
1[9, 3]	→ -36.21 + 5.41 i

Output 2:



$$\begin{matrix} 3 \\ 7 \\ -6 \\ 1 \\ 10 \\ -9 \end{matrix}$$

1[6, 0]	→ 2.03694 - 17.4565 i
1[6, 1]	→ -8.58447 - 0.762101 i
1[6, 2]	→ 4.8 - 18.21 i
1[6, 3]	→ -4.82 - 9.4 i
1[9, 0]	→ -27.6281 + 1.38585 i
1[9, 1]	→ -1.59865 - 21.357 i
1[9, 2]	→ -9.71865 - 12.704 i
1[9, 3]	→ -36.21 + 5.41 i

$$\begin{matrix} 1 \\ 10 \\ -9 \\ 3 \\ 7 \\ -6 \end{matrix}$$

1[6, 0]	→ 5.42262 - 34.3212 i
1[6, 1]	→ 1.19213 - 24.4841 i
1[6, 2]	→ -2.80943 + 3.11726 i
1[6, 3]	→ 6.12 - 24.21 i
1[9, 0]	→ -20.2529 + 20.5593 i
1[9, 1]	→ -7.76915 + 35.7108 i
1[9, 2]	→ -5.45 - 10.45 i
1[9, 3]	→ -36.21 + 5.41 i

In the preceding **Input**, the function `cutSols` numerically solves the cut equations implied by `cg`. The function `osdSolutionTable` takes the cut graph and numerical solutions, and constructs a list of the form

$$\{\dots, \{\{g1, wbList1, sol1\}, \{g2, wbList2, sol2\}\}, \dots\}.$$

In this list, `g1` and `g2` are complementary¹ colored graphs, the `wbList`'s are the list of white and black vertices in corresponding graphs, and the `sol`'s are the numerical values of the loop momenta. In the on-shell diagrams, the green-colored vertices indicate valency $v > 3$.

If some components of the loop momenta are unconstrained by the cut equations, then those components are set to random rational values to improve the speed of the numerical solver. Some components of the momenta are unconstrained here because there are only five constraints for the eight components of momentum. Thus the components ℓ_6^3 , ℓ_9^2 , and ℓ_9^3 are random rational numbers – a fact apparent in the preceding **Outputs**. The other values for the components of the of loop momenta are calculated by solving the cut equations and using the previous-displayed external kinematics from `loadKinematics[4,1]`.

Confirming that the numerical cut solutions generate the on-shell diagram matching Fig. 4.2 is a good first step before attempting to solve cut equations analytically.

The solution in Eq. (4.29) is input as

¹Complementary here means the black and white vertices are exchanged.

Input:

```

ClearAll[lSol];
lSol[5, u[a1_], u[a2_]] :=
  opExp[5, a1,
    a2, {{1, 1}, {2, 2}, {1, 2}, {2, 1}}, {(
      s[k[1], k[2]] - s[k[1], k[2]] \[Delta][]) / (
      s[k[1], k[2]] + s[k[1], k[3]] \[Delta][]) - 1, -1, 0, 0}];
lSol[6, u[a1_], u[a2_]] :=
  opExp[6, a1,
    a2, {{3, 3}, {4, 4}, {3, 4}, {4, 3}}, {\[Delta][], 0, 0, 0}];
lSolProps;
allASols := Join[aSols[5], aSols[6]];
{lSol[5, u, u], lSol[6, u, u]} //. allASols // spAlg // niceP

```

Output:

$$\begin{aligned}
& - | 1 \rangle [1 | - | 2 \rangle [2 | + \frac{| 1 \rangle [1 | s_{1,2}}{s_{1,2} + \delta s_{1,3}} - \frac{\delta | 1 \rangle [1 | s_{1,2}}{s_{1,2} + \delta s_{1,3}} \\
& \delta | 3 \rangle [3 |
\end{aligned}$$

where the two momenta are “nicely printed”. The symbol `\[Delta][[]]` is Mathematica syntax for the free parameter δ , and the empty square brackets are required so certain functions correctly recognize the parameter. The `opExp` is an outer-product expansion of the loop momenta in terms of external kinematics with specified coefficients.

A first check that this solution is correct is to confirm that the literature value for the amplitude, Eq. (4.16) indeed vanishes at this kinematic point.

The canonical numerators with the \mathcal{K} factor of Eq. (2.27) restored are

Input:

```

factor = s[k[1], k[2]] s[k[2], k[3]] (ptb[1] //. ptbe //. ptu);
nOld[1] = factor*s[k[1], k[2]];
nOld[2] = factor*s[k[1], k[2]];
nOld[i_] := 0 /; i > 2;
{nOld[1], nOld[2]} //. ptu // niceP

```

Output:

$$\frac{s_{1,2}^2 s_{2,3}}{\langle 1 | 2 \rangle \langle 2 | 3 \rangle \langle 3 | 4 \rangle \langle 4 | 1 \rangle}$$

$$\frac{s_{1,2}^2 s_{2,3}}{\langle 1 | 2 \rangle \langle 2 | 3 \rangle \langle 3 | 4 \rangle \langle 4 | 1 \rangle}$$

where `ptb[1]` is PT(1234) and where the `ptbe` and `ptu` commands handle logistics of the Parke-Taylor factors.

The cut of the amplitude can be constructed either analytically or numerically; since there is an analytic analysis in the previous section, here it is done numerically. To actually compute the cut from `cg`:

Input:

```

loadKinematics[4, 1]
cut = (constructCut[cg, allDiags, nOld] /. momConsGraph[diag[1]]);
cut = cut // spc // spAs // colorElim;
tn[cut //. ptu] // Together

```

Output:

0

The first line loads pseudo-random external kinematics at four-points (the first argument) and with random seed one (the second argument).

The `constructCut` function in line two does most of the work in all calculations. The function determines all graphs that contribute on the cut represented by `cg`. It first blows up all graphs with vertices of valency $v > 3$ into trivalent graphs, then keeps only those graphs isomorphic to graphs in the set of `allDiags`, and then relabels the numerators `nOld` into the labels of the cut. The result is that `cut` is exactly Eq. (4.33) where the $N^{(x)}$'s are the old values of the numerators. The replacement at the end of line three `momConsGraph[diag[1]]` ensures the loop momenta appearing in the expression are ℓ_5 and ℓ_6 , so that this expression can be evaluated with the spinor expressions defined by `lSol[5,u,u]` and `lSol[6,u,u]`.

In the third line, `spc` applies algebraic identities to `cut`, `spAs` substitutes in the loop momenta defined by the `lSol[_]`'s, and `colorElim` reduces `cut` to an independent color basis.

In the last line, `tn` converts the analytic expression to a numerical expression using the pseudo-random external kinematics already loaded. Since `cut` is a rational function of δ , to see it vanish requires going to a common denominator using `Together`.

To compute the cut with the new numerator, the process is nearly identical. The main difference is in defining the ansatz:

Input:

```
ClearAll[nAnsatz];
nAnsatz[1, 1] = s[k[1], k[2]]^2 s[k[2], k[3]];
nAnsatz[1] =
  a[1, 1] pt[u[k /@ {1, 2, 3, 4}]] nAnsatz[1, 1] +
  a[1, 2] pt[u[k /@ {1, 2, 4, 3}]] nAnsatz[1, 1];
nAnsatz[2, 1] = s[k[1], k[2]] s[k[1], k[3]] sq[l[5] - k[3]];
nAnsatz[2, 2] = s[k[1], k[2]] s[k[2], k[3]] sq[l[5] - k[4]];
nAnsatz[2] =
  a[2, 1, 1] pt[u[k /@ {1, 2, 3, 4}]] nAnsatz[2, 1] +
  a[2, 1, 2] pt[u[k /@ {1, 2, 4, 3}]] nAnsatz[2, 1] +
  a[2, 2, 1] pt[u[k /@ {1, 2, 3, 4}]] nAnsatz[2, 2] +
  a[2, 2, 2] pt[u[k /@ {1, 2, 4, 3}]] nAnsatz[2, 2];
(* Output 1 *)
nAnsatz[1] //. ptu // niceP
(* Output 2 *)
(List@@nAnsatz[2]) //. ptu // niceP
```

Output 1:

$$\frac{a_{1,1} s_{1,2}^2 s_{2,3}}{\langle 1 | 2 \rangle \langle 2 | 3 \rangle \langle 3 | 4 \rangle \langle 4 | 1 \rangle} + \frac{a_{1,2} s_{1,2}^2 s_{2,3}}{\langle 1 | 2 \rangle \langle 2 | 4 \rangle \langle 3 | 1 \rangle \langle 4 | 3 \rangle}$$

Output 2:

$$\frac{(-k_3+l_5)^2 s_{1,2} s_{1,3} a_{2,1,1}}{\langle 1 | 2 \rangle \langle 2 | 3 \rangle \langle 3 | 4 \rangle \langle 4 | 1 \rangle}$$
$$\frac{(-k_3+l_5)^2 s_{1,2} s_{1,3} a_{2,1,2}}{\langle 1 | 2 \rangle \langle 2 | 4 \rangle \langle 3 | 1 \rangle \langle 4 | 3 \rangle}$$
$$\frac{(-k_4+l_5)^2 s_{1,2} s_{2,3} a_{2,2,1}}{\langle 1 | 2 \rangle \langle 2 | 3 \rangle \langle 3 | 4 \rangle \langle 4 | 1 \rangle}$$
$$\frac{(-k_4+l_5)^2 s_{1,2} s_{2,3} a_{2,2,2}}{\langle 1 | 2 \rangle \langle 2 | 4 \rangle \langle 3 | 1 \rangle \langle 4 | 3 \rangle}$$

where the lines are summed in **Output 2**².

Now `constructCut` can construct the pure integrand amplitude ansatz on the cut in terms of all external momenta:

Input:

```
cut = (
constructCut[cg, allDiags, nAnsatz] /.
momConsGraph[diag[1]]
);
jac = s + u \[Delta] [];
cut = cut / jac;
cut = cut // spc // spAs // colorElim;
(List@@cut)//niceP
```

Output:

$$\begin{aligned}
& - \frac{c[3] (a_{1,1} \text{PT}_{1,2,3,4} + a_{1,2} \text{PT}_{1,2,4,3})}{(-1+\delta) \delta} \\
& - \frac{s (2 c[1] - c[2] + c[3]) (a_{1,2} \text{PT}_{1,4,2,3} + a_{1,1} \text{PT}_{1,4,3,2})}{\delta (s+(t+u) \delta)} \\
& \frac{(c[1] - c[2]) ((a_{2,1,1} + a_{2,2,1}) \text{PT}_{3,4,1,2} + (a_{2,1,2} + a_{2,2,2}) \text{PT}_{3,4,2,1})}{(-1+\delta) \delta} \\
& - \frac{u (-1+\delta) c[1] ((a_{2,1,1} + a_{2,2,1}) \text{PT}_{2,3,1,4} + (a_{2,1,2} + a_{2,2,2}) \text{PT}_{2,3,4,1})}{\delta (s+t-u (-2+\delta) \delta)} \\
& \frac{c[1] ((a_{2,1,1} + a_{2,2,1}) \text{PT}_{1,4,2,3} + (a_{2,1,2} + a_{2,2,2}) \text{PT}_{1,4,3,2})}{(-1+\delta) \delta} \\
& - \frac{u (-1+\delta) (c[1] - c[2]) ((a_{2,1,1} + a_{2,2,1}) \text{PT}_{1,2,3,4} + (a_{2,1,2} + a_{2,2,2}) \text{PT}_{1,2,4,3})}{\delta (s+t-u (-2+\delta) \delta)} \\
& - \frac{u (-1+\delta) c[2] ((a_{2,1,1} - a_{2,2,1}) \text{PT}_{2,4,1,3} + (a_{2,1,2} - a_{2,2,2}) \text{PT}_{2,4,3,1})}{\delta (s+t-u (-2+\delta) \delta)}
\end{aligned}$$

The `constructCut` function was discussed above. Again the sum is split onto multiple lines to make the expression fit on the page. The Jacobian `jac` is put in by hand, but all it does is cancel a factor to make the expression smaller. The `c[_]`'s are the independent color factors.

²The sum in `nAnsatz[2]` is split into multiple lines for printing purposes.

This expression has to vanish. Here `osdn` could analytically set the coefficients of all basis elements to zero, which is how Sec. 4.1.3 was originally generated. Alternatively, the expression can be evaluated multiple times for different random external kinematic points. Proceeding in this way:

Input:

```
equations =
  ParallelTable[
    loadKinematics[4, ri];
    Expand[Numerator[Together[tn[cut /. ptu]]]]
  ,
  {ri, 1, 12}
  ];
equations[[1]] // N
```

Output:

```
(-0.000222088 - 0.000461302 I) a[1, 1] c[1]
+(0.000245818 + 0.000114917 I) a[1, 2] c[1]
+<<48>>
+(-0.000672096 + 0.000716818 I) a[2, 2, 2] c[2] \[Delta][]^3
+(-0.000335076 + 8.28822*10^-6 I) a[1, 2] c[3] \[Delta][]^3
```

The variable `equations` is a list of length 12 – one entry per random seed `ri`. The **Output** shows one of the entries of `equations`, and is truncated to show only four of the 52 total terms, indicated by the “+<<48>>”. The working precision is 200 digits and so the `N` function rounds the **Output** to a legible number of digits. The cut is now a function of the parameters of the ansatz, the color factors, and the single uncut parameter δ . Relations between the parameters are determined by setting the coefficients of the `c[_]`’s and powers of δ to zero:

Input:

```
(* Rename delta for syntax reasons *)
equations = equations /. {\[Delta][_] -> \[Delta][0]};
solution = (coeffEqns[equations, {c, \[Delta]}] == 0);
solution = solution // Solve // Chop // Rationalize // Flatten;
solution // TableForm
```

Output:

```
{
a[1, 2] -> 0,
a[2, 1, 1] -> 0,
a[2, 1, 2] -> -a[1, 1],
a[2, 2, 1] -> -a[1, 1],
a[2, 2, 2] -> 0
}
```

The `coeffEqns` command reads the coefficients of the `c[_]`'s and δ 's. Solving the system requires the `Chop` and `Rationalize` operations to convert the 200-digit precision numbers to integers. This of course matches the solution Eq. (4.40).

It is worth reiterating: the `osdn` package does much more than illustrated here. I used these functions to generate or check everything appearing in our publications and in this dissertation. This section was meant to be a small illustration of what the functions of `osdn` can do.

4.2 Two-loop Five-point Super-Yang–Mills Amplitude

In this section, the two-loop five-point amplitude is written in the pure integrand basis. For an overview of the pure integrand basis, see Sec. 2.3.3. This section will be sparse on details, but the method is similar to the much more detailed Sec. 4.1.2.

The integrand for the two-loop five-point amplitude was first obtained in Ref. [67] in a format that makes the duality between color and kinematics manifest. With respect to that representation, the pure integrand representation has the additional feature that it is manifestly free of spurious poles in external kinematics.

Construction of the pure integrand basis starts from a general sYM power counting of loop momenta as in Sec. 2.3.2. For the pure integrand basis, the overall mass dimension of $d\mathcal{I}_j$ is zero, since there is no \mathcal{K} (Eq. (2.27)) factored out. The basis elements are split according to diagram topologies; trivalent diagrams are termed parent diagrams; diagrams with valency ($v > 3$) vertices are called contact terms. The numerators of each pure integrand are given in Tab. 4.1.

In Tab. 4.1 there is a relabeling notation $N|_{i \leftrightarrow j}^{(a)}$: “redraw the graph associated with numerator N with the indicated exchanges of external momenta i, j and also relabel loop momenta accordingly.” As a simple example,

$$N_2^{(a)} = N_1^{(a)} \Big|_{\substack{1 \leftrightarrow 2 \\ 4 \leftrightarrow 5}} \quad (4.41)$$

requires the relabelings:

$$k_1 \leftrightarrow k_2, \quad k_4 \leftrightarrow k_5, \quad \ell_6 \leftrightarrow \ell_6 - k_1 - k_2, \quad \ell_7 \leftrightarrow \ell_7 - k_4 - k_5. \quad (4.42)$$

For this amplitude, there is an additional pure integrand listed in Tab. 4.2. This integrand is not a basis element because it is linearly dependent on two other basis elements: $N_1^{(h)} - N_2^{(h)} + N_1^{(j)}(\ell_6 - k_1)^2 = 0$. It is a choice to take $N_1^{(h)}$ and $N_2^{(h)}$ as the linearly independent pure integrands, and $N_1^{(j)}$ may be interesting in future studies.

It is useful here to use spinor helicity variables associated with external momenta. Specifically, several of the expressions in Tab. 4.1 have the structure $(\ell + \alpha\lambda_i\tilde{\lambda}_j)^2$, where α is such that both mass dimension and little group weights are consistent. For example, the penta-box numerator

$$N_1^{(b)} \sim \left(\ell_6 + \frac{Q_{45} \cdot \tilde{\lambda}_3 \tilde{\lambda}_1}{[13]} \right)^2 = (\ell_6 - \ell_6^*)^2, \quad (4.43)$$

is a “chiral” numerator that manifestly vanishes on the $\overline{\text{MHV}}$ solution $\ell_6 = \ell_6^*$ [98]. The notation is $Q_{ij} = k_i + k_j$.

The amplitude is assembled from the basis numerators as

$$\mathcal{A}_5^{(2)} = \sum_{\mathcal{S}_5} \sum_x \frac{1}{S_x} \int d^4\ell_6 d^4\ell_7 \frac{\mathcal{N}^{(x)}}{\prod_{\alpha_x} p_{\alpha_x}^2}, \quad (4.44)$$

where the sum over x runs over all diagrams in the basis listed in Tab. 4.1, the sum over \mathcal{S}_5 is a sum over all 120 permutations of the external legs, and S_x is the symmetry factor of diagram x . The product over α_x indicates the product of Feynman propagators $p_{\alpha_x}^2$ of diagram x , as read from the graphs in Tab. 4.1.

The following set of independent five-point Parke-Taylor factors are chosen as the Parke-Taylor basis

$$\begin{aligned} \text{PT}_1 &= \text{PT}(12345), & \text{PT}_2 &= \text{PT}(12354), & \text{PT}_3 &= \text{PT}(12453), \\ \text{PT}_4 &= \text{PT}(12534), & \text{PT}_5 &= \text{PT}(13425), & \text{PT}_6 &= \text{PT}(15423). \end{aligned} \quad (4.45)$$

The basis elements $\overline{N}^{(x)}$ in Tab. 4.3 do not contribute to the MHV amplitude so those data are omitted from the $\mathfrak{a}_{\nu\sigma}^{(x)}$.

There is additional information about how to use Tab. 4.3 and 4.1 in the discussion of the three-loop four-point pure integrand representation in Sec. 5.2. Though the specifics there are different, the mechanics are the same.

Finally, paralleling the discussion of the two-loop four-point amplitude in Sec. 4.1.3, the two-loop five-point pure integrand amplitude can be correctly constrained up to an overall

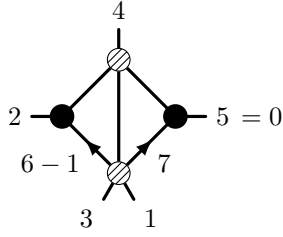


Figure 4.4: The two-loop five-point MHV amplitude vanishes on this cut. The five-point tree at the bottom of the diagram has $k = 2$ or $k = 3$, so the overall helicity counting is $k = 3$ or $k = 4$.

coefficient by matching one cut where the amplitude must vanish. I did this for Ref. [3] using the software discussed in Sec. 2.6 and using the cut in Fig. 4.4.

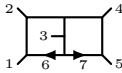

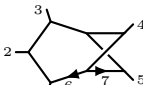
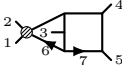
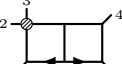
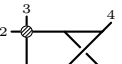
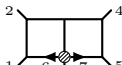

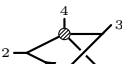
Diagram	Numerators
(a) 	$N_1^{(a)} = \langle 13 \rangle \langle 24 \rangle \left[[24][13] \left(\ell_7 + \frac{[45]}{[24]} \lambda_5 \tilde{\lambda}_2 \right)^2 \left(\ell_6 - \frac{Q_{12} \cdot \tilde{\lambda}_3 \tilde{\lambda}_1}{[13]} \right)^2 - [14][23] \left(\ell_7 + \frac{[45]}{[14]} \lambda_5 \tilde{\lambda}_1 \right)^2 \left(\ell_6 - \frac{Q_{12} \cdot \tilde{\lambda}_3 \tilde{\lambda}_2}{[23]} \right)^2 \right],$ $N_2^{(a)} = N_1^{(a)} \Big _{\substack{1 \leftrightarrow 2 \\ 4 \leftrightarrow 5}}, \quad N_3^{(a)} = N_1^{(a)} \Big _{\substack{2 \leftrightarrow 4 \\ 1 \leftrightarrow 5}}, \quad N_4^{(a)} = N_1^{(a)} \Big _{\substack{1 \leftrightarrow 4 \\ 2 \leftrightarrow 5}},$ $N_5^{(a)} = \overline{N}_1^{(a)}, \quad N_6^{(a)} = \overline{N}_2^{(a)}, \quad N_7^{(a)} = \overline{N}_3^{(a)}, \quad N_8^{(a)} = \overline{N}_4^{(a)},$
(b) 	$N_1^{(b)} = \langle 15 \rangle [45] \langle 43 \rangle s_{45} [13] \left(\ell_6 + \frac{Q_{45} \cdot \tilde{\lambda}_3 \tilde{\lambda}_1}{[13]} \right)^2,$ $N_2^{(b)} = \overline{N}_1^{(b)},$
(c) 	$N_1^{(c)} = [13] \left(\ell_6 + \frac{Q_{45} \cdot \tilde{\lambda}_3 \tilde{\lambda}_1}{[13]} \right)^2 \langle 15 \rangle [54] \langle 43 \rangle (\ell_6 + k_4)^2,$ $N_2^{(c)} = N_1^{(c)} \Big _{4 \leftrightarrow 5}, \quad N_3^{(c)} = \overline{N}_1^{(c)}, \quad N_4^{(c)} = \overline{N}_2^{(c)},$
(d) 	$N_1^{(d)} = s_{34} (s_{34} + s_{35}) \left(\ell_7 - k_5 + \frac{\langle 35 \rangle}{\langle 34 \rangle} \lambda_4 \tilde{\lambda}_5 \right)^2,$ $N_2^{(d)} = N_1^{(d)} \Big _{4 \leftrightarrow 5}, \quad N_3^{(d)} = \overline{N}_1^{(d)}, \quad N_4^{(d)} = \overline{N}_2^{(d)},$
(e) 	$N_1^{(e)} = s_{15} s_{45}^2,$
(f) 	$N_1^{(f)} = s_{14} s_{45} (\ell_6 + k_5)^2, \quad N_2^{(f)} = N_1^{(f)} \Big _{4 \leftrightarrow 5},$
(g) 	$N_1^{(g)} = s_{12} s_{45} s_{24},$
(h) 	$N_1^{(h)} = \langle 15 \rangle [35] \langle 23 \rangle [12] \left(\ell_6 - \frac{\langle 12 \rangle}{\langle 32 \rangle} \lambda_3 \tilde{\lambda}_1 \right)^2, \quad N_2^{(h)} = N_1^{(h)} \Big _{3 \leftrightarrow 5},$ $N_3^{(h)} = s_{12} \langle 13 \rangle [15] \langle 5 \ell_6 3 \rangle, \quad N_4^{(h)} = s_{12} [13] \langle 15 \rangle \langle 3 \ell_6 5 \rangle,$ $N_5^{(h)} = \overline{N}_1^{(h)}, \quad N_6^{(h)} = \overline{N}_2^{(h)},$
(i) 	$N_1^{(i)} = \langle 2 4 3 \rangle \langle 3 5 2 \rangle - \langle 3 4 2 \rangle \langle 2 5 3 \rangle.$

Table 4.1: The parent diagram numerators that give pure integrands for the two-loop five-point amplitude. Each basis diagram is consistent with requiring logarithmic singularities and no poles at infinity. Hatched dots indicate contact terms. The overline notation means $[\cdot] \leftrightarrow \langle \cdot \rangle$.

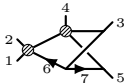
Diagram	Numerators
(j) 	$N_1^{(j)} = s_{12}s_{35} = (N_2^{(h)} - N_1^{(h)})/(\ell_6 - k_1)^2,$

Table 4.2: A diagram and numerator that gives a pure integrand. However, as indicated in the table and explained in the text, it is not a an independent basis element. Hatched dots indicate contact terms.

Color Dressed Numerators	PT Matrices
$\mathcal{N}^{(a)} = c_{12345}^{(a)} \sum_{\substack{1 \leq \nu \leq 4 \\ 1 \leq \sigma \leq 6}} N_\nu^{(a)} a_{\nu\sigma}^{(a)} \text{PT}_\sigma,$	$a_{\nu\sigma}^{(a)} = \frac{1}{4} \begin{pmatrix} -1 & 0 & 1 & 0 & 0 & 2 \\ 1 & 0 & -1 & 0 & 0 & 2 \\ -3 & 0 & -1 & 0 & 0 & 2 \\ -1 & 0 & -3 & 0 & 0 & 2 \end{pmatrix},$
$\mathcal{N}^{(b)} = c_{12345}^{(b)} \sum_{1 \leq \sigma \leq 6} N_1^{(b)} a_{1\sigma}^{(b)} \text{PT}_\sigma,$	$a_{1\nu}^{(b)} = (-1 \ 0 \ 0 \ 0 \ 0 \ 0),$
$\mathcal{N}^{(c)} = c_{12345}^{(c)} \sum_{\substack{1 \leq \nu \leq 2 \\ 1 \leq \sigma \leq 6}} N_\nu^{(c)} a_{\nu\sigma}^{(c)} \text{PT}_\sigma,$	$a_{\nu\sigma}^{(c)} = \begin{pmatrix} -1 & 0 & 0 & 0 & 0 & 0 \\ 0 & -1 & 0 & 0 & 0 & 0 \end{pmatrix},$
$\mathcal{N}^{(d)} = \mathcal{N}^{(e)} = \mathcal{N}^{(f)} = 0,$	
$\mathcal{N}^{(g)} = c_{12345}^{(a)} \sum_{1 \leq \sigma \leq 6} N_1^{(g)} a_{1\sigma, (12345)}^{(g)} \text{PT}_\sigma$ $+ c_{31245}^{(b)} \sum_{1 \leq \sigma \leq 6} N_1^{(g)} a_{1\sigma, (31245)}^{(g)} \text{PT}_\sigma,$	$a_{1\sigma, (12345)}^{(g)} = \frac{1}{4} (1 \ 0 \ 3 \ 0 \ 0 \ -2),$ $a_{1\sigma, (31245)}^{(g)} = (0 \ 0 \ -1 \ 0 \ 0 \ 0),$
$\mathcal{N}^{(h)} = c_{12345}^{(a)} \sum_{\substack{1 \leq \nu \leq 4 \\ 1 \leq \sigma \leq 6}} N_\nu^{(h)} a_{\nu\sigma, (12345)}^{(h)} \text{PT}_\sigma$ $+ c_{12543}^{(a)} \sum_{\substack{1 \leq \nu \leq 4 \\ 1 \leq \sigma \leq 6}} N_\nu^{(h)} a_{\nu\sigma, (12543)}^{(h)} \text{PT}_\sigma,$	$a_{\nu\sigma, (12345)}^{(h)} = \frac{1}{4} \begin{pmatrix} 4 & 0 & 4 & 0 & 0 & -4 \\ 2 & 0 & 3 & 0 & 1 & -2 \\ -2 & 0 & -3 & 0 & -1 & 2 \\ 4 & 0 & 4 & 0 & 0 & -4 \end{pmatrix},$ $a_{\nu\sigma, (12543)}^{(h)} = a_{\nu\sigma, (12345)}^{(h)},$
$\mathcal{N}^{(i)} = c_{12345}^{(a)} \sum_{1 \leq \sigma \leq 6} N_1^{(i)} a_{1\sigma, (12345)}^{(i)} \text{PT}_\sigma$ $+ c_{13245}^{(a)} \sum_{1 \leq \sigma \leq 6} N_1^{(i)} a_{1\sigma, (13245)}^{(i)} \text{PT}_\sigma$ $+ c_{12543}^{(a)} \sum_{1 \leq \sigma \leq 6} N_1^{(i)} a_{1\sigma, (12543)}^{(i)} \text{PT}_\sigma$ $+ c_{15243}^{(a)} \sum_{1 \leq \sigma \leq 6} N_1^{(i)} a_{1\sigma, (15243)}^{(i)} \text{PT}_\sigma,$	$a_{1\sigma, (12345)}^{(i)} = 2 (0 \ 0 \ -1 \ 0 \ 0 \ 1),$ $a_{1\sigma, (13245)}^{(i)} = 2 (0 \ 0 \ 0 \ 0 \ 0 \ 1),$ $a_{1\sigma, (12543)}^{(i)} = 2 (1 \ 0 \ 1 \ 0 \ 1 \ -1),$ $a_{1\sigma, (15243)}^{(i)} = 2 (0 \ 0 \ 0 \ 0 \ -1 \ 0).$

Table 4.3: The two-loop five-point numerators that contribute to the amplitude. The $N_\nu^{(x)}$ are listed in Tab. 4.1. The five-point PT_σ are listed in Eq. (4.45). Numerators including color information are denoted by $\mathcal{N}^{(x)}$.

4.3 Two-loop n -point Super-Yang–Mills Amplitude

This section summarizes preliminary work on constructing the two-loop n -point amplitude.

The method parallels Ref. [99], in which the two-loop n -point planar amplitude was constructed. The main goal is to determine all possible cuts that the amplitude must satisfy and to selectively construct a set of basis integrals that is guaranteed to have unit leading singularities and no poles at infinity. This is a close relative of the pure integrand basis of Sec. 2.3.3.

A tentative outline of the process is:

- Determine all cuts of the amplitude, sorting from the most composite cuts to the least.
- Determine an independent set of the cuts.
- Build a basis of integrals that has unit leading singularities on all independent cuts.
- Check examples for specific n (=6,7 point).
- Check collinear limits.

The first point in the outline can be done exhaustively. The “most composite cuts” are graphs that have six edges in Fig. 4.5. A cut of the two-loop amplitude must localize eight degrees of freedom, and so the six on-shell conditions represented by such graphs do not localize all degrees of freedom. It is possible to localize the additional degrees of freedom by “double-cutting” two of the propagators. More precisely, a double cut is a specific residue of the integrand that falls under the class of composite cuts; see Sec. 2.1.

Starting from a list of all connected graphs with $v \leq 9$ vertices, it is straightforward to systematically select all diagrams that meet the requirements for being cuts of the amplitude: an on-shell diagram is valid if it is possible to generate it by taking a co-dimension eight residue of any two-loop graph. This generates some heuristic rules, such as all on-shell

diagrams must have at most eight propagators, and it must be possible to cut any loop momentum four times, double cuts included.

In practice this is done by generating a complete set of “skeleton” graphs as appearing in Fig. 4.5. These can then be dressed with massless or massive external particles, and the propagators can be dressed according to how many times they are cut. For example, the six-cut-propagator nonplanar diagram in the upper-left corner of Fig. 4.5 must have two propagators double-cut to localize all eight degrees of freedom in the loop momentum. Additionally, there are several ways to distribute massive and massless external legs around the skeleton graph. In Fig. 4.6, the double-cut propagators are denoted by dashed lines rather than solid. Massless corners are denoted by one external leg, and massive corners by two. As a first step in generating the list of all cuts, I have done this for all the relevant diagrams in Fig. 4.5.

For the second point in the outline: the on-shell diagrams are not independent. The diagrams represent both cuts of the amplitude and on-shell functions. The on-shell functions obey residue theorems that result in a web of identities connecting the diagrams. It may be possible to generate all such residue and thereby determine a basis, or it may be more tractable to just check by hand for residues that are closely connected.

Constructing the basis of unit leading singularities is mechanically identical to constructing the two-loop five-point pure integrands of Tab. 4.1.

As for checking specific examples, doing so is straightforward in the planar limit, where BCFW [100, 101] recursion relations exist. It is less clear how to proceed in the full theory. Potential tests are the two-loop six- and seven-point amplitudes. These amplitudes do not exist in the literature, and even generating all the diagrams that contribute to the amplitude – Figs. 4.7 and 4.8 – was a non-trivial first step in this direction. One way we will confirm the final result is by checking specific homogeneous cuts (Sec. 2.4)

Another potential test is computing various collinear limits of the integrands in the spirit of Ref. [102]. This is on-going work.

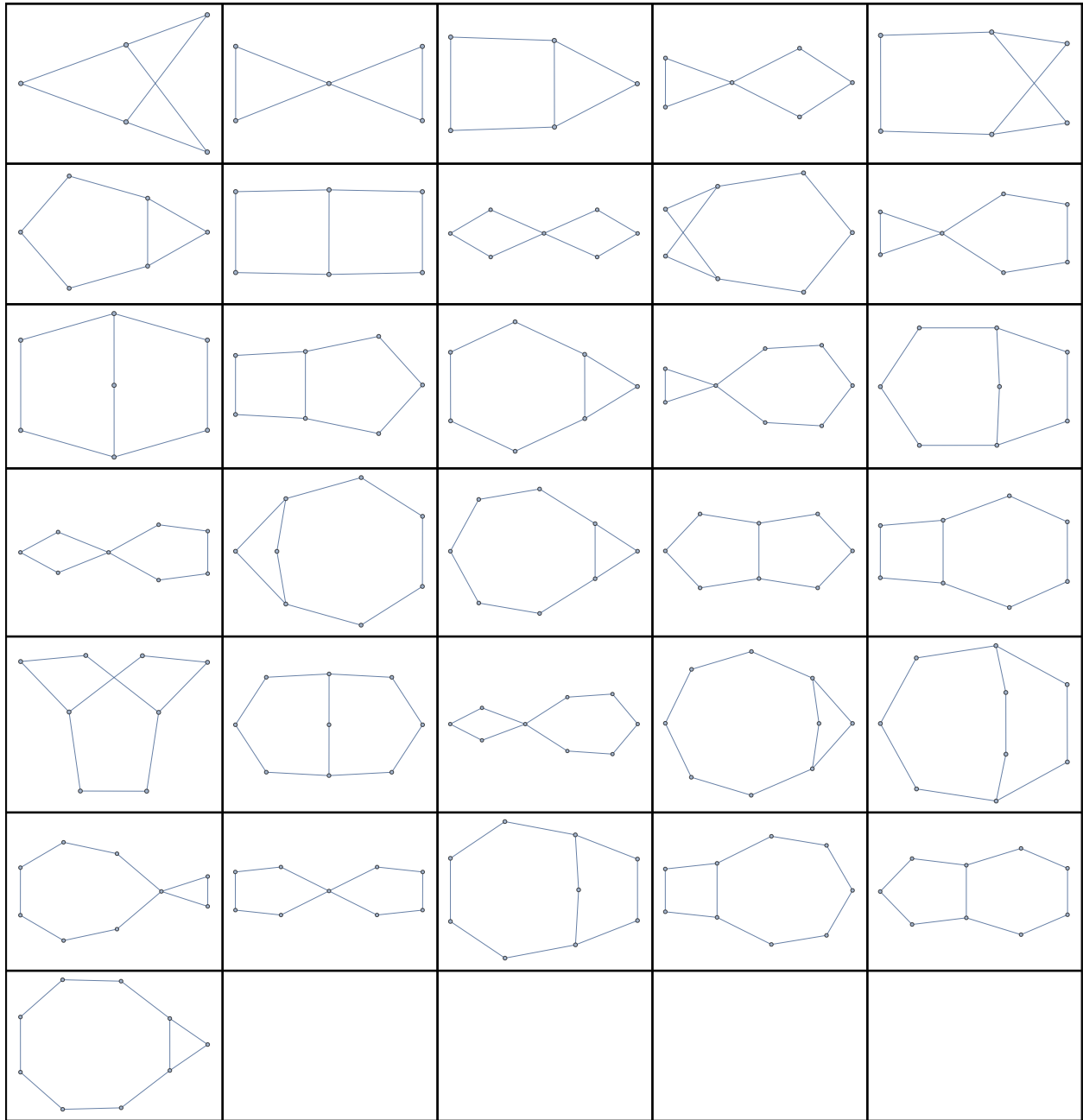


Figure 4.5: The set of “skeleton” graphs for two-loop n -point on-shell diagrams and integrals. Dressing the vertices and edges of these skeleton graphs yields the on-shell diagrams associated with cuts of the amplitude; see Fig. 4.6 for an example.

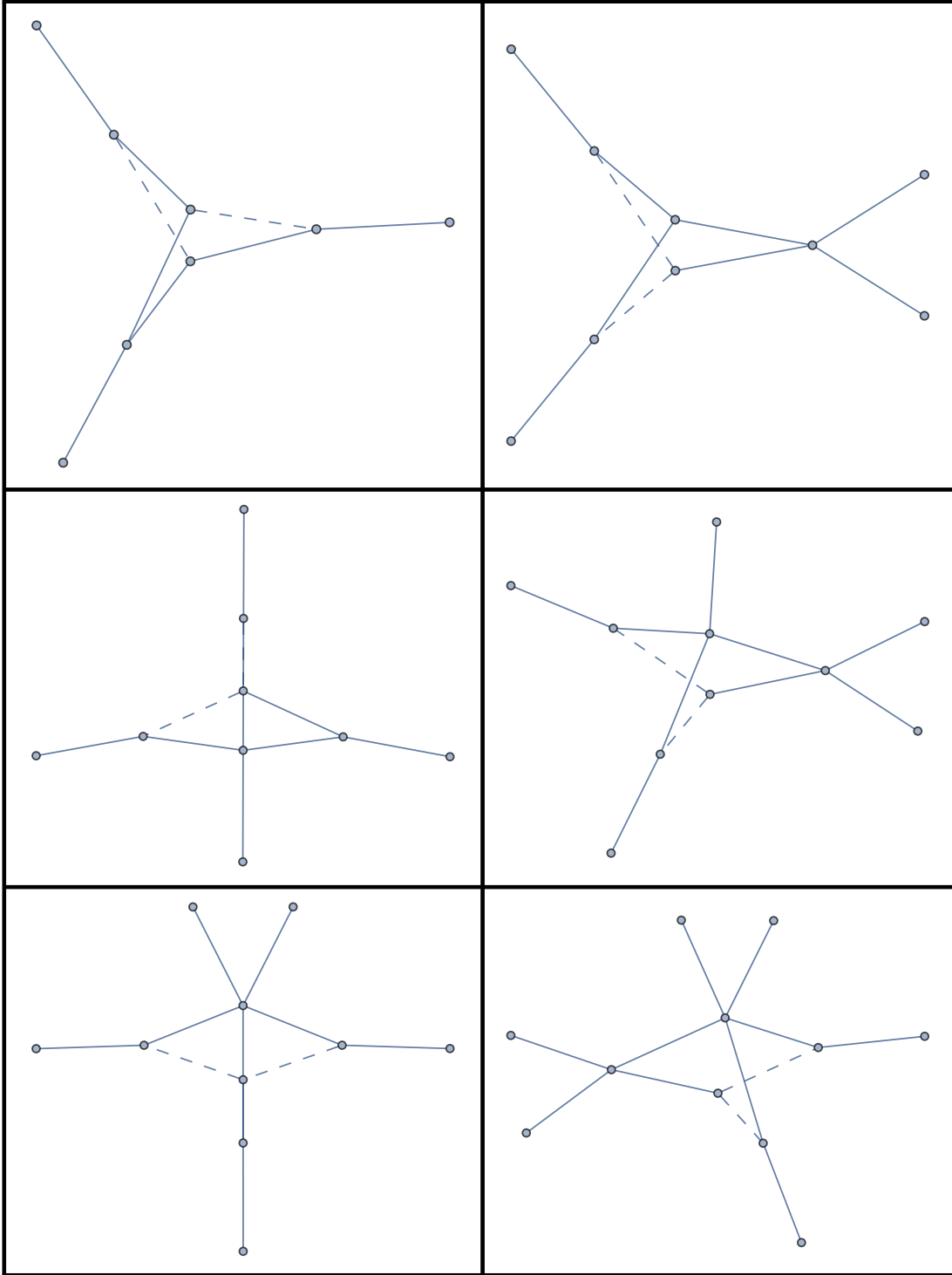


Figure 4.6: All possible ways of dressing the upper-left skeleton diagram in Fig. 4.5. One external leg indicates a massless corner; two indicate a massive corner. A dashed edge indicates a double-cut propagator.

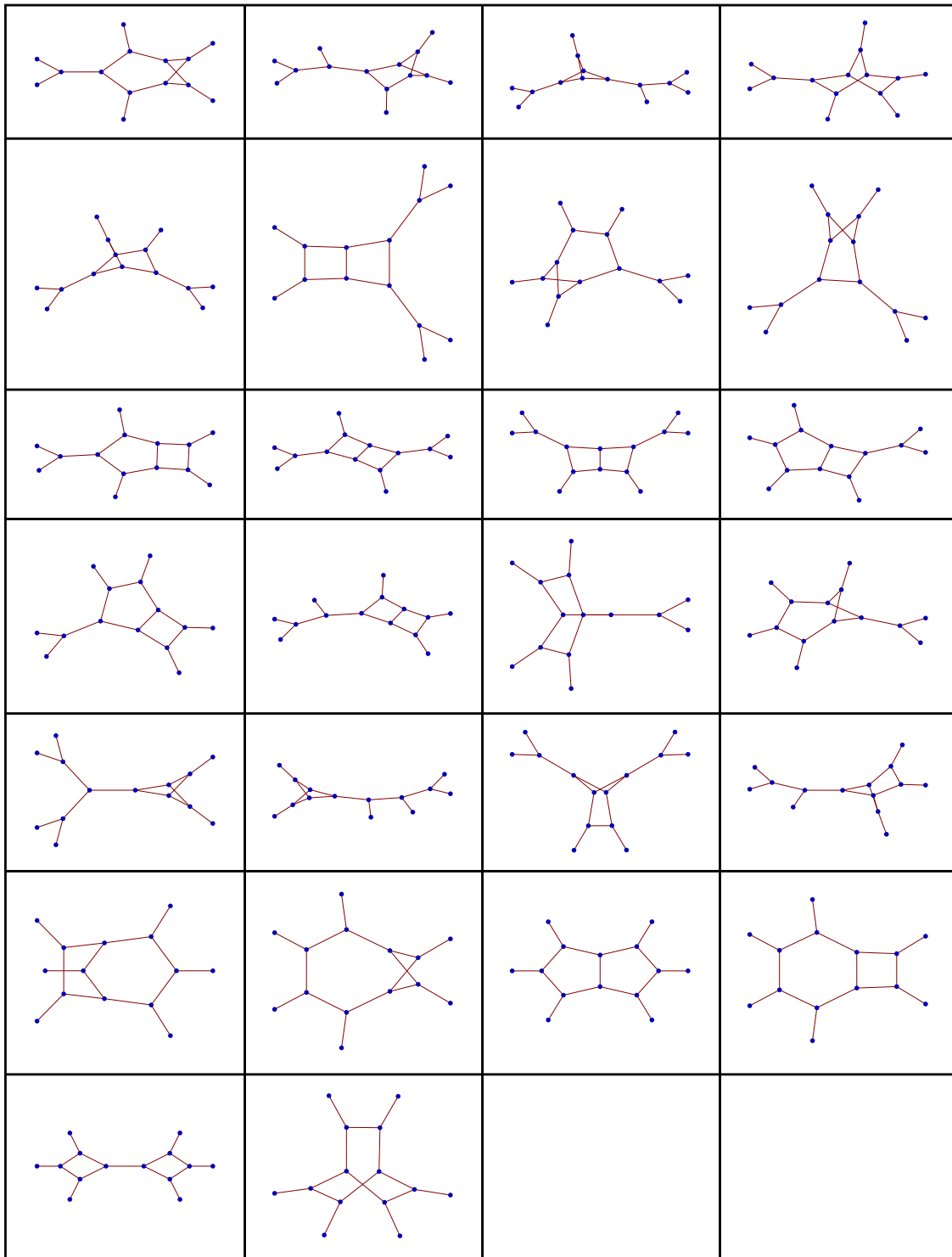


Figure 4.7: The set of trivalent two-loop six-point graphs. The graphs are intentionally not labeled.

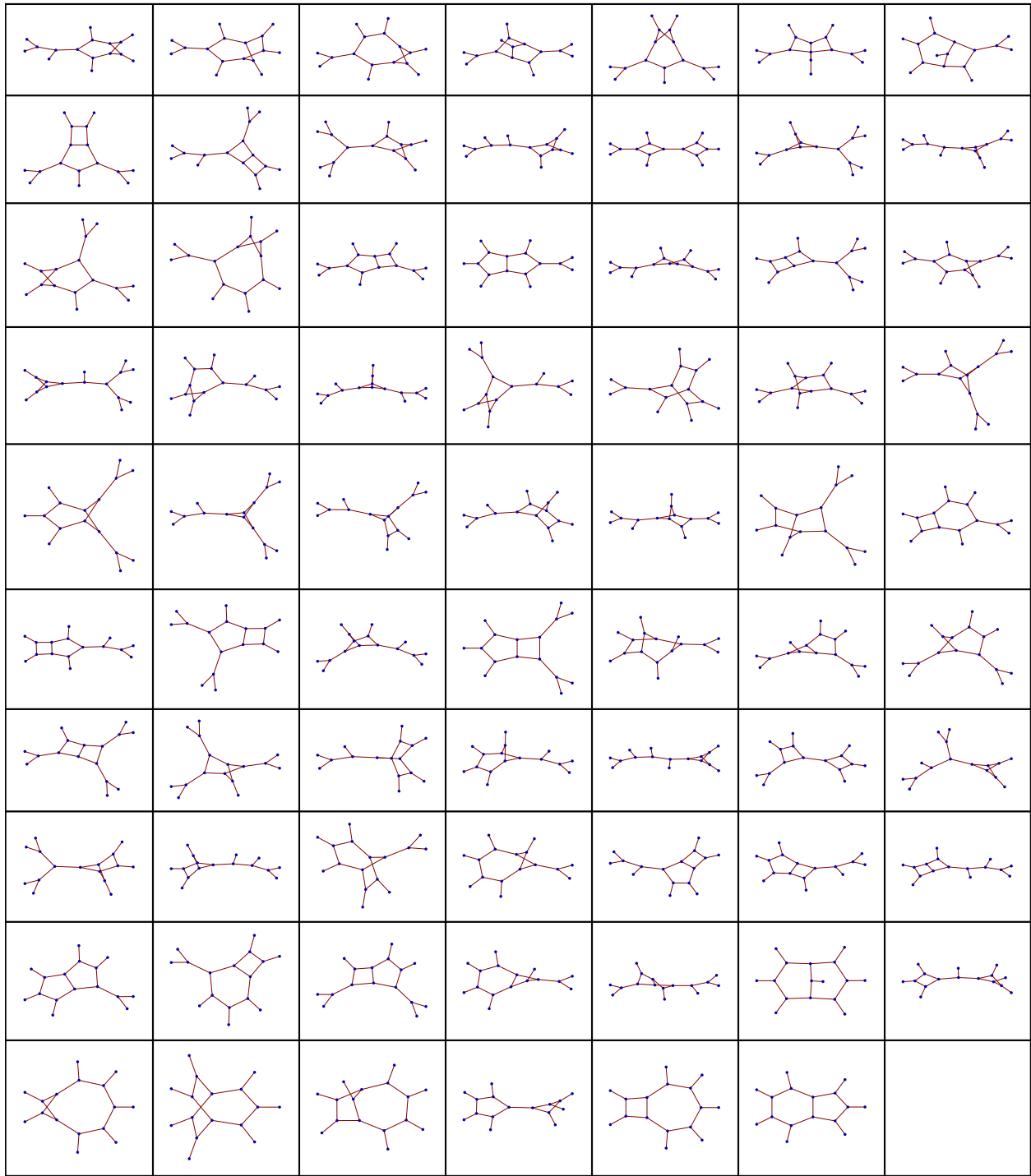


Figure 4.8: The set of trivalent two-loop seven-point graphs. The graphs are intentionally not labeled.

CHAPTER 5

Three-Loop Four-Point Super-Yang–Mills Amplitude

The three-loop four-point sYM amplitude is constructed in two different ways in this chapter. In Sec. 5.1, the amplitude is presented in a $d\log$ representation, in line with the discussion of Sec. 2.3; this is analogous to the two-loop four-point amplitude in Sec. 4.1.1. In Sec. 5.2, the amplitude is written in the pure integrand basis explained in Sec. 2.3.3; the discussion is similar to that surrounding the two-loop five-point pure integrand representation in Sec. 4.2. For both constructions, the details in this chapter are largely excised in favor of the discussion surrounding the simpler two-loop four-point amplitude in Sec. 4.1.

5.1 $d\log$ Form

This section follows the recipe of Sec. 2.3 to find a basis of three-loop diagram integrands that have only logarithmic singularities and no poles at infinity. The three-loop four-point parent diagrams are shown in Tab. 5.1. These were classified in Ref. [66, 103], where an un-integrated representation of the three-loop four-point full sYM amplitude was first obtained. As in Sec. 2.3, the parent diagrams are restricted to those where no bubble or triangle diagrams appear as subdiagrams. Diagrams with contact terms can be incorporated into a parent diagram by including in the numerator inverse propagators that cancel propagators.

Applying the power-counting rules in Sec. 2.3, the maximum powers of allowed loop

momenta for each parent diagram are

$$\begin{aligned}
N^{(a)} &= \mathcal{O}(1), \\
N^{(b)} &= \mathcal{O}(\ell_6^2), \\
N^{(c)} &= \mathcal{O}(\ell_5^2, (\ell_5 \cdot \ell_7), \ell_7^2), \\
N^{(d)} &= \mathcal{O}(\ell_6^4), \\
N^{(e)} &= \mathcal{O}(\ell_5^2), \\
N^{(f)} &= \mathcal{O}(\ell_5^4), \\
N^{(g)} &= \mathcal{O}(\ell_5^2 \ell_6^2), \\
N^{(h)} &= \mathcal{O}(\ell_5^2 \ell_6^2, \ell_5^2 \ell_7^2, \ell_5^2 (\ell_6 \cdot \ell_7)), \\
N^{(i)} &= \mathcal{O}(\ell_5^2 \ell_6^2), \tag{5.1}
\end{aligned}$$

where the choice of independent loop momenta in Tab. 5.1 gives the most stringent power counts. Diagram (h) requires combining restrictions from a variety of labelings to arrive at this stringent power count. Ignoring the overall prefactor of \mathcal{K} , the overall dimension of each numerator is $\mathcal{O}(p^4)$, including external momenta.

5.1.1 Diagram Numerators

The next step is to write down the most general diagram numerators that are consistent with the power count in Eq. (5.1), respect diagram symmetry, are built only from Lorentz dot products of the loop and external momenta, have only logarithmic singularities and have no poles at infinity. Although the construction is straightforward, the complete list of conditions is lengthy. Included here are only a few examples of how to construct the $d \log$ numerators, followed by a table of numerators, Tab. 5.1, that satisfy the $d \log$ constraints.

Diagram (a)

Diagram (a) in Tab. 5.1 is a simple first example. The required numerators are simple to write down by following the same logic as in the two-loop example in Sec. 4.1.1. Since the numerator of diagram (a) is independent of all loop momenta as noted in Eq. (5.1), only numerators that depend on the Mandelstam invariants s and t are allowed. There are three numerators that are consistent with the overall dimension,

$$N_1^{(a)} = s^2, \quad N_2^{(a)} = st, \quad N_3^{(a)} = t^2. \quad (5.2)$$

Following similar logic as in the two-loop four-point example, it is straightforward to check that there are no double poles or poles at infinity.

Diagram (b)

The numerator for diagram (b) is also easy to obtain, this time by following the logic of the two-loop nonplanar diagram. From Eq. (5.1), the numerator may only depend on loop-momentum ℓ_6 . The two-loop subdiagram on the right side of diagram (b) in Tab. 5.1 containing ℓ_6 is just the two-loop nonplanar double box already analyzed in Sec. 4.1.1. Repeating the earlier nonplanar box procedure for this subdiagram produces the most general possible numerator for diagram (b),

$$N_1^{(b)} = s((\ell_6 - k_3)^2 + (\ell_6 - k_4)^2). \quad (5.3)$$

This is just the two-loop nonplanar numerator with an extra factor of s . A factor of t instead of s is disallowed because it violates the $k_3 \leftrightarrow k_4$ symmetry of diagram (b).

Diagram (e)

As a somewhat more complicated example, consider diagram (e) in Tab. 5.1. Because this diagram is planar, it could be constructed by enforcing dual conformal invariance. This

is a first example where the d log requirements supplant dual conformal invariance – see Sec. 6.1 for further discussion.

From Eq. (5.1), the numerator depends on the loop momentum ℓ_5 at most quadratically. Therefore a valid ansatz for it is

$$N^{(e)} = (c_1 s + c_2 t) (\ell_5^2 + d_1 (\ell_5 \cdot Q) + d_2 s + d_3 t), \quad (5.4)$$

where Q is a vector independent of all loop momenta and the c_i and d_i are numerical constants. The overall factor $(c_1 s + c_2 t)$ is included so that the numerator has the correct overall dimensions, but this factor does not play a role in canceling unwanted singularities of the integrand.

Canceling any hidden double poles and poles at infinity in the integrand imposes constraints on this numerator ansatz Eq. (5.4). The starting integrand is

$$\begin{aligned} \mathcal{I}^{(e)} &= \frac{N^{(e)}}{\ell_6^2 (\ell_6 + \ell_5)^2 (\ell_6 + \ell_7)^2 (\ell_6 + k_4)^2 (\ell_7 - \ell_5)^2 (\ell_7 - k_1 - k_2)^2 (\ell_7 + k_4)^2} \\ &\quad \times \frac{1}{\ell_5^2 (\ell_5 - k_1)^2 (\ell_5 - k_1 - k_2)^2}. \end{aligned} \quad (5.5)$$

Since the numerator ansatz (5.4) is a function of ℓ_5 , it is convenient to localize to on-shell values for ℓ_6 and ℓ_7 . This leaves the numerator ansatz unaltered, making it straightforward to determine all coefficients in $N^{(e)}$. To locate a double pole, consider the cut sequence

$$\text{cut} = \{B(\ell_6), B(\ell_7, \ell_7)\}, \quad (5.6)$$

using the notation of Sec. 2.1, so that $B(\ell_7, \ell_7)$ indicates that cutting the $1/\ell_7^2$ propagator produced by the $B(\ell_6)$ cut. This produces an overall Jacobian

$$J_{6,7} = s [(\ell_5 + k_4)^2]^2. \quad (5.7)$$

After this sequence of cuts, the integrand of Eq. (5.5) becomes:

$$\text{Res}_{\substack{\ell_6\text{-cut} \\ \ell_7\text{-cut}}} [\mathcal{I}^{(e)}] = \frac{N^{(e)}}{\ell_5^2(\ell_5 - k_1)^2(\ell_5 - k_1 - k_2)^2 [(\ell_5 + k_4)^2]^2 s}, \quad (5.8)$$

exposing a double pole at $(\ell_5 + k_4)^2 = 0$.

To impose the d log constraints on the integrand, cancel the double pole in the denominator with an appropriate numerator. Choosing the ansatz in Eq. (5.4) to have $Q = k_4$, $d_1 = 2$, $d_2 = 0$, $d_3 = 0$ gives a final form of the allowed numerator,

$$N^{(e)} = (c_1 s + c_2 t)(\ell_5 + k_4)^2, \quad (5.9)$$

so that there are two basis numerators,

$$N_1^{(e)} = s(\ell_5 + k_4)^2, \quad N_2^{(e)} = t(\ell_5 + k_4)^2. \quad (5.10)$$

For Ref. [2], we checked that this numerator passes all other double-pole constraints coming from different regions of momentum space; we also checked that it has no poles at infinity. It is interesting that, up to a factor depending only on external momenta, these are precisely the numerators consistent with dual conformal symmetry. As discussed in Sec. 6.1, this is no accident.

Diagram (d)

Next consider diagram (d) in Tab. 5.1. From the power counting arguments summarized in Eq. (5.1), the numerator for this diagram is a quartic function of momentum ℓ_6 , and it depends on neither ℓ_5 nor ℓ_7 .

When constructing numerators algorithmically it is standard to start with a general ansatz, but to more easily illustrate the role of contact terms, consider instead starting from the natural guess that diagram (d) is closely related to a product of two two-loop nonplanar

double boxes. Thus an educated initial guess is that the desired numerator is the product of numerators corresponding to the two-loop nonplanar subdiagrams:

$$\tilde{N}^{(d)} = [(\ell_6 + k_1)^2 + (\ell_6 + k_2)^2] [(\ell_6 - k_3)^2 + (\ell_6 - k_4)^2]. \quad (5.11)$$

This numerator is labeled $\tilde{N}^{(d)}$ because it is not quite the numerator $N^{(d)}$ that satisfies the $d \log$ constraints. Note that this numerator satisfies the symmetries of the diagram.

This ansatz satisfies nearly all constraints on double poles and poles at infinity. There is though a double pole not removed by the numerator in the kinematic region:

$$\text{cut} = \{\ell_5^2, (\ell_5 + k_2)^2, \ell_7^2, (\ell_7 - k_3)^2, B(\ell_6)\}. \quad (5.12)$$

To unveil the double pole, first solve the ℓ_5 and ℓ_7 dependent cut conditions in terms of two parameters α and β :

$$\ell_5 = \alpha k_2, \quad \ell_7 = -\beta k_3. \quad (5.13)$$

The final $B(\ell_6)$ represents a box-cut of four of the six remaining propagators that depend on α and β :

$$(\ell_6 - \alpha k_2)^2 = (\ell_6 - \alpha k_2 + k_1)^2 = (\ell_6 + \beta k_3)^2 = (\ell_6 + \beta k_3 - k_4)^2 = 0. \quad (5.14)$$

Before cutting the $B(\ell_6)$ propagators, the integrand is

$$\text{Res}_{\substack{\ell_5\text{-cut} \\ \ell_7\text{-cut}}} \tilde{\mathcal{I}}^{(d)} = \frac{\tilde{N}^{(d)}}{\ell_6^2 (\ell_6 + k_1 + k_2)^2 (\ell_6 - \alpha k_2)^2 (\ell_6 - \alpha k_2 + k_1)^2} \quad (5.15)$$

$$\times \frac{1}{(\ell_6 + \beta k_3)^2 (\ell_6 + \beta k_3 - k_4)^2}. \quad (5.16)$$

Localizing further to the $B(\ell_6)$ cuts produces a Jacobian

$$J_6 = su(\alpha - \beta)^2, \quad (5.17)$$

while a solution to the box-cut conditions of Eq. (5.14)

$$\ell_6^* = \alpha \lambda_4 \tilde{\lambda}_2 \frac{\langle 12 \rangle}{\langle 14 \rangle} - \beta \lambda_1 \tilde{\lambda}_3 \frac{\langle 34 \rangle}{\langle 14 \rangle}, \quad (5.18)$$

turns the remaining uncut propagators of Eq. (5.16) into:

$$\ell_6^2 = s\alpha\beta, \quad (\ell_6 + k_1 + k_2)^2 = s(1 + \alpha)(1 + \beta). \quad (5.19)$$

The result of completely localizing all momenta in this way is:

$$\text{Res}_{\text{cuts}} \tilde{\mathcal{I}}^{(d)} = -\frac{s^2(\alpha(1 + \beta) + \beta(1 + \alpha))^2}{s^3 u \alpha \beta (1 + \alpha)(1 + \beta)(\alpha - \beta)^2}. \quad (5.20)$$

This manifestly has a double pole located at $\alpha - \beta = 0$. To cancel this double pole requires adding an extra term to the numerator. A natural choice is a term that collapses both propagators connecting the two two-loop nonplanar subdiagrams: $\ell_6^2(\ell_6 + k_1 + k_2)^2$. On the support of the cut solutions Eq. (5.18), this becomes $s^2\alpha\beta(\alpha + 1)(\beta + 1)$. The double pole at $\alpha - \beta = 0$ in Eq. (5.20) can be canceled by choosing the linear combination

$$N_1^{(d)} = [(\ell_6 + k_1)^2 + (\ell_6 + k_2)^2] [(\ell_6 - k_3)^2 + (\ell_6 - k_4)^2] - 4\ell_6^2(\ell_6 + k_1 + k_2)^2. \quad (5.21)$$

Indeed, with this numerator the diagram lacks even a single pole at $\alpha - \beta = 0$.

It is interesting to note that relaxing the condition that the numerator respects the diagram symmetry $k_1 \leftrightarrow k_2$ and $k_3 \leftrightarrow k_4$, there are four independent numerators with no double pole. For example,

$$\tilde{N}^{(d)} = (\ell_6 + k_1)^2(\ell_6 - k_3)^2 - \ell_6^2(\ell_6 + k_1 + k_2)^2, \quad (5.22)$$

is a d log numerator. Requiring $N^{(d)}$ to respect diagram symmetry requires summing the first four terms in Eq. (5.21), each with its own ‘‘correction’’ term $-\ell_6^2(\ell_6 + k_1 + k_2)^2$. This accounts for the factor of four on the last term in Eq. (5.21).

For Ref. [2], we carried out detailed checks of all potentially dangerous regions of the integrand of diagram (d) showing that the numerator of Eq. (5.21) results in a diagram with only logarithmic singularities and no poles at infinity. In fact, the numerator (5.21) is the only one respecting the symmetries of diagram (d) with these properties. This follows by starting with a general ansatz subject to the power counting constraint in Eq. (5.1) and showing that no other solution exists other than the one in Eq. (5.21).

All Diagrams

For Ref. [2], we went through the diagrams in Tab. 5.1 in great detail, finding the numerators that respect diagram symmetry including color signs, and that have only logarithmic singularities and no poles at infinity. This results in a set of basis $d\log$ numerators associated with each diagram. For the diagrams where numerator factors do not cancel any propagators, the set of numerators is collected in Tab. 5.1.

In addition, there are also diagrams where numerators do cancel propagators. For the purpose of constructing amplitudes, it is convenient to absorb these contact contributions into the parent diagrams of Tab. 5.1 to make color assignments manifest. This makes it tractable to treat all contributions on an equal footing, such that color factors can be read directly from the associated parent diagram by dressing each three vertex with an \tilde{f}^{abc} . This distributes the contact term diagrams in Tab. 5.3 among the parent diagrams, listed in Tab. 5.2. When distributing the contact terms to the parent diagrams, change the momentum labels to those of each parent diagram and then multiply and divide by the missing propagator(s). The reason the numerators in Tab. 5.2 appear more complicated than those in Tab. 5.3 is that a single term from Tab. 5.3 can appear with multiple momentum relabelings in order to enforce the symmetries of the parent diagrams on the numerators.

As an example of the correspondence between the numerators in Tab. 5.2 and Tab. 5.3, consider diagram (j) and the associated numerators, $N_1^{(j)}$ and $N_2^{(j)}$, in Tab. 5.3. To convert this into a contribution to diagram (i) in Tab. 5.2, multiply and divide by the missing

propagator $1/(\ell_5 + \ell_6 + k_4)^2$. Then take the appropriate linear combination so that the diagram (i) anti-symmetry, including the color sign, under $\{k_1 \leftrightarrow k_3, \ell_5 \leftrightarrow \ell_6, \ell_7 \leftrightarrow -\ell_7\}$ is satisfied. This gives,

$$N_2^{(i)} = \frac{1}{3}(\ell_5 + \ell_6 + k_4)^2 [t - s] . \quad (5.23)$$

In fact, there are three alternative propagators that can be inserted instead of $1/(\ell_5 + \ell_6 + k_4)^2$ which are all equivalent to the three relabelings of external lines for diagram (i). This requires a combinatorial factor of $\frac{1}{3}$, which is absorbed into the definition of the numerator because of the differing symmetries between diagram (i) in Tab. 5.2 and diagram (j) in Tab. 5.3.

As a second example, consider diagram (k) in Tab. 5.3, corresponding to the basis element $N_1^{(k)}$. Restoring the two missing propagators by multiplying and dividing by the appropriate inverse propagators, the contribution from diagram (k) in Tab. 5.3, corresponds to numerators $N_2^{(c)}$, $N_2^{(f)}$, $N_5^{(g)}$, $N_6^{(g)}$, $N_2^{(h)}$ and $N_3^{(i)}$ in Tab. 5.2.

In summary, the diagrams along with the numerators in Tab. 5.1 and 5.2 are a complete set for expanding the three-loop four-point sYM amplitude with the desired power counting. The integrands have only logarithmic singularities and no poles at infinity. They are also constructed to satisfy diagram symmetries, including color signs.

5.1.2 Determining the Coefficients

Now the three-loop four-point sYM amplitude can be written in a way that each term is free of double poles and poles at infinity. This is done by expressing the numerators in Eq. (2.26) directly in terms of the d log basis via Eq. (2.32). Because each basis numerator reflects diagram symmetry, only one numerator need be specified for each diagram topology since permutations of external legs then correspond to relabelings.

The coefficients in front of all basis elements are straightforward to determine using simple unitarity cuts, together with previously determined representations of the three-loop amplitude. The sYM numerators from Ref. [66] in the choice of momentum labels of Tab. 5.1

Diagram	Numerators
(a)	$N_1^{(a)} = s^2, \quad N_2^{(a)} = st, \quad N_3^{(a)} = t^2,$
(b)	$N_1^{(b)} = s [(\ell_6 - k_3)^2 + (\ell_6 - k_4)^2],$
(c)	$N_1^{(c)} = s [(\ell_5 - \ell_7)^2 + (\ell_5 + \ell_7 + k_1 + k_2)^2],$
(d)	$N_1^{(d)} = [(\ell_6 + k_1)^2 + (\ell_6 + k_2)^2]^2 - 4\ell_6^2(\ell_6 + k_1 + k_2)^2,$
(e)	$N_1^{(e)} = s(\ell_5 + k_4)^2, \quad N_2^{(e)} = t(\ell_5 + k_4)^2,$
(f)	$N_1^{(f)} = (\ell_5 + k_4)^2 [(\ell_5 + k_3)^2 + (\ell_5 + k_4)^2],$
(g)	$N_1^{(g)} = s(\ell_5 + \ell_6 + k_3)^2,$ $N_2^{(g)} = t(\ell_5 + \ell_6 + k_3)^2,$ $N_3^{(g)} = (\ell_5 + k_3)^2(\ell_6 + k_1 + k_2)^2,$ $N_4^{(g)} = (\ell_5 + k_4)^2(\ell_6 + k_1 + k_2)^2,$
(h)	$N_1^{(h)} = \left[(\ell_6 + \ell_7)^2(\ell_5 + k_2 + k_3)^2 - \ell_5^2(\ell_6 + \ell_7 - k_1 - k_2)^2 \right. \\ \left. - (\ell_5 + \ell_6)^2(\ell_7 + k_2 + k_3)^2 - (\ell_5 + \ell_6 + k_2 + k_3)^2\ell_7^2 \right. \\ \left. - (\ell_6 + k_1 + k_4)^2(\ell_5 - \ell_7)^2 - (\ell_5 - \ell_7 + k_2 + k_3)^2\ell_6^2 \right] \\ - \left[[(\ell_5 - k_1)^2 + (\ell_5 - k_4)^2][(\ell_6 + \ell_7 - k_1)^2 + (\ell_6 + \ell_7 - k_2)^2] \right. \\ \left. - 4 \times \ell_5^2(\ell_6 + \ell_7 - k_1 - k_2)^2 \right. \\ \left. - (\ell_7 + k_4)^2(\ell_5 + \ell_6 - k_1)^2 - (\ell_7 + k_3)^2(\ell_5 + \ell_6 - k_2)^2 \right. \\ \left. - (\ell_6 + k_4)^2(\ell_5 - \ell_7 + k_1)^2 - (\ell_6 + k_3)^2(\ell_5 - \ell_7 + k_2)^2 \right],$
(i)	$N_1^{(i)} = (\ell_6 + k_4)^2 [(\ell_5 - k_1 - k_2)^2 + (\ell_5 - k_1 - k_3)^2] \\ - (\ell_5 + k_4)^2 [(\ell_6 + k_1 + k_4)^2 + (\ell_6 + k_2 + k_4)^2] \\ - \ell_5^2(\ell_6 - k_2)^2 + \ell_6^2(\ell_5 - k_2)^2.$

Table 5.1: The parent numerator basis elements. The basis elements respect the symmetries of the diagrams.

Diagram	Numerator
(c)	$N_2^{(c)} = (\ell_5)^2 (\ell_7)^2 + (\ell_5 + k_1 + k_2)^2 (\ell_7)^2 + (\ell_5)^2 (\ell_7 + k_1 + k_2)^2$ $+ (\ell_5 + k_1 + k_2)^2 (\ell_7 + k_1 + k_2)^2,$
(f)	$N_2^{(f)} = \ell_5^2 (\ell_5 - k_1 - k_2)^2,$
(g)	$N_5^{(g)} = (\ell_5 - k_1 - k_2)^2 (\ell_6 - k_4)^2,$ $N_6^{(g)} = \ell_5^2 (\ell_6 - k_4)^2,$
(h)	$N_2^{(h)} = \ell_6^2 (\ell_5 - \ell_7)^2 + \ell_7^2 (\ell_5 + \ell_6)^2 + (\ell_6 + k_4)^2 (\ell_5 - \ell_7 + k_2)^2$ $+ (\ell_5 + \ell_6 - k_1)^2 (\ell_7 + k_3)^2,$
(i)	$N_2^{(i)} = \frac{1}{3} (\ell_5 + \ell_6 + k_4)^2 [t - s],$ $N_3^{(i)} = (\ell_6)^2 (\ell_5 - k_1)^2 - (\ell_5)^2 (\ell_6 - k_3)^2.$

Table 5.2: The parent diagram numerator basis elements where a numerator factor cancels a propagator. Each term in brackets does not cancel a propagator, while the remaining factors each cancel a propagator. Each basis numerator maintains the symmetries of the associated diagram, including color signs. The associated color factor can be read off from each diagram.

Diagram	Numerator
(j)	$N_1^{(j)} = s, \quad N_2^{(j)} = t,$
(k)	$N_1^{(k)} = 1.$

Table 5.3: The numerator basis elements correspond to the contact term diagrams. Hatched dots indicate contact terms. Written this way, the numerators are simple, but the color factors cannot be read off from the diagrams.

are

$$\begin{aligned}
N_{\text{old}}^{(\text{a})} &= N_{\text{old}}^{(\text{b})} = N_{\text{old}}^{(\text{c})} = N_{\text{old}}^{(\text{d})} = s^2, \\
N_{\text{old}}^{(\text{e})} &= N_{\text{old}}^{(\text{f})} = N_{\text{old}}^{(\text{g})} = s(\ell_5 + k_4)^2, \\
N_{\text{old}}^{(\text{h})} &= -st + 2s(k_2 + k_3) \cdot \ell_5 + 2t(\ell_6 + \ell_7) \cdot (k_1 + k_2), \\
N_{\text{old}}^{(\text{i})} &= s(k_4 + \ell_5)^2 - t(k_4 + \ell_6)^2 - \frac{1}{3}(s - t)(k_4 + \ell_5 + \ell_6)^2.
\end{aligned} \tag{5.24}$$

To fix coefficients in the d log basis, start with maximal cuts in which all propagators of each diagram are placed on shell. The complete set of maximal cut solutions are unique to each diagram, so coefficients can be matched by considering only a single diagram at a time. Starting with diagram (a) in Tab. 5.1: the d log numerator is a linear combination of three basis elements

$$N^{(\text{a})} = a_1^{(\text{a})} N_1^{(\text{a})} + a_2^{(\text{a})} N_2^{(\text{a})} + a_3^{(\text{a})} N_3^{(\text{a})}, \tag{5.25}$$

corresponding to $N_j^{(\text{a})}$ in Tab. 5.1. The $a_j^{(\text{a})}$ are rational numbers to be determined. The maximal cuts have no effect because both the new and old numerators are independent of loop momentum. Functionally matching the two numerators, the coefficients in front of the numerator basis elements are $a_1^{(\text{a})} = 1$, $a_2^{(\text{a})} = 0$ and $a_3^{(\text{a})} = 0$.

Now consider diagram (b) in Tab. 5.1. Here the basis element is of a different form compared to the old version of the numerator in Eq. (5.24). The new form of the numerator is

$$N^{(\text{b})} = a_1^{(\text{b})} N_1^{(\text{b})} = a_1^{(\text{b})} s [(\ell_6 - k_3)^2 + (\ell_6 - k_4)^2]. \tag{5.26}$$

In order to make the comparison to the old version, impose the maximal cut conditions involving only ℓ_6 :

$$\ell_6^2 = 0, \quad (\ell_6 - k_2 - k_3)^2 = 0. \tag{5.27}$$

Applying these conditions:

$$[(\ell_6 - k_3)^2 + (\ell_6 - k_4)^2] \rightarrow -s. \tag{5.28}$$

Comparing to $N_{\text{old}}^{(b)}$ in Eq. (5.24) yields the coefficient $a_1^{(b)} = -1$.

As a more complicated example, consider diagram (i). In this case the numerators depend only on ℓ_5 and ℓ_6 . The relevant cut conditions read off from Tab. 5.1(i) are

$$\ell_5^2 = \ell_6^2 = (\ell_5 - k_1)^2 = (\ell_6 - k_3)^2 = (\ell_5 + \ell_6 - k_3 - k_1)^2 = (\ell_5 + \ell_6 + k_4)^2 = 0. \quad (5.29)$$

With these cut conditions, the old numerator in Eq. (5.24) becomes

$$N_{\text{old}}^{(i)}|_{\text{cut}} = 2s(k_4 \cdot \ell_5) - 2t(k_4 \cdot \ell_6). \quad (5.30)$$

The full numerator for diagram (i) is a linear combination of the three basis elements for diagram (i) in Tab. 5.1 and 5.2,

$$N^{(i)} = a_1^{(i)} N_1^{(i)} + a_2^{(i)} N_2^{(i)} + a_3^{(i)} N_3^{(i)}. \quad (5.31)$$

The maximal cut conditions immediately set to zero the last two of these numerators because they contain inverse propagators. Applying the cut conditions Eq. (5.29) to the non-vanishing term results in

$$N^{(i)}|_{\text{cut}} = a_1^{(i)} [-2(\ell_6 \cdot k_4)t + 2(\ell_5 \cdot k_4)s]. \quad (5.32)$$

Comparing Eq. (5.30) to Eq. (5.32) fixes $a_1^{(i)} = 1$. The two other coefficients for diagram (i), $a_2^{(i)}$ and $a_3^{(i)}$ cannot be fixed from the maximal cuts since they multiply inverse propagators and so vanish.

In order to determine all coefficients and prove that the answer is complete and correct requires evaluating next-to-maximal and next-to-next-to-maximal cuts. Cuts up to only this level are sufficient for fixing all parameters because of the especially good power counting of sYM. For Ref. [2], I automated these checks with the software outlined in Sec. 2.6. Using

these cuts results in numerators in terms of the basis elements:

$$\begin{aligned}
N^{(a)} &= N_1^{(a)} , \\
N^{(b)} &= -N_1^{(b)} , \\
N^{(c)} &= -N_1^{(c)} + 2d_1 N_2^{(c)} , \\
N^{(d)} &= N_1^{(d)} , \\
N^{(e)} &= N_1^{(e)} , \\
N^{(f)} &= -N_1^{(f)} + 2d_2 N_2^{(f)} , \\
N^{(g)} &= -N_1^{(g)} + N_3^{(g)} + N_4^{(g)} + (d_1 + d_3 - 1)N_5^{(g)} + (d_1 - d_2)N_6^{(g)} , \\
N^{(h)} &= N_1^{(h)} + 2d_3 N_2^{(h)} , \\
N^{(i)} &= N_1^{(i)} + N_2^{(i)} + (d_3 - d_2)N_3^{(i)} ,
\end{aligned} \tag{5.33}$$

where the three d_i are free parameters not fixed by any physical constraint.

The ambiguity represented by the three free parameters, d_i in Eq. (5.33), derives from color factors being not independent but rather related via the color Jacobi identity. This allows contact terms to move between different diagrams without altering the amplitude. Different choices of d_1, d_2, d_3 correspond to three degrees of freedom from color Jacobi identities. This freedom allows moving contact contributions of diagram (k), where two propagators are collapsed, between different parent diagrams. The contact term in diagram (j) of Tab. 5.3 does not generate a fourth degree of freedom because the three resulting parent diagrams are all the same topology, corresponding to relabelings of the external legs of diagram (i); the potential freedom in this case cancels within the single diagram. We explicitly checked that the d_i parameters in Eq. (5.33) drop out of the full amplitude after using appropriate color Jacobi identities. One choice of free parameters is to take them to all vanish

$$d_1 = 0, \quad d_2 = 0, \quad d_3 = 0. \tag{5.34}$$

In this case every remaining non-vanishing numerical coefficient in front of a basis elements

is ± 1 ¹. Of course this is not some “best” choice of the d_i , given that the amplitude is unchanged for any other choice of d_i .

5.2 Pure Integrand Basis

The $d \log$ representation of the amplitude is closely related to the pure integrand representation of the amplitude. Much as with the two-loop four-point amplitude in Sec. 4.1, the only difference between the $d \log$ and pure integrand representation of the three-loop four-point amplitude are that some of the basis elements in Tab. 5.1 and 5.2 must be split and re-scaled.

In particular, the elements of Tab. 5.1 and 5.2 are split and re-scaled so that *any* leading singularity² is either ± 1 or 0. This is exactly the same reason Eq. (4.22) is rewritten as Eq. (4.23) in the two-loop four-point example in Sec. 4.1.2. The resulting basis numerators yielding pure integrands are summarized in Tab. 5.4.

The notation “ $N|_{i \leftrightarrow j}$ ” in Tab. 5.4 means: “redraw the graph associated with numerator N with the indicated exchanges of external momenta i, j and also relabel loop momenta accordingly.” A simple example is $N_2^{(i)} = N_1^{(i)}|_{1 \leftrightarrow 3}$, where

$$N_1^{(i)} = tu(\ell_6 + k_4)^2(\ell_5 - k_1 - k_2)^2. \quad (5.35)$$

Under this relabeling, the Mandelstam variables s and t transform into one another $s = (k_1 + k_2)^2 \leftrightarrow (k_3 + k_2)^2 = t$ and u stays invariant. In addition to changing the external labels, the loop momenta must be relabeled as well. In the chosen example, this corresponds

¹Recall that $N_2^{(i)}$ absorbed the 1/3 combinatorial factor mismatch between diagram (i) and diagram (j).

²See Sec. 2.1 for the definition of leading singularities.

to interchanging $\ell_5 \leftrightarrow \ell_6$, so that

$$N_2^{(i)} = N_1^{(i)}|_{1 \leftrightarrow 3} = su(\ell_5 + k_4)^2(\ell_6 - k_3 - k_2)^2. \quad (5.36)$$

The amplitude is assembled from the basis numerators as

$$\mathcal{A}_4^{(3)} = \sum_{\mathcal{S}_4} \sum_{(x)} \frac{1}{S^{(x)}} \int d^4\ell_5 d^4\ell_6 d^4\ell_7 \frac{\mathcal{N}^{(x)}}{\prod_{\alpha^{(x)}} p_{\alpha^{(x)}}^2}, \quad (5.37)$$

analogously to Eq. (4.24). Now the sum over x runs over all diagrams in the basis listed in Tab. 5.4, the sum over \mathcal{S}_4 is a sum over all 24 permutations of the external legs, and S_x is the symmetry factor of diagram x determined by counting the number of automorphisms of diagram x . The product over α_x indicates the product of Feynman propagators $p_{\alpha_x}^2$ of diagram x , as read from the graphs in Tab. 5.4. The Parke-Taylor factors, color factors, and coefficients are absorbed in $\mathcal{N}^{(x)}$, which are listed in Tab. 5.5.

For four external particles, there are only two independent Parke-Taylor factors:

$$\text{PT}_1 = \text{PT}(1234), \quad \text{PT}_2 = \text{PT}(1243). \quad (5.38)$$

The third possible factor, $\text{PT}(1423)$, is related to the other two by a $U(1)$ decoupling identity or dual Ward identity [104]

$$\text{PT}(1423) = -\text{PT}(1234) - \text{PT}(1243), \quad (5.39)$$

and is therefore linearly dependent on PT_1 and PT_2 .

When checking cuts of the amplitude, certain cuts may combine contributions from different terms in the permutation sum of Eq. (5.37), resulting in a cut expression that involves diagrams that are relabelings of those in Tab. 5.4. In that case, the procedure is to relabel the numerators, propagators, Parke-Taylor factors, and color factors given in the tables into the cut labels. The resulting Parke-Taylor factors may not be in the original basis of

Parke-Taylor factors; however just as in Eq. (5.39), every Parke-Taylor factor in the relabeled expression can be expanded in the original Parke-Taylor basis of Eq. (5.38).

The diagrams with 10 propagators contain only three-point vertices and therefore have unique color factors included in $\mathcal{N}^{(x)}$. For the two diagrams with less than 10 propagators, the ansatz for \mathcal{N} includes all independent color factors from all 10-propagator diagrams that are related to the lower-propagator diagrams by collapsing internal legs. For example, three 10-propagator diagrams are related to diagram (j) in this way, with color factors $c_{1234}^{(i)}$, $c_{1243}^{(i)}$ and $c_{3241}^{(i)}$, where

$$c_{1234}^{(i)} = \tilde{f}^{a_1 a_8 a_5} \tilde{f}^{a_6 a_2 a_9} \tilde{f}^{a_3 a_{11} a_{10}} \tilde{f}^{a_{12} a_4 a_{13}} \tilde{f}^{a_9 a_{10} a_8} \tilde{f}^{a_{11} a_{12} a_{14}} \tilde{f}^{a_{13} a_5 a_7} \tilde{f}^{a_{14} a_7 a_6} , \quad (5.40)$$

is the standard color factor in terms of appropriately normalized structure constants, and the others c 's are relabelings of 1234 of this color factor. The Jacobi relation between the three color factors allows eliminating, for example, $c_{1243}^{(i)}$. This is exactly how diagram (j) is written. In diagram (k), there are nine contributing parent diagrams. Typically there are four independent color factors in the solution to the set of six Jacobi relations, but in this case two of the color factors that contribute happen to be identical up to a sign, and thus there are only three independent color factors.

In Eq. (5.33), the final representation of the amplitude contained arbitrary free parameters associated with the color Jacobi identity that allowed contact terms to be moved between parent diagrams without altering the amplitude. This freedom is absent in Tab. 5.5 because contact terms are assigned to their own diagrams, and each contact term is expanded in a basis of color factors.

One advantage of the Parke-Taylor expansion of the amplitude is that the amplitude can be compactly expressed in the set of matrices listed on the right of Tab. 5.5. For example, $\mathcal{N}^{(i)}$ can be read off from the table as

$$\mathcal{N}^{(i)} = c_{1234}^{(i)}(-1)(N_1^{(i)}(\text{PT}_1 + \text{PT}_2) + N_2^{(i)}\text{PT}_2 - N_3^{(i)}\text{PT}_1 + N_4^{(i)}\text{PT}_1) . \quad (5.41)$$

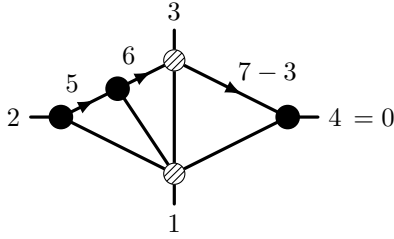


Figure 5.1: The three-loop four-point MHV amplitude vanishes on this cut. The five-point tree at the bottom of the diagram has $k = 2$ or $k = 3$, so the overall helicity counting is $k = 3$ or $k = 4$.

This expression supplies the Parke-Taylor and color dependence for Eq. (5.37), in agreement with the general form of Eq. (2.35).

Finally, paralleling the discussion of the two-loop four-point amplitude in Sec. 4.1.3, the three-loop four-point pure integrand amplitude can be correctly constrained up to an overall coefficient by matching one cut where the amplitude must vanish. I did this for Ref. [3] using the software discussed in Sec. 2.6 and using the cut in Fig. 5.1.

Diagram	Numerators
(a)	$N_1^{(a)} = s^3 t,$
(b)	$N_1^{(b)} = s^2 u (\ell_6 - k_3)^2, \quad N_2^{(b)} = N_1^{(b)} _{3 \leftrightarrow 4},$
(c)	$N_1^{(c)} = s^2 u (\ell_5 - \ell_7)^2, \quad N_2^{(c)} = N_1^{(c)} _{1 \leftrightarrow 2},$
(d)	$N_1^{(d)} = su [(\ell_6 - k_1)^2 (\ell_6 + k_3)^2 - \ell_6^2 (\ell_6 - k_1 - k_2)^2],$ $N_2^{(d)} = N_1^{(d)} _{3 \leftrightarrow 4}, \quad N_3^{(d)} = N_1^{(d)} _{1 \leftrightarrow 2}, \quad N_4^{(d)} = N_1^{(d)} _{1 \leftrightarrow 2, 3 \leftrightarrow 4},$
(e)	$N_1^{(e)} = s^2 t (\ell_5 + k_4)^2,$
(f)	$N_1^{(f)} = st (\ell_5 + k_4)^2 (\ell_5 + k_3)^2, \quad N_2^{(f)} = su (\ell_5 + k_4)^2 (\ell_5 + k_4)^2,$
(g)	$N_1^{(g)} = s^2 t (\ell_5 + \ell_6 + k_3)^2,$ $N_2^{(g)} = st (\ell_5 + k_3)^2 (\ell_6 + k_1 + k_2)^2, \quad N_3^{(g)} = N_2^{(g)} _{3 \leftrightarrow 4},$
(h)	$N_1^{(h)} = st [(\ell_6 + \ell_7)^2 (\ell_5 + k_2 + k_3)^2 - \ell_5^2 (\ell_6 + \ell_7 - k_1 - k_2)^2$ $- (\ell_5 + \ell_6)^2 (\ell_7 + k_2 + k_3)^2 - (\ell_5 + \ell_6 + k_2 + k_3)^2 \ell_7^2$ $- (\ell_6 + k_1 + k_4)^2 (\ell_5 - \ell_7)^2 - (\ell_5 - \ell_7 + k_2 + k_3)^2 \ell_6^2],$ $N_2^{(h)} = tu [((\ell_5 - k_1)^2 + (\ell_5 - k_4)^2)[(\ell_6 + \ell_7 - k_1)^2 + (\ell_6 + \ell_7 - k_2)^2]$ $- 4 \ell_5^2 (\ell_6 + \ell_7 - k_1 - k_2)^2$ $- (\ell_7 + k_4)^2 (\ell_5 + \ell_6 - k_1)^2 - (\ell_7 + k_3)^2 (\ell_5 + \ell_6 - k_2)^2$ $- (\ell_6 + k_4)^2 (\ell_5 - \ell_7 + k_1)^2 - (\ell_6 + k_3)^2 (\ell_5 - \ell_7 + k_2)^2],$ $N_3^{(h)} = N_1^{(h)} _{2 \leftrightarrow 4}, \quad N_4^{(h)} = N_2^{(h)} _{2 \leftrightarrow 4},$
(i)	$N_1^{(i)} = tu (\ell_6 + k_4)^2 (\ell_5 - k_1 - k_2)^2, \quad N_2^{(i)} = N_1^{(i)} _{1 \leftrightarrow 3}$ $N_3^{(i)} = st [(\ell_6 + k_4)^2 (\ell_5 - k_1 - k_3)^2 - \ell_5^2 (\ell_6 - k_2)^2], \quad N_4^{(i)} = N_3^{(i)} _{1 \leftrightarrow 3}$
(j)	$N^{(j)} = stu.$
(k)	$N^{(k)} = su,$

Table 5.4: The basis of numerators for pure integrands for the three-loop four-point amplitude. Hatched dots indicate contact terms. The notation $N|_{i \leftrightarrow j}$ is defined in the text.

Color Dressed Numerators	PT Matrices
$\mathcal{N}^{(a)} = c_{1234}^{(a)} \sum_{1 \leq \sigma \leq 2} N_1^{(a)} a_{1\sigma}^{(a)} \text{PT}_\sigma,$	$a_{1\sigma}^{(a)} = \begin{pmatrix} 1 & 0 \end{pmatrix},$
$\mathcal{N}^{(b)} = c_{1234}^{(b)} \sum_{\substack{1 \leq \nu \leq 2 \\ 1 \leq \sigma \leq 2}} N_\nu^{(b)} a_{\nu\sigma}^{(b)} \text{PT}_\sigma,$	$a_{\nu\sigma}^{(b)} = (-1) \begin{pmatrix} 0 & 1 \\ 1 & 0 \end{pmatrix},$
$\mathcal{N}^{(c)} = c_{1234}^{(c)} \sum_{\substack{1 \leq \nu \leq 2 \\ 1 \leq \sigma \leq 2}} N_\nu^{(c)} a_{\nu\sigma}^{(c)} \text{PT}_\sigma,$	$a_{\nu\sigma}^{(c)} = (-1) \begin{pmatrix} 0 & 1 \\ 1 & 0 \end{pmatrix},$
$\mathcal{N}^{(d)} = c_{1234}^{(d)} \sum_{\substack{1 \leq \nu \leq 4 \\ 1 \leq \sigma \leq 2}} N_\nu^{(d)} a_{\nu\sigma}^{(d)} \text{PT}_\sigma,$	$a_{\nu\sigma}^{(d)} = \begin{pmatrix} 0 & 1 & 1 & 0 \\ 1 & 0 & 0 & 1 \end{pmatrix}^T,$
$\mathcal{N}^{(e)} = c_{1234}^{(e)} \sum_{1 \leq \sigma \leq 2} N_1^{(e)} a_{1\sigma}^{(e)} \text{PT}_\sigma,$	$a_{1\sigma}^{(e)} = \begin{pmatrix} 1 & 0 \end{pmatrix},$
$\mathcal{N}^{(f)} = c_{1234}^{(f)} \sum_{\substack{1 \leq \nu \leq 2 \\ 1 \leq \sigma \leq 2}} N_\nu^{(f)} a_{\nu\sigma}^{(f)} \text{PT}_\sigma,$	$a_{\nu\sigma}^{(f)} = (-1) \begin{pmatrix} 1 & 0 \\ 0 & 1 \end{pmatrix},$
$\mathcal{N}^{(g)} = c_{1234}^{(g)} \sum_{\substack{1 \leq \nu \leq 3 \\ 1 \leq \sigma \leq 2}} N_\nu^{(g)} a_{\nu\sigma}^{(g)} \text{PT}_\sigma,$	$a_{\nu\sigma}^{(g)} = \begin{pmatrix} -1 & 1 & 0 \\ 0 & 0 & 1 \end{pmatrix}^T,$
$\mathcal{N}^{(h)} = c_{1234}^{(h)} \sum_{\substack{1 \leq \nu \leq 4 \\ 1 \leq \sigma \leq 2}} N_\nu^{(h)} a_{\nu\sigma}^{(h)} \text{PT}_\sigma,$	$a_{\nu\sigma}^{(h)} = \frac{1}{2} \begin{pmatrix} 1 & 1 & 1 & 0 \\ 0 & 1 & 0 & -1 \end{pmatrix}^T,$
$\mathcal{N}^{(i)} = c_{1234}^{(i)} \sum_{\substack{1 \leq \nu \leq 4 \\ 1 \leq \sigma \leq 2}} N_\nu^{(i)} a_{\nu\sigma}^{(i)} \text{PT}_\sigma,$	$a_{\nu\sigma}^{(i)} = (-1) \begin{pmatrix} 1 & 0 & -1 & 1 \\ 1 & 1 & 0 & 0 \end{pmatrix}^T,$
$\mathcal{N}^{(j)} = c_{1234}^{(j)} \sum_{1 \leq \sigma \leq 2} N_1^{(j)} a_{1\sigma, (1234)}^{(j)} \text{PT}_\sigma$ $+ c_{3241}^{(j)} \sum_{1 \leq \sigma \leq 2} N_1^{(j)} a_{1\sigma, (3241)}^{(j)} \text{PT}_\sigma,$	$a_{1\sigma, (1234)}^{(j)} = \begin{pmatrix} 1 & 1 \end{pmatrix},$ $a_{1\sigma, (3241)}^{(j)} = \begin{pmatrix} -1 & 0 \end{pmatrix},$
$\mathcal{N}^{(k)} = c_{1234}^{(g)} \sum_{1 \leq \sigma \leq 2} N_1^{(k)} a_{1\sigma, (1234)}^{(k)} \text{PT}_\sigma$ $+ c_{4312}^{(g)} \sum_{1 \leq \sigma \leq 2} N_1^{(k)} a_{1\sigma, (4312)}^{(k)} \text{PT}_\sigma$ $+ c_{2431}^{(f)} \sum_{1 \leq \sigma \leq 2} N_1^{(k)} a_{1\sigma, (2431)}^{(k)} \text{PT}_\sigma.$	$a_{1\sigma, (1234)}^{(k)} = \begin{pmatrix} -2 & 0 \end{pmatrix},$ $a_{1\sigma, (4312)}^{(k)} = 0,$ $a_{1\sigma, (2431)}^{(k)} = 0.$

Table 5.5: The three-loop four-point numerators that contribute to the amplitude. The $N_\nu^{(x)}$ are listed in Tab. 5.4. The four-point Parke-Taylor factors PT_σ are listed in Eq. (5.38). The numerators including color factors are denoted as $\mathcal{N}^{(x)}$. The symbol ‘ T ’ denotes a transpose.

CHAPTER 6

Higher-loop Four-point Planar Amplitudes

This chapter contains two topics. Discussed in Sec. 6.1 are the implications of requiring the planar L -loop amplitude for $4 \leq L \leq 7$ to be written in terms of diagrams with no double poles and no poles at infinity. In Sec. 6.2 is a discussion of the mSUGRA amplitude.

6.1 Higher-loop Planar Super-Yang–Mills Amplitudes

Requiring that every diagram of the amplitude be free of double poles and poles at infinity constrains the diagrams that contribute to the planar amplitude. In Ref. [2] we conjectured:

Logarithmic singularities and absence of poles at infinity
imply dual conformal invariance of local integrand forms
to all loop orders in the planar sector.

This suggests using the singularity structure of the integrand as a guide to finding a generalization of dual conformal invariance in full sYM.

In Sec. 6.1.1 is a brief introduction to dual conformal invariance. In Sec. 6.1.2 is an algorithm for detecting bad poles in the amplitude. In Sec. 6.1.3 the algorithm is applied to four- through seven-loop planar diagrams, explaining why many dual conformal integrands do not contribute to the amplitude.

6.1.1 Dual Conformal Invariance

Dual conformal symmetry [20–22] has been extensively studied for planar sYM amplitudes. Dual or region variables are the natural variables to make dual conformal symmetry manifest. Dual variables correspond to vertices placed in the face of each planar momentum-space graph. These are indicated in the following sections with a red (shaded) dot and labeled with a red (shaded) number. This is illustrated in Fig. 6.2 for example.

The relation between external momenta k_i and external dual variables x_i is

$$k_i = x_{i+1} - x_i, \quad i = 1, 2, 3, 4, \quad x_5 \equiv x_1. \quad (6.1)$$

In term of dual variables, the Mandelstam invariants are

$$s = (k_1 + k_2)^2 \equiv x_{13}^2, \quad t = (k_2 + k_3)^2 \equiv x_{24}^2. \quad (6.2)$$

The internal faces are parametrized by additional x_j , with $j = 5, 6, \dots, 4 + L$ corresponding to loop momenta. In terms of the dual coordinates, loop momenta are defined from the diagrams as:

$$\ell = x_{\text{right}} - x_{\text{left}}, \quad (6.3)$$

where x_{right} is the dual coordinate to the right of ℓ when traveling in the direction of ℓ , and x_{left} is the dual coordinate to the left of ℓ when traveling in the direction of ℓ .

The key symmetry property of dual conformal invariance is inversion, $x_i^\mu \rightarrow x_i^\mu/x_i^2$ so that

$$x_{ij}^2 \rightarrow \frac{x_{ij}^2}{x_i^2 x_j^2}, \quad d^4 x_i \rightarrow \frac{d^4 x_i}{x_i^2}. \quad (6.4)$$

A four-point planar integrand form is dual conformally invariant (DCI) if $d\mathcal{I} \rightarrow d\mathcal{I}$ under this transformation.

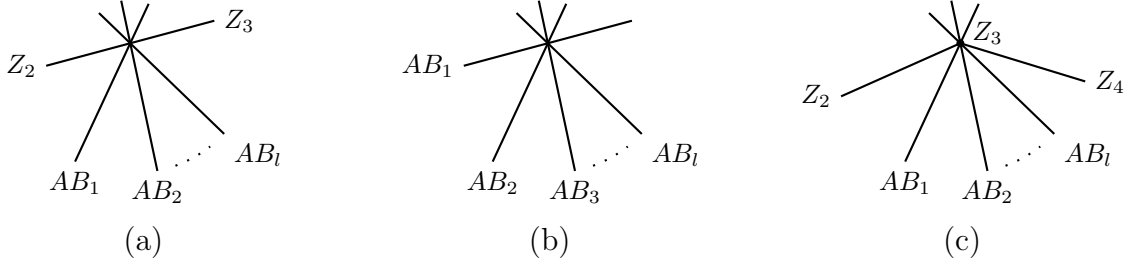


Figure 6.1: Cut configurations in momentum twistor geometry. The type I conditions correspond to (b), type II to (a) and type III to (c).

6.1.2 Algorithm for Vanishing Integrands

At a given loop order, it is straightforward to write down all dual conformal invariant integrands by generating all planar graphs, then writing down all possible numerators that balance the dual conformal weight of the propagators. The set of integrands so generated is an overcomplete basis for writing the amplitude; said another way: many of these integrands have zero coefficient in the planar amplitude.

In Ref. [25], Drummond, Korchemsky, and Sokatchev (DKS) showed that certain integrands have infrared divergences and so can not be DCI. The DKS constraint is then a way to set the coefficient of some DCI integrands to zero in the amplitude.

In Ref. [2], we showed that the DKS constraint could be rephrased in dual momentum twistor variables, and then generalized. In momentum twistor space, the l loop variables $\{x_{i_1}, \dots, x_{i_l}\}$ correspond to l lines $(AB)_1, \dots, (AB)_l$. Taking a specific point, say x_3 , in dual coordinates corresponds to the line Z_2Z_3 in momentum twistor space. The DKS constraint then corresponds to a configuration in momentum twistor space for which all l lines intersect the line Z_2Z_3 at the same point, as in Fig. 6.1(a).

This geometric reasoning then generalizes to two similar cases: all lines $(AB)_i$ intersect at a generic point as in Fig. 6.1(b), or all lines intersect at a given external point as in Fig. 6.1(c). Algebraic rearrangement¹ of the integrand yields inequalities on the integrands

¹See Ref. [2] for exact details.

that must be satisfied for the integrand to have no double poles and no poles at infinity. In particular, consider cutting some subset of propagators in a given diagram. Then the inequalities are in terms of

- N the number of numerator factors that vanish on the cut
- P the number of propagators that are cut
- The subset of l loop dual coordinates $\{x\}_L \equiv \{x_{i_1}, \dots, x_{i_l}\}$ that appear in the set of cut propagators.

Corresponding to each of the diagrams in Fig. 6.1, there are three conditions:

- Type I (Fig. 6.1(b)):

$$P < N + 2l - 2, \quad (6.5)$$

in the limit that loop dual coordinates are light-like separated from each other: $x_{ij}^2 = 0$ for all $x_i, x_j \in \{x\}_L$.

- Type II (Fig. 6.1(a)):

$$P < N + 2l, \quad (6.6)$$

in the limit that loop dual coordinates are light-like separated from each other and from one external point: $x_{ij}^2 = x_{ki}^2 = 0$ for all $x_i, x_j \in \{x\}_L$, $k = 1, 2, 3, 4$

- Type III (Fig. 6.1(c)):

$$P < N + 2l + 1, \quad (6.7)$$

in the limit that loop dual coordinates are light-like separated from each other and from two external points: $x_{ij}^2 = x_{ki}^2 = x_{k'i}^2 = 0$, for all $x_i, x_j \in \{x\}_L$, $k, k' = 1, 2, 3, 4$.²

If cutting any subset of propagators of a diagram fails to satisfy all of these conditions, then the diagram has non-logarithmic poles. Several examples at various loop orders follow.

²The equations $x_{ki}^2 = x_{k'i}^2 = 0$ have two solutions so we have to choose the same solution for all x_i .

6.1.3 Applying the Algorithm

Starting from the set of all dual conformal numerators allowed by power counting at various loop levels, the goal is to eliminate numerators that do not pass the inequalities of Sec. 6.1.2.

Four-loop Planar Super-Yang–Mills Amplitudes

As a first example, consider diagram Fig. 6.2(4d). This diagram contains two pentagon subdiagrams parametrized by ℓ_5 and ℓ_7 and so has a numerator scaling as $N^{(4f)} \sim \mathcal{O}(\ell_5^2, \ell_7^2)$. There are four³ independent numerators allowed by dual conformal invariance

$$N_1^{(4d)} = s^2(\ell_5 - \ell_7)^2 = (x_{13}^2)^2 x_{57}^2, \quad (6.8)$$

$$N_2^{(4d)} = s\ell_7^2(\ell_5 + k_1 + k_2)^2 = x_{13}^2 x_{37}^2 x_{15}^2 \longrightarrow N^{(4d_2)} = x_{13}^2. \quad (6.9)$$

$$N_3^{(4d)} = x_{13}^2 x_{27}^2 x_{45}^2, \quad (6.10)$$

$$N_4^{(4d)} = x_{13}^2 x_{25}^2 x_{47}^2 \longrightarrow N^{(4d')} = x_{13}^2. \quad (6.11)$$

In Eq. (6.9), the notation $N_2^{(4d)} \longrightarrow N^{(4d_2)}$ indicates that the numerator $N_2^{(4d)}$ cancels two propagators to produce exactly Fig. 6.3(4d₂), with numerator $N^{(4d_2)}$. Similarly in Eq. (6.11), $N_4^{(4d)}$ reduces to diagram (4d') in Fig. 6.3 upon canceling propagators.

To apply the algorithm, first select some subset of the propagators. In this case, cutting all propagators

$$x_{ij}^2, \quad i, j \in \{2, 3, 5, 6, 7, 8\}, \quad (6.12)$$

splits the set of all numerators in Eqs. (6.8)-(6.11) into two sets. The numerator $N_1^{(4d)} = (x_{13}^2)^2 x_{57}^2$ has $N = 1$, while there are $l = 4$ loops, and there are a total of $P = 8$ propagators

³There is a fifth numerator $s\ell_7^2(\ell_5 + k_1 + k_2)^2$ that is a relabeling of $N_2^{(4d)}$ under automorphisms of diagram (4d). Here and below such relabelings are omitted.

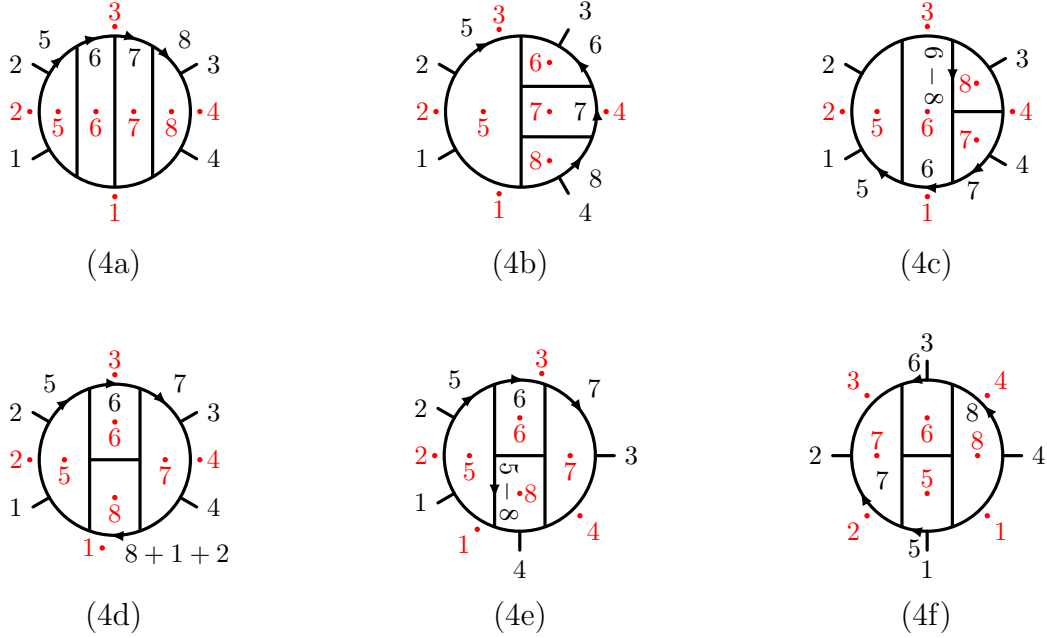


Figure 6.2: Parent diagrams contributing to the four-loop planar amplitude. The red (shaded) dots indicate the face or dual labels of the planar graph.

from the specified subset Eq. (6.12). In this case

$$P = 8 < 9 = 1 + 2 \cdot 4 = N + 2l, \quad (6.13)$$

and so the numerator is allowed by this double pole constraint. In fact, both numerators $N_1^{(4d)}$ and $N_2^{(4d)}$ from Eqs. (6.8) and (6.9) have the same values of P , l , and N , and so each passes this double pole test and has only single poles. In contrast, the numerators $N_3^{(4d)}$ and $N_4^{(4d)}$ from Eqs. (6.10) and (6.11) have $N = 0$ and fail the inequality, so they have double poles and do not contribute to the amplitude.

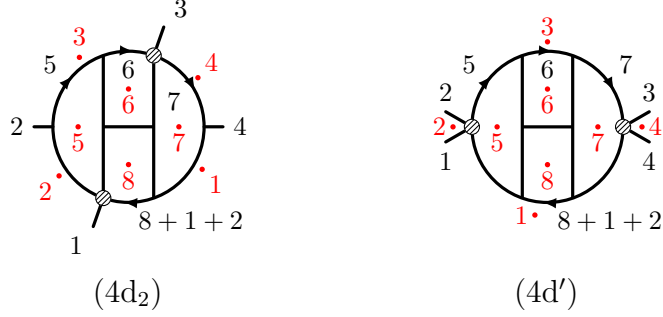


Figure 6.3: Diagram $(4d_2)$ contributes to the planar amplitude at four-loops. Diagram $(4d')$ does not. Red (shaded) dots represent dual coordinates. Hatched dots represent contact terms.

Five-loop Planar Super-Yang–Mills Amplitudes

As a first five-loop example, consider the trivalent graph Fig. 6.4.

The dual conformal numerators that do not collapse any propagators in Fig. 6.4 are

$$\begin{aligned}
 N_1^{(5a)} &= x_{24}^2 x_{35}^2 x_{17}^2 x_{68}^2, & N_2^{(5a)} &= -x_{13}^2 x_{24}^2 x_{57}^2 x_{68}^2, \\
 N_3^{(5a)} &= x_{18}^2 x_{27}^2 x_{36}^2 x_{45}^2, & &
 \end{aligned}
 \tag{6.14}$$

where any dual conformal numerators that are relabelings of these numerators under automorphisms of the diagram are omitted. These three numerators correspond to diagrams 21, 22 and 35, respectively, of Ref. [71]. However, notice that in the notation used here an overall factor of $st = x_{13}^2 x_{24}^2$ has been stripped off. For the three kinematic conditions of the rules, this diagram has three different values of P :

$$P_I = 8, \quad P_{II} = 10, \quad \text{and} \quad P_{III} = 12,
 \tag{6.15}$$

where the subscript corresponds to the inequality of the previous section. The type I kinematics is most constraining in this example, and for $l = 5$ requires $N > 0$. Converting this back to a statement about the numerator, implies that all $d \log$ numerators for this diagram must have at least one factor of the form $x_{l_1 l_2}$, for x_{l_1} and x_{l_2} in the set of loop face variables.

Only $N_1^{(5a)}$ and $N_2^{(5a)}$ have this correct loop dependence. So both $N_1^{(5a)}$ and $N_2^{(5a)}$ can appear in the amplitude, while $N_3^{(5a)}$ yields an integrand with non-logarithmic poles, and so has coefficient zero in the amplitude.

In addition to the numerators in Eq. (6.14), there are other dual conformal numerators that cancel propagators of the parent diagram, resulting in contact-term diagrams depicted in Figs. 6.5 and 6.6. Considering only the contact terms that can be obtained from the diagram in Fig. 6.4, the numerators that pass the three inequalities are

$$\begin{aligned} N^{(5b)} &= -x_{24}^2 x_{17}^2 x_{36}^2, & N^{(5c)} &= x_{13}^2 x_{24}^2, \\ N^{(5d)} &= -x_{13}^2 x_{27}^2, & N^{(5e)} &= x_{24}^2, \end{aligned} \tag{6.16}$$

where the four numerators respectively correspond to diagrams 31, 32, 33, and 34 in Ref. [71]. Besides $N_3^{(5a)}$, there are four more numerators that display DCI at the integrand level, but are invalid by applying the type II rules:

$$\begin{aligned} N^{(5f)} &= x_{18}^2 x_{36}^2, & N^{(5g)} &= 1, \\ N^{(5h)} &= x_{17}^2 x_{36}^2 x_{48}^2, & N^{(5i)} &= x_{35}^2. \end{aligned} \tag{6.17}$$

These correspond to diagrams 36, 37, 38 and 39, respectively, of Ref. [71]. The numerators listed in Eq. (6.16) are numerators for the lower-propagator topologies in Fig. 6.5, and the numerators listed in Eq. (6.17) are numerators for the lower-propagator topologies in Fig. 6.6. Again the other dual conformal numerators that are relabelings of these numerators under automorphism of the diagram are omitted.

This analysis does not prove $N_{1,2}^{(5a)}$ through $N^{(5e)}$ can be written as d log forms; it only shows that the corresponding integrands do not contain the types of non-logarithmic singularities detected by the three inequalities. It is still possible for those integrands to have non-logarithmic poles buried in certain kinematic regimes deeper in the cut structure. Indeed, under more careful scrutiny, such additional constraints appear from the requirements

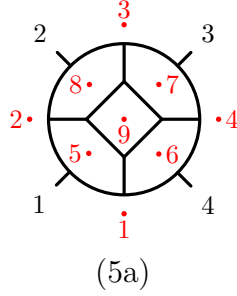


Figure 6.4: A sample five-loop planar diagram. Red (shaded) dots and labels represent dual coordinates.

of no double poles. In particular only the following combinations of integrands corresponding to Figs. 6.4 and 6.5 are free of double poles:

$$\mathcal{I}^{(A)} = \mathcal{I}_1^{(5a)} + \mathcal{I}^{(5b)} + \mathcal{I}^{(5e)}, \quad \mathcal{I}^{(B)} = \mathcal{I}_2^{(5a)} + \mathcal{I}^{(5c)}, \quad \mathcal{I}^{(D)} = \mathcal{I}^{(5d)}. \quad (6.18)$$

The notation is, for example, that the integrand $\mathcal{I}_1^{(5a)}$ has the propagators of diagram (5a) and the numerator $N_1^{(5a)}$ in Eq. (6.14). Similarly, the corresponding numerators for the integrands of diagrams (5b)–(5e) are given in Eq. (6.16). The integrand for diagram (5a) with numerator $N_3^{(5a)}$ is not present, because no contact terms can remove all double poles of $\mathcal{I}_3^{(5a)}$. In this case, all cancellations of double poles are between the parent and descendant diagrams. However, at higher loops the situation can very well be more complicated: unwanted singularities could cancel between different parent diagrams as well.

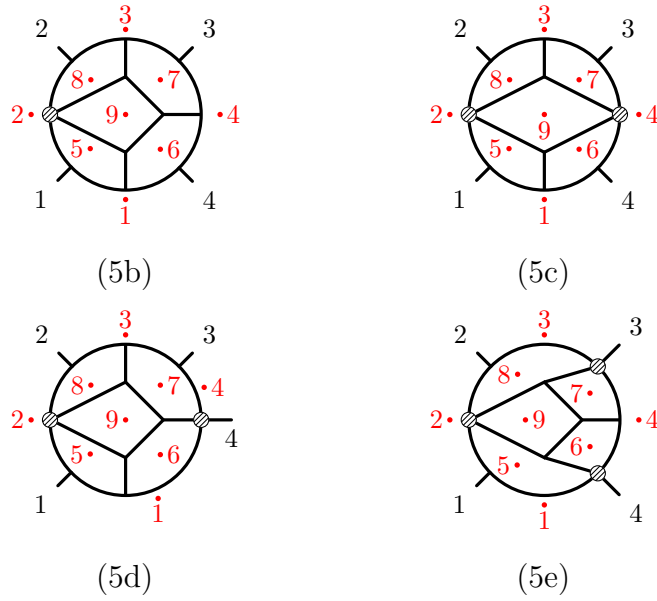


Figure 6.5: Descendants of the five-loop planar diagram of Fig. 6.4 with numerator coefficients determined to be *non-zero* by testing for non-logarithmic singularities.

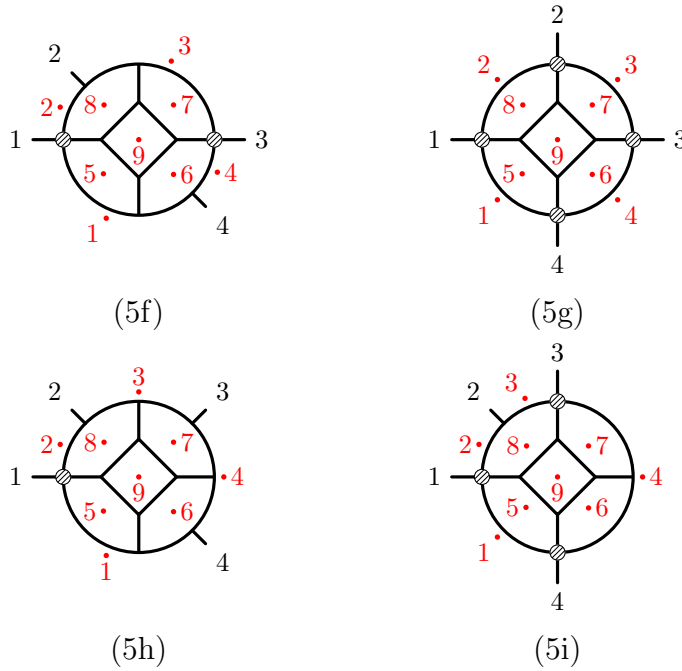


Figure 6.6: Descendants of the five-loop planar diagram of Fig. 6.4 with numerator coefficients determined to be zero by testing positive for non-logarithmic singularities.

Six- and Seven-loop Planar Super-Yang–Mills Amplitudes

Finally, consider two six-loop examples that both fall outside the type II inequality from Sec. 6.1.2. This means both numerators escape detection by the original DKS rule, and so far could not be easily identified as DCI integrands that do not contribute to the amplitude. The two examples are the six-loop “bow-tie” in Fig. 6.7(6a) and another six-loop diagram with two contact terms in Fig. 6.7(6b). The dual conformal numerators of these diagrams are [105]⁴

$$N^{(6a)} = x_{13}^3 x_{24}, \quad N^{(6b)} = x_{24}^2 x_{27}^2 x_{45}^2. \quad (6.19)$$

There are other dual conformal numerators for (6b), but they belong to lower-propagator diagrams, and so are omitted here.

This integrand (6a) does not satisfy inequality III from Sec. 6.1.2. Choosing the seven propagators

$$x_{25}^2 = x_{26}^2 = x_{36}^2 = x_{37}^2 = x_{56}^2 = x_{57}^2 = x_{67}^2 = 0, \quad (6.20)$$

selects $l = 3$, $N = 0$, $P = 7$ and the corresponding inequality $P < N + 2l + 1$ is violated. This means the non-logarithmic rules immediately offer a reason why this diagram contributes to the amplitude with coefficient zero. This agrees with Ref. [105].

The six-loop example (6b) in Fig. 6.7 is more subtle, since it is not ruled out by the three inequalities. However, it does have a double pole. From Ref. [105], this diagram with numerator $N^{(6b)}$ does not enter the expansion of the amplitude but has coefficient zero. Presumably, the double pole cannot cancel against other diagrams.

For Ref. [2], we also conducted a variety of checks at seven loops using the integrand given in Ref. [105]. There are 2329 planar integrands at seven loops, and all 456 contributions that failed the tests did not appear in the amplitude, as expected. We also checked dozens of

⁴These diagrams and numerators can be found in the associated files of Ref. [105] in the list of six loop integrands that do not contribute to the amplitude. Here a factor of $st = x_{13}^2 x_{24}^2$ is stripped off.

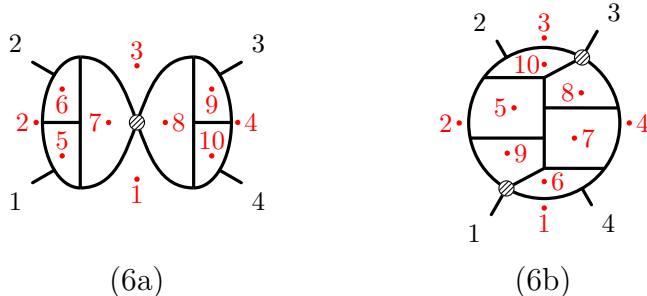


Figure 6.7: Two six-loop diagrams that have coefficient zero in the amplitude because they have non-logarithmic singularities. Diagram (6a) has non-logarithmic poles detected by the inequalities. Diagram (6b) requires explicit checks to locate double poles.

examples that have vanishing coefficients and were able to identify problematic singularities in all cases. More generally there were examples of double poles canceling non-trivially between different diagrams, just as at five-loops.

The key implication from this section is that it should be possible to carry the consequences of dual conformal symmetry to the nonplanar sector by considering the singularity structure of the integrand.

6.2 Maximal Supergravity Poles

Continuing with the chapter theme, in this section is an analysis of the singularity structure of mSUGRA amplitudes. In Sec. 6.2.1, is a conjecture that mSUGRA amplitudes have only logarithmic poles at finite loop momentum, with supporting evidence from the three-loop four-point mSUGRA amplitude. In Sec. 6.2.2, a certain easy-to-analyze planar ($L \geq 4$)-loop diagram highlights the analytic structure of the mSUGRA amplitude for infinite values of loop momentum.

6.2.1 Logarithmic Singularities

In Ref. [2], we conjectured:

For finite loop momentum, the four-point momentum-space mSUGRA integrand forms have only logarithmic singularities.

This follows in a straightforward way from the color-kinematics duality, Sec. 2.5, when one of the copies is in $d \log$ form.

As an explicit example, consider the three-loop four-point sYM amplitude, double-copied into the three-loop four-point mSUGRA amplitude. Using the BCJ numerators from Ref. [61] in conjunction with the $d \log$ representation of the sYM amplitude in Eq. (5.33) yields the mSUGRA amplitude in a format that makes the singularity structure manifest for finite loop momentum. Since the BCJ numerators are known for this sYM amplitude, so too are the mSUGRA numerators:

$$N_{\text{mSUGRA}}^{(x)} = N^{(x)} N_{\text{BCJ}}^{(x)}, \quad (6.21)$$

where (x) labels the diagram, $N^{(x)}$ is one of the numerators in Eq. (5.33), and $N_{\text{BCJ}}^{(x)}$ is one of the BCJ numerators from Ref. [61]. For example, consider the mSUGRA numerator of integrand (f) in Tab. 5.1. Multiplying the sYM $d \log$ numerator $N^{(f)}$ in Eq. (5.33) by the corresponding BCJ numerator yields the mSUGRA numerator:

$$N_{\text{mSUGRA}}^{(f)} = - \left[(\ell_5 + k_4)^2 ((\ell_5 + k_3)^2 + (\ell_5 + k_4)^2) \right] \\ \times \left[(s(-\tau_{35} + \tau_{45} + t) - t(\tau_{25} + \tau_{45}) + u(\tau_{25} - \tau_{35}) - s^2)/3 \right], \quad (6.22)$$

where $\tau_{ij} = 2k_i \cdot \ell_j$. Just like in the sYM case, overall factors of \mathcal{K} , as defined in Eq. (2.27), are factored out.

This representation of the mSUGRA amplitude has new nontrivial properties compared to other representations. Since the mSUGRA and sYM diagrams have identical propagators, and each mSUGRA numerator has a factor of $N^{(x)}$, all double poles located at finite values of loop momentum in the mSUGRA amplitude are canceled.

In general the factor $N_{\text{BCJ}}^{(x)}$ in Eq. (6.21) carries additional powers of loop momenta. These extra powers of loop momenta in the numerator compared to the sYM case generically lead

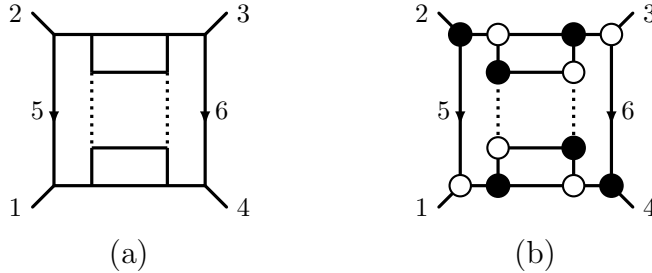


Figure 6.8: At $L \geq 4$ loops, diagram (a) contains a pole at infinity that cannot cancel against other diagrams. Cutting all propagators in diagram (a) yields the corresponding on-shell diagram (b). Diagram (b) encodes a residue of the amplitude on one of the solutions of the L -loop maximal cut. In both diagrams, the dashed lines indicate possible additional rungs.

to poles at infinity. However, because the three-loop four-point BCJ numerators are at most linear in loop momentum, only single poles can develop at infinity. At higher loops, the BCJ numerators contribute ever larger powers of loop momenta. These additional loop momenta generate non-logarithmic singularities as the orders of the poles at infinity grow. This is the content of Sec. 6.2.2

6.2.2 Poles at Infinity

In this section, the mSUGRA integrand is shown to have a pole at infinity by considering the planar, ($L \geq 4$)-loop diagram in Fig. 6.8(a) and the cut, Fig. 6.8(b), of the amplitude on which only diagram (a) contributes.

While the four-point mSUGRA amplitude at five or higher loops is unknown, there is partial information about the structure of the amplitude to all loop orders. In particular, the value of the maximal cut of the diagram in Fig. 6.8(a) that is displayed in Fig. 6.8(b) is known. Through either direct computation of superspace sums [106, 107] or using the rung rule [97], the value for the numerator is

$$N = [(\ell_5 + \ell_6 + k_2 + k_3)^2]^{\delta(L-3)}, \quad (6.23)$$

up to terms that vanish on the cut. Here $\delta = 1$ for sYM theory and $\delta = 2$ for mSUGRA. As usual factors of \mathcal{K} have been removed.

To approach Fig. 6.8(b) so that only a single diagram is selected requires some care⁵. On this solution, the two loop momenta labeled in Fig. 6.8 have solutions

$$\ell_5 = \alpha \lambda_1 \tilde{\lambda}_2, \quad \ell_6 = \beta \lambda_3 \tilde{\lambda}_4, \quad (6.24)$$

matching the discussion in Sec. 2.4.2 for mapping between cut solutions and on-shell diagrams. The Jacobian for this cut is

$$J = s^2 \alpha \beta [(\ell_5 + \ell_6 + k_2 + k_3)^2]^{L-2} F(\sigma_1, \dots, \sigma_{L-3}), \quad (6.25)$$

where the function F depends on the remaining $L - 3$ parameters, σ_i , of the cut solution, and not on α or β . On the cut, the parametrization Eq. (6.24) implies that

$$(\ell_5 + \ell_6 + k_2 + k_3)^2|_{\text{cut}} = (\alpha \langle 13 \rangle + \langle 23 \rangle)(\beta [24] + [23]). \quad (6.26)$$

Then the residue in the sYM case is

$$\text{Res}_{\text{cut}} d\mathcal{I}_{\text{sYM}} \sim \frac{d\alpha}{\alpha(\alpha - \alpha_0)} \wedge \frac{d\beta}{\beta(\beta - \beta_0)} \wedge \frac{d\sigma_1 \dots d\sigma_{L-3}}{F(\sigma_1, \dots, \sigma_{L-3})}, \quad (6.27)$$

with $\alpha_0 = -\langle 23 \rangle / \langle 13 \rangle$, $\beta_0 = -[23] / [24]$. So the sYM integrand has only logarithmic singularities and no pole at infinity in α or β . On the other hand, in the mSUGRA case the residue is

$$\text{Res}_{\text{cut}} d\mathcal{I}_{\text{mSUGRA}} \sim \frac{d\alpha}{\alpha(\alpha - \alpha_0)^{4-L}} \wedge \frac{d\beta}{\beta(\beta - \beta_0)^{4-L}} \wedge \frac{d\sigma_1 \dots d\sigma_{L-3}}{F(\sigma_1, \dots, \sigma_{L-3})}. \quad (6.28)$$

The mSUGRA residues have the same structure as the sYM residues for $L = 3$, but not

⁵To avoid mixing in any additional diagrams, first take a next-to-maximal cut, then make a final cut to hone in on the single solution in Eq. (6.24).

for $L > 3$. In the latter case, the sYM expression in Eq. (6.27) stays logarithmic with no poles at $\alpha, \beta \rightarrow \infty$, while the mSUGRA residue Eq. (6.28) loses the poles at α_0 and β_0 for $L = 4$ and develops a logarithmic pole at infinity. However, for $L \geq 5$ the poles at infinity become non-logarithmic, and the degree grows linearly with L . Since the cut was carefully chosen so that no other diagrams can mix with Fig. 6.8(a), the poles at infinity identified in Eq. (6.28) for $L \geq 4$ cannot cancel against other diagrams, and so the mSUGRA amplitudes indeed have poles at infinity. This can also be verified by the direct evaluation of the on-shell diagram in Fig. 6.8(b). Thus, in contrast to sYM, mSUGRA amplitudes have poles at infinity with a degree that grows linearly with the loop order.

As a final comment, the role that these poles at infinity play in the ultraviolet behavior of mSUGRA amplitudes is still an open question. While it is true that a lack of poles at infinity implies an amplitude is ultraviolet finite, the converse argument that poles at infinity imply divergences is not necessarily true. We discuss several reasons to believe the converse fails in Ref. [2].

CHAPTER 7

Five-loop Four-point Amplitudes

In Sec. 7.1 is a brief discussion of the motivation for computing the five-loop four-point mSUGRA amplitude. Current on-going work on this topic is covered in Sec. 7.2.

7.1 Motivation

At present, it is unknown if the five-loop contribution to the four-point mSUGRA amplitude, $\mathcal{A}_4^{(5)}$, is finite or divergent in $D = 4$. If this mSUGRA amplitude is indeed finite, understanding the mechanism responsible for reeling in its apparent power-counting divergences would have a large impact on general understanding of quantum gravity. A finite amplitude would also raise interesting questions about the necessity of quantum gravity ultraviolet completions such as string theory.

To date, the most efficient way to compute mSUGRA ultraviolet divergences is through the color-kinematics duality, reviewed in Sec. 2.5. Numerators for the four-point sYM amplitude that satisfy Jacobi relations have been found through four-loops [72]. Using the color-kinematics duality through four-loops, it happens to be that the dimensions in which the mSUGRA amplitude converges exactly matches [108] the dimensions in which the sYM amplitude converges

$$D < 8, \quad L = 1, \tag{7.1}$$

$$D < 4 + \frac{6}{L}, \quad L > 1 \tag{7.2}$$

for spacetime dimension D [109]. Note that the contributions to the sYM amplitude are

finite to all loop orders in $D = 4$, reflected in Eq. (7.2). If the pattern holds and the mSUGRA critical dimension continues to match the sYM critical dimension for $L \geq 5$, then mSUGRA would be finite in $D = 4$ dimensions like sYM. Such a result would be surprising as it runs counter to the results predicted by standard arguments based on symmetries of the Lagrangian and superspace methods.

So far, direct attempts to construct the five-loop four-point BCJ representation of the sYM amplitude have hit technical obstructions. Unfortunately the way in which direct construction fails is not enlightening. Just like in constructing the d log numerators by ansatz (Sec. 2.3.2), the BCJ numerators are written as ansätze, then subjected to constraints – Jacobi relations in this case. The resulting set of constraint equations for the parameters cannot be solved.

As a troubleshooting step, Ref. [110] computed a minimally constrained¹ representation of the sYM amplitude and its divergences. The work outlined in Sec. 7.2 here is a path from the troubleshooting representation of Ref. [110] towards a BCJ representation.

7.2 Color-Kinematics Duality on Cuts

Heuristically, the aim is to construct a five-loop four-point sYM amplitude that, while not completely BCJ, retains the properties of the BCJ representation that allows the sYM amplitude to double-copy into the mSUGRA amplitude. The method of *BCJ-on-the-cuts* [111] does exactly this.

The main idea of BCJ-on-the-cuts is to impose that the kinematic numerators obey color Jacobi identities on all unitarity cuts, rather than functionally for all values of loop momenta. The traditional approach was to impose

$$N_s + N_t + N_u = 0 \quad \forall \quad \{\ell\} \tag{7.3}$$

¹The only constraint was that the amplitude had all correct unitarity cuts.

whenever

$$c_s + c_t + c_u = 0, \tag{7.4}$$

while the new BCJ-on-the-cuts approach is to require

$$(N_s + N_t + N_u)|_{\{\ell^*\}} = 0 \tag{7.5}$$

where $\{\ell^*\}$ denotes any cut in a spanning set of unitarity cuts, the numerators N_i are numerators of integrands and are implicitly functions of the loop and external momenta:

$$N_i = N_i(k_1, k_2, k_3, \ell_5, \ell_6, \ell_7, \ell_8, \ell_9), \tag{7.6}$$

and the s , t , and u subscripts denote the three diagrams contributing to a color Jacobi relation as in Fig. 2.4. Preserving the Jacobi identities on cuts ensures that the double copy procedure will yield a mSUGRA amplitude that satisfies all unitarity cuts; satisfying all unitarity cuts in turn means the resulting mSUGRA amplitude is correct.

While all the technology for tackling the problem in this way already exists, the main issue is the size of the system of equations that results.

For a sense of scale, there are 910 diagrams that contribute to the five-loop sYM amplitude; see a selection in Fig. 7.1. It is not known for five-loops what power counting each diagram must have for the BCJ representation, but at four loops it was sufficient to include no powers of loop momentum for a box subdiagram, one power for a pentagon, two for a hexagon, and so on. This counting defines a *minimal BCJ power counting*. For the 910 five-loop diagrams with all numerator ansätze so designed, this results in $\mathcal{O}(10^6)$ parameters. While the ansätze are designed so that the constraint equations are linear between these parameters, the number of parameters and constraint equations quickly approaches technological limits for matrix inversion.

As a first step towards applying BCJ-on-the-cuts, it is sensible to seek any representation

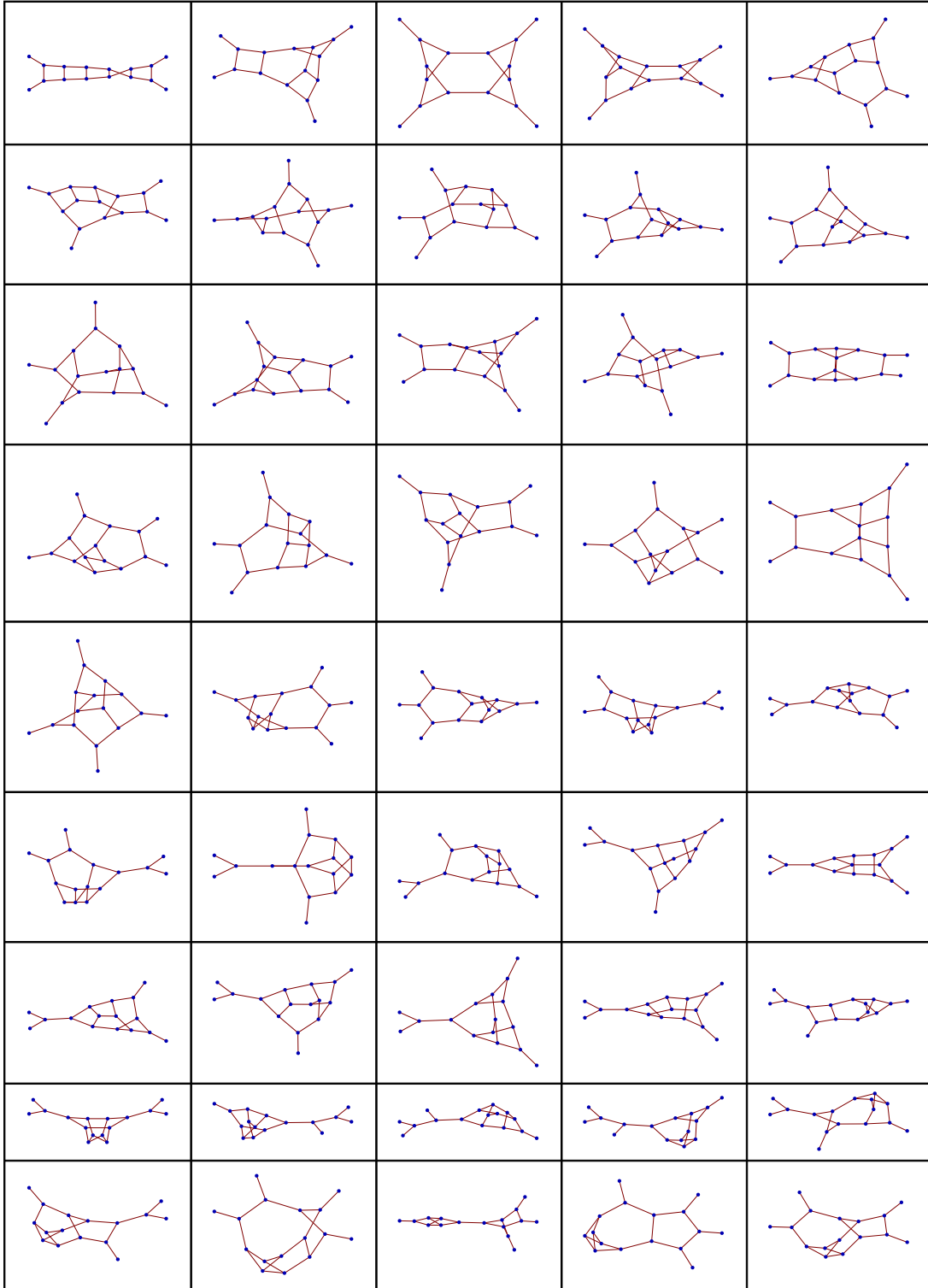


Figure 7.1: A sample subset of the diagrams contributing to the five-loop four-point amplitude. The graphs are intentionally not labeled.

of the sYM amplitude with minimal BCJ power counting. Mathematically, this first step is to constrain a numerator ansatz for a new representation of the amplitude, $\mathcal{A}_{4,\text{new}}^{(5)}$, so that

$$0 = \left(\mathcal{A}_{4,\text{new}}^{(5)} - \mathcal{A}_{4,\text{old}}^{(5)} \right) \Big|_{\text{cut}} \quad \forall \text{ cuts}, \quad (7.7)$$

where $\mathcal{A}_{4,\text{old}}^{(5)}$ is the representation from Ref. [110].

The authors of Ref. [110] made unpublished progress in this direction a few years ago. The goal now is to continue and complete that work. There are several questions to address:

- What is the correct set of five-loop diagrams?
- How should diagrams with vanishing color factor be treated?
- Is it possible to work analytically rather than numerically?

Each of these points are addressed below.

Among the set of 910 five-loop graphs, there is a subset of 178 graphs that contain the two-loop three-point subdiagram of Fig. 7.2(a); an example diagram is shown in Fig. 7.2(b). Such graphs would not appear in a traditional BCJ representation, since such graphs can always be rewritten as a linear combination of graphs with triangle diagrams which are assumed to vanish. Since the new approach considers BCJ for specific values of loop momenta, it is possible that these new graphs could be non-zero in the new representation.

As for the second point, the two-loop three-point subdiagram of Fig. 7.2(a) has an additional property: the associated color factor vanishes. This happens because the product of color factors is both symmetric and anti-symmetric in at least one of the sum indices. In the sYM amplitude, written schematically as

$$\mathcal{A} = \sum \int d\ell \frac{cN_{\text{BCJ}}}{\text{props}}, \quad (7.8)$$

a vanishing color factor implies a diagram does not contribute. On the other hand, such graphs might appear when double copying to obtain the gravity amplitude, since then the

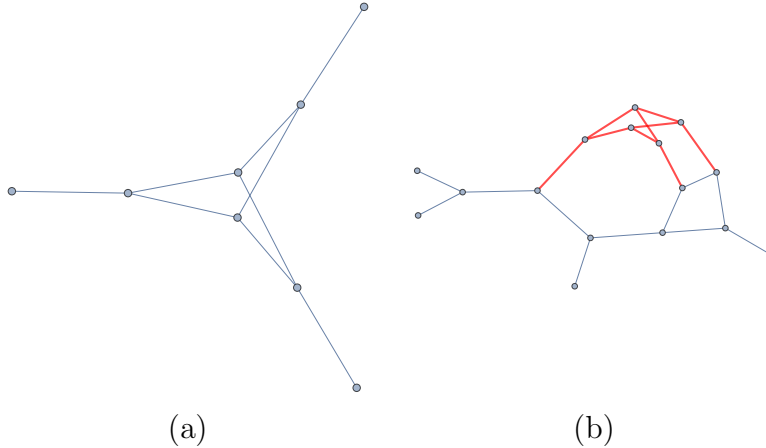


Figure 7.2: Figure (a) is a two-loop three-point graph that, under a Jacobi relation, can be written as a linear combination of two graphs with triangle subdiagrams. Figure (a) also has vanishing color factor. Figure (b) is an example of how (a) might be embedded in a five-loop graph; graph (a) is highlighted red in graph (b).

amplitude takes the form

$$\mathcal{M} = \sum \int d\ell \frac{\tilde{N}_{\text{any}} N_{\text{BCJ}}}{\text{props}}, \quad (7.9)$$

where the vanishing color factor is replaced by a not-necessarily-vanishing numerator: $c \rightarrow \tilde{N}_{\text{any}}$. This already happens in the four-loop BCJ construction [72]. In fact, even at five-loops there are six diagrams that contribute to the five-loop sYM amplitude of Ref. [111] that have color factors that vanish from subdiagrams other than Fig. 7.2(a).

The standard procedure for constraining amplitude numerators is to require that under relabeling of external legs the numerator changes sign in the same way as the color factor. One way to relax constraints that might be causing issues with imposing BCJ-on-the-cuts, or even standard BCJ, is to skip any constraints that result from graphs that have vanishing color factors. This is ongoing work.

Finally, it is simplest to work with Eq. (7.7) by reducing the expression to an independent set of Lorentz invariants, then converting the invariants to random integers². Converting to numerics in this way simplifies the large expressions that may arise from cuts, yet there is

²Integers allow for infinite precision in Mathematica.

non-zero risk of a numerical equation solver returning a particular rather than a general solution. The obvious way around this is to not use numerics but to instead keep analytic expressions. This has technical challenges, especially when trying to construct and analyze (next-to-)^k-max cuts where for $k > 2$ tens or hundreds of diagrams might contribute.

There have been recent technological leaps forward³ that have allowed for a dramatic increase in ansatz size. This is particularly important for the minimal power representation because every diagram must have its own ansatz, unlike traditional BCJ where a very tiny subset of diagrams dictates the remainder. With a better understanding of such an ansatz, future steps will be to impose BCJ-on-the-cuts conditions, Eq. (7.5), while increasing the size of the numerator ansätze so that the resulting system is consistent.

³Andreas von Manteuffel and Robert Schabinger in private correspondences.

CHAPTER 8

Conclusion

A successful and oft-repeated message in modern high energy theory research is that “There are better ways than Feynman diagrams to calculate scattering amplitudes.” This dissertation toed that party line. In particular, this dissertation reviewed several novel, non-Feynman-diagram-based techniques for constructing sYM and mSUGRA amplitudes. At both tree and loop level the analytic structure of the amplitude served as the guide for constructing the amplitude. Tools for constructing sYM and mSUGRA amplitudes based on the analytic properties of the amplitudes were detailed in Ch. 2.

At tree-level in Ch. 3, the fact that residues of the sYM amplitude obeyed BCJ amplitude relations implied the existence of residue numerators that double copied sYM residues into mSUGRA residues.

In explicit examples at loop level the pole structure of the sYM amplitude was shown to have only logarithmic singularities and no poles at infinity; that is to say the sYM amplitude admits a $d \log$ representation. This was the content of Sec. 4.1.1 (two-loop four-point), Sec. 5.1 (three-loop four-point), and Ch. 6 (more-than-three-loop four-point planar). This laid the foundation for a pure integrand representation of the amplitude, in which the amplitude is expanded in a basis of integrands that have only unit leading singularities and no poles at infinity. Such representations were made explicit in Sec. 4.1.2 (two-loop four-point), Sec. 4.2 (two-loop five-point), and Sec. 5.2 (three-loop four-point). Such a representation may generalize to n arbitrary particles, per the discussion in Sec. 4.3.

Based on the compelling story of the planar theory, the full sYM amplitude was constructed by considering only one specific value in loop momentum space where the amplitude

has to vanish. The process for such a construction was detailed in Sec. 4.1.3. This success hints that the structure of the planar theory is likely an echo of currently hidden structure in the full theory.

With the duality between color and kinematics in hand (Sec. 2.5), it becomes trivial to check what new sYM representations imply about mSUGRA. Carefully choosing a specific cut of a planar ($L \geq 4$)-loop diagram proved that the mSUGRA amplitude has poles at infinity; this was shown in Sec. 6.2. It is an open question if the five-loop four-point mSUGRA amplitude is finite in $D = 4$ spacetime dimensions. Current work on this topic was the content of Ch. 7. In particular, that chapter addressed current work towards finding the sYM five-loop four-point amplitude that satisfies BCJ on the cuts.

Finally, the set of Mathematica functions collectively referred to in this dissertation as `osdn` were used to generate and check all the work appearing in this dissertation and the associated publications. Some functions were briefly listed in Sec. 2.6. In Sec. 4.1.4 was an example on how to use `osdn` to generate the two-loop four-point pure integrand basis from one homogeneous constraint.

BIBLIOGRAPHY

- [1] Sean Litsey and James Stankowicz. Kinematic numerators and a double-copy formula for $\mathcal{N} = 4$ super-Yang-Mills residues. *Phys. Rev.*, D90(2):025013, 2014.
- [2] Zvi Bern, Enrico Herrmann, Sean Litsey, James Stankowicz, and Jaroslav Trnka. Logarithmic Singularities and Maximally Supersymmetric Amplitudes. *JHEP*, 06:202, 2015.
- [3] Zvi Bern, Enrico Herrmann, Sean Litsey, James Stankowicz, and Jaroslav Trnka. Evidence for a Nonplanar Amplituhedron. 2015.
- [4] Henriette Elvang and Yu-tin Huang. *Scattering Amplitudes in Gauge Theory and Gravity*. Cambridge University Press, 2015.
- [5] V. P. Nair. A Current Algebra for Some Gauge Theory Amplitudes. *Phys. Lett.*, B214:215, 1988.
- [6] James M. Drummond, Johannes M. Henn, and Jan Plefka. Yangian symmetry of scattering amplitudes in $\mathcal{N} = 4$ super Yang-Mills theory. *JHEP*, 05:046, 2009.
- [7] C. N. Yang and R. L. Mills. Conservation of isotopic spin and isotopic gauge invariance. *Phys. Rev.*, 96:191–195, Oct 1954.
- [8] Lance J. Dixon, James M. Drummond, Matt von Hippel, and Jeffrey Pennington. Hexagon functions and the three-loop remainder function. *JHEP*, 12:049, 2013.
- [9] Lance J. Dixon and Matt von Hippel. Bootstrapping an NMHV amplitude through three loops. *JHEP*, 10:065, 2014.
- [10] Lance J. Dixon, Matt von Hippel, and Andrew J. McLeod. The four-loop six-gluon NMHV ratio function. *JHEP*, 01:053, 2016.
- [11] Johannes M. Henn. Lectures on differential equations for Feynman integrals. *J. Phys.*, A48:153001, 2015.

- [12] Alexander B. Goncharov, Marcus Spradlin, C. Vergu, and Anastasia Volovich. Classical Polylogarithms for Amplitudes and Wilson Loops. *Phys. Rev. Lett.*, 105:151605, 2010.
- [13] John Golden, Alexander B. Goncharov, Marcus Spradlin, Cristian Vergu, and Anastasia Volovich. Motivic Amplitudes and Cluster Coordinates. *JHEP*, 01:091, 2014.
- [14] James M. Drummond, Georgios Papathanasiou, and Marcus Spradlin. A Symbol of Uniqueness: The Cluster Bootstrap for the 3-Loop MHV Heptagon. *JHEP*, 03:072, 2015.
- [15] Daniel Parker, Adam Scherlis, Marcus Spradlin, and Anastasia Volovich. Hedgehog bases for A_n cluster polylogarithms and an application to six-point amplitudes. *JHEP*, 11:136, 2015.
- [16] Arthur E. Lipstein and Lionel Mason. From d logs to dilogs the super Yang-Mills MHV amplitude revisited. *JHEP*, 01:169, 2014.
- [17] J. B. Tausk. Nonplanar massless two loop Feynman diagrams with four on-shell legs. *Phys. Lett.*, B469:225–234, 1999.
- [18] Vladimir A. Smirnov. Evaluating feynman integrals by uniformly transcendent differential equations. Radcor Loopfest, 2015.
- [19] Z. Bern, J. J. M. Carrasco, and Henrik Johansson. New Relations for Gauge-Theory Amplitudes. *Phys. Rev.*, D78:085011, 2008.
- [20] J. M. Drummond, J. Henn, V. A. Smirnov, and E. Sokatchev. Magic identities for conformal four-point integrals. *JHEP*, 01:064, 2007.
- [21] Luis F. Alday and Juan Martin Maldacena. Gluon scattering amplitudes at strong coupling. *JHEP*, 06:064, 2007.
- [22] J. M. Drummond, J. Henn, G. P. Korchemsky, and E. Sokatchev. Dual superconformal symmetry of scattering amplitudes in $\mathcal{N} = 4$ super-Yang-Mills theory. *Nucl. Phys.*, B828:317–374, 2010.

- [23] Niklas Beisert and Matthias Staudacher. The $\mathcal{N} = 4$ SYM integrable super spin chain. *Nucl. Phys.*, B670:439–463, 2003.
- [24] Niklas Beisert, Burkhard Eden, and Matthias Staudacher. Transcendentality and Crossing. *J. Stat. Mech.*, 0701:P01021, 2007.
- [25] J. M. Drummond, G. P. Korchemsky, and E. Sokatchev. Conformal properties of four-gluon planar amplitudes and Wilson loops. *Nucl. Phys.*, B795:385–408, 2008.
- [26] J. M. Drummond, J. Henn, G. P. Korchemsky, and E. Sokatchev. Conformal Ward identities for Wilson loops and a test of the duality with gluon amplitudes. *Nucl. Phys.*, B826:337–364, 2010.
- [27] Andreas Brandhuber, Paul Heslop, and Gabriele Travaglini. MHV amplitudes in $\mathcal{N} = 4$ super Yang-Mills and Wilson loops. *Nucl. Phys.*, B794:231–243, 2008.
- [28] L. J. Mason and David Skinner. The Complete Planar S-matrix of $\mathcal{N} = 4$ SYM as a Wilson Loop in Twistor Space. *JHEP*, 12:018, 2010.
- [29] Simon Caron-Huot. Notes on the scattering amplitude / Wilson loop duality. *JHEP*, 07:058, 2011.
- [30] Luis F. Alday, Burkhard Eden, Gregory P. Korchemsky, Juan Maldacena, and Emery Sokatchev. From correlation functions to Wilson loops. *JHEP*, 09:123, 2011.
- [31] Benjamin Basso, Amit Sever, and Pedro Vieira. Spacetime and Flux Tube S-Matrices at Finite Coupling for $\mathcal{N} = 4$ Supersymmetric Yang-Mills Theory. *Phys. Rev. Lett.*, 111(9):091602, 2013.
- [32] Benjamin Basso, Joao Caetano, Lucia Cordova, Amit Sever, and Pedro Vieira. OPE for all Helicity Amplitudes. *JHEP*, 08:018, 2015.
- [33] Benjamin Basso, Amit Sever, and Pedro Vieira. Hexagonal Wilson Loops in Planar $\mathcal{N} = 4$ SYM Theory at Finite Coupling. 2015.

- [34] Nima Arkani-Hamed, Freddy Cachazo, Clifford Cheung, and Jared Kaplan. A Duality For The S Matrix. *JHEP*, 03:020, 2010.
- [35] Nima Arkani-Hamed, Freddy Cachazo, and Clifford Cheung. The Grassmannian Origin Of Dual Superconformal Invariance. *JHEP*, 03:036, 2010.
- [36] L. J. Mason and David Skinner. Dual Superconformal Invariance, Momentum Twistors and Grassmannians. *JHEP*, 11:045, 2009.
- [37] Nima Arkani-Hamed, Jacob Bourjaily, Freddy Cachazo, and Jaroslav Trnka. Unification of Residues and Grassmannian Dualities. *JHEP*, 01:049, 2011.
- [38] Nima Arkani-Hamed, Jacob Bourjaily, Freddy Cachazo, and Jaroslav Trnka. Local Spacetime Physics from the Grassmannian. *JHEP*, 01:108, 2011.
- [39] Nima Arkani-Hamed, Jacob L. Bourjaily, Freddy Cachazo, Simon Caron-Huot, and Jaroslav Trnka. The All-Loop Integrand For Scattering Amplitudes in Planar $\mathcal{N} = 4$ SYM. *JHEP*, 01:041, 2011.
- [40] Nima Arkani-Hamed, Jacob L. Bourjaily, Freddy Cachazo, Alexander B. Goncharov, Alexander Postnikov, and Jaroslav Trnka. *Scattering Amplitudes and the Positive Grassmannian*. Cambridge University Press, 2012.
- [41] Yu-Tin Huang and Congkao Wen. ABJM amplitudes and the positive orthogonal grassmannian. *JHEP*, 02:104, 2014.
- [42] Yu-tin Huang, Congkao Wen, and Dan Xie. The Positive orthogonal Grassmannian and loop amplitudes of ABJM. *J. Phys.*, A47(47):474008, 2014.
- [43] Joonho Kim and Sangmin Lee. Positroid Stratification of Orthogonal Grassmannian and ABJM Amplitudes. *JHEP*, 09:085, 2014.
- [44] Henriette Elvang, Yu-tin Huang, Cynthia Keeler, Thomas Lam, Timothy M. Olson, Samuel B. Roland, and David E. Speyer. Grassmannians for scattering amplitudes in 4d $\mathcal{N} = 4$ SYM and 3d ABJM. *JHEP*, 12:181, 2014.

- [45] Nima Arkani-Hamed and Jaroslav Trnka. The Amplituhedron. *JHEP*, 10:030, 2014.
- [46] Nima Arkani-Hamed and Jaroslav Trnka. Into the Amplituhedron. *JHEP*, 12:182, 2014.
- [47] Sebastian Franco, Daniele Galloni, Alberto Mariotti, and Jaroslav Trnka. Anatomy of the Amplituhedron. *JHEP*, 03:128, 2015.
- [48] Yuntao Bai and Song He. The Amplituhedron from Momentum Twistor Diagrams. *JHEP*, 02:065, 2015.
- [49] Nima Arkani-Hamed, Andrew Hodges, and Jaroslav Trnka. Positive Amplitudes In The Amplituhedron. *JHEP*, 08:030, 2015.
- [50] Thomas Lam. Amplituhedron cells and Stanley symmetric functions. *Commun. Math. Phys.*, 343(3):1025–1037, 2016.
- [51] Yuntao Bai, Song He, and Thomas Lam. The Amplituhedron and the One-loop Grassmannian Measure. *JHEP*, 01:112, 2016.
- [52] Livia Ferro, Tomasz Lukowski, Andrea Orta, and Matteo Parisi. Towards the Amplituhedron Volume. *JHEP*, 03:014, 2016.
- [53] G. Lusztig. Total positivity in partial flag manifolds. *Represent. Theory*, 2:70–78, 1998.
- [54] A. Postnikov. Total Positivity, Grassmannians, and Networks. *ArXiv Mathematics e-prints*, September 2006.
- [55] A. Postnikov, D. Speyer, and L. Williams. Matching Polytopes, Toric Geometry, and the Non-negative Part of the Grassmannian. *ArXiv e-prints*, June 2007.
- [56] L. K. Williams. Enumeration of Totally Positive Grassmann Cells. *ArXiv Mathematics e-prints*, July 2003.
- [57] A. B. Goncharov and R. Kenyon. Dimers and Cluster Integrable Systems. *ArXiv e-prints*, July 2011.

- [58] A. Knutson, T. Lam, and D. Speyer. Positroid Varieties: Juggling and Geometry. *ArXiv e-prints*, November 2011.
- [59] Sebastian Franco, Daniele Galloni, Brenda Penante, and Congkao Wen. Non-Planar On-Shell Diagrams. *JHEP*, 06:199, 2015.
- [60] Rouven Frassek and David Meidinger. Yangian-type symmetries of non-planar leading singularities. 2016.
- [61] Zvi Bern, John Joseph M. Carrasco, and Henrik Johansson. Perturbative Quantum Gravity as a Double Copy of Gauge Theory. *Phys. Rev. Lett.*, 105:061602, 2010.
- [62] Nima Arkani-Hamed, Jacob L. Bourjaily, Freddy Cachazo, and Jaroslav Trnka. Singularity Structure of Maximally Supersymmetric Scattering Amplitudes. *Phys. Rev. Lett.*, 113(26):261603, 2014.
- [63] Stephen J. Parke and T. R. Taylor. An Amplitude for n Gluon Scattering. *Phys. Rev. Lett.*, 56:2459, 1986.
- [64] Michelangelo L. Mangano, Stephen J. Parke, and Zhan Xu. Duality and Multi-Gluon Scattering. *Nucl. Phys.*, B298:653, 1988.
- [65] Nima Arkani-Hamed, Jacob L. Bourjaily, Freddy Cachazo, Alexander Postnikov, and Jaroslav Trnka. On-Shell Structures of MHV Amplitudes Beyond the Planar Limit. *JHEP*, 06:179, 2015.
- [66] Z. Bern, J. J. Carrasco, Lance J. Dixon, Henrik Johansson, D. A. Kosower, and R. Roiban. Three-Loop Superfiniteness of $\mathcal{N} = 8$ Supergravity. *Phys. Rev. Lett.*, 98:161303, 2007.
- [67] John Joseph M. Carrasco and Henrik Johansson. Five-Point Amplitudes in $\mathcal{N} = 4$ Super-Yang-Mills Theory and $\mathcal{N} = 8$ Supergravity. *Phys. Rev.*, D85:025006, 2012.

- [68] Zvi Bern, Lance J. Dixon, David C. Dunbar, and David A. Kosower. One loop n point gauge theory amplitudes, unitarity and collinear limits. *Nucl. Phys.*, B425:217–260, 1994.
- [69] Freddy Cachazo. Sharpening The Leading Singularity. 2008.
- [70] Zvi Bern, Lance J. Dixon, and David A. Kosower. Dimensionally regulated pentagon integrals. *Nucl. Phys.*, B412:751–816, 1994.
- [71] Z. Bern, J. J. M. Carrasco, Henrik Johansson, and D. A. Kosower. Maximally supersymmetric planar Yang-Mills amplitudes at five loops. *Phys. Rev.*, D76:125020, 2007.
- [72] Z. Bern, J. J. M. Carrasco, L. J. Dixon, H. Johansson, and R. Roiban. Simplifying Multiloop Integrands and Ultraviolet Divergences of Gauge Theory and Gravity Amplitudes. *Phys. Rev.*, D85:105014, 2012.
- [73] N.E.J. Bjerrum-Bohr and Pierre Vanhove. Absence of Triangles in Maximal Supergravity Amplitudes. *JHEP*, 0810:006, 2008.
- [74] Nima Arkani-Hamed, Freddy Cachazo, and Jared Kaplan. What is the Simplest Quantum Field Theory? *JHEP*, 09:016, 2010.
- [75] Edward Witten. Perturbative gauge theory as a string theory in twistor space. *Commun. Math. Phys.*, 252:189–258, 2004.
- [76] Nathan Berkovits. An Alternative string theory in twistor space for $\mathcal{N} = 4$ superYang-Mills. *Phys. Rev. Lett.*, 93:011601, 2004.
- [77] Radu Roiban, Marcus Spradlin, and Anastasia Volovich. A Googly amplitude from the B model in twistor space. *JHEP*, 04:012, 2004.
- [78] Radu Roiban, Marcus Spradlin, and Anastasia Volovich. On the tree level S matrix of Yang-Mills theory. *Phys. Rev.*, D70:026009, 2004.

- [79] Marcus Spradlin and Anastasia Volovich. From Twistor String Theory To Recursion Relations. *Phys. Rev.*, D80:085022, 2009.
- [80] Dung Nguyen, Marcus Spradlin, Anastasia Volovich, and Congkao Wen. The Tree Formula for MHV Graviton Amplitudes. *JHEP*, 07:045, 2010.
- [81] Andrew Hodges. New expressions for gravitational scattering amplitudes. *JHEP*, 07:075, 2013.
- [82] Andrew Hodges. A simple formula for gravitational MHV amplitudes. 2012.
- [83] Freddy Cachazo and Yvonne Geyer. A 'Twistor String' Inspired Formula For Tree-Level Scattering Amplitudes in $\mathcal{N} = 8$ SUGRA. 2012.
- [84] Freddy Cachazo and David Skinner. Gravity from Rational Curves in Twistor Space. *Phys. Rev. Lett.*, 110(16):161301, 2013.
- [85] Freddy Cachazo, Lionel Mason, and David Skinner. Gravity in Twistor Space and its Grassmannian Formulation. *SIGMA*, 10:051, 2014.
- [86] Song He. A Link Representation for Gravity Amplitudes. *JHEP*, 10:139, 2013.
- [87] Diana Vaman and York-Peng Yao. Constraints and Generalized Gauge Transformations on Tree-Level Gluon and Graviton Amplitudes. *JHEP*, 11:028, 2010.
- [88] Rutger H. Boels and Reinke Sven Isermann. On powercounting in perturbative quantum gravity theories through color-kinematic duality. *JHEP*, 06:017, 2013.
- [89] Vittorio Del Duca, Lance J. Dixon, and Fabio Maltoni. New color decompositions for gauge amplitudes at tree and loop level. *Nucl. Phys.*, B571:51–70, 2000.
- [90] Ronald Kleiss and Hans Kuijf. Multi - Gluon Cross-sections and Five Jet Production at Hadron Colliders. *Nucl. Phys.*, B312:616, 1989.
- [91] H. Kawai, D. C. Lewellen, and S. H. H. Tye. A Relation Between Tree Amplitudes of Closed and Open Strings. *Nucl. Phys.*, B269:1, 1986.

- [92] A. Ben-Israel and T. N. E. Greville. *Generalized inverses: theory and applications*. CMS books in mathematics No. 15, 2003.
- [93] Carlos R. Mafra, Oliver Schlotterer, and Stephan Stieberger. Explicit BCJ Numerators from Pure Spinors. *JHEP*, 07:092, 2011.
- [94] N. E. J. Bjerrum-Bohr, Poul H. Damgaard, Thomas Sondergaard, and Pierre Vanhove. The Momentum Kernel of Gauge and Gravity Theories. *JHEP*, 01:001, 2011.
- [95] Freddy Cachazo, Song He, and Ellis Ye Yuan. Scattering of Massless Particles in Arbitrary Dimensions. *Phys. Rev. Lett.*, 113(17):171601, 2014.
- [96] Zvi Bern, Tristan Dennen, Yu-tin Huang, and Michael Kiermaier. Gravity as the Square of Gauge Theory. *Phys. Rev.*, D82:065003, 2010.
- [97] Z. Bern, J. S. Rozowsky, and B. Yan. Two loop four gluon amplitudes in $\mathcal{N} = 4$ superYang-Mills. *Phys. Lett.*, B401:273–282, 1997.
- [98] Nima Arkani-Hamed, Jacob L. Bourjaily, Freddy Cachazo, and Jaroslav Trnka. Local Integrals for Planar Scattering Amplitudes. *JHEP*, 06:125, 2012.
- [99] Jacob L. Bourjaily and Jaroslav Trnka. Local Integrand Representations of All Two-Loop Amplitudes in Planar SYM. *JHEP*, 08:119, 2015.
- [100] Ruth Britto, Freddy Cachazo, and Bo Feng. New recursion relations for tree amplitudes of gluons. *Nucl. Phys.*, B715:499–522, 2005.
- [101] Ruth Britto, Freddy Cachazo, Bo Feng, and Edward Witten. Direct proof of tree-level recursion relation in Yang-Mills theory. *Phys. Rev. Lett.*, 94:181602, 2005.
- [102] Zvi Bern and Gordon Chalmers. Factorization in one loop gauge theory. *Nucl. Phys.*, B447:465–518, 1995.

- [103] Z. Bern, J. J. M. Carrasco, Lance J. Dixon, Henrik Johansson, and R. Roiban. Manifest Ultraviolet Behavior for the Three-Loop Four-Point Amplitude of $\mathcal{N} = 8$ Supergravity. *Phys. Rev.*, D78:105019, 2008.
- [104] Michelangelo L. Mangano and Stephen J. Parke. Multiparton Amplitudes in Gauge Theories. *Phys. Rept.*, 200:301–367, 1991.
- [105] Jacob L. Bourjaily, Alexander DiRe, Amin Shaikh, Marcus Spradlin, and Anastasia Volovich. The Soft-Collinear Bootstrap: $\mathcal{N} = 4$ Yang-Mills Amplitudes at Six and Seven Loops. *JHEP*, 1203:032, 2012.
- [106] Henriette Elvang, Daniel Z. Freedman, and Michael Kiermaier. Recursion Relations, Generating Functions, and Unitarity Sums in $\mathcal{N} = 4$ SYM Theory. *JHEP*, 04:009, 2009.
- [107] Z. Bern, J. J. M. Carrasco, H. Ita, H. Johansson, and R. Roiban. On the Structure of Supersymmetric Sums in Multi-Loop Unitarity Cuts. *Phys. Rev.*, D80:065029, 2009.
- [108] Z. Bern, J. J. M. Carrasco, Lance J. Dixon, H. Johansson, and R. Roiban. The Complete Four-Loop Four-Point Amplitude in $\mathcal{N} = 4$ Super-Yang-Mills Theory. *Phys. Rev.*, D82:125040, 2010.
- [109] Z. Bern, Lance J. Dixon, D. C. Dunbar, M. Perelstein, and J. S. Rozowsky. On the relationship between Yang-Mills theory and gravity and its implication for ultraviolet divergences. *Nucl. Phys.*, B530:401–456, 1998.
- [110] Z. Bern, J. J. M. Carrasco, H. Johansson, and R. Roiban. The Five-Loop Four-Point Amplitude of $\mathcal{N} = 4$ super-Yang-Mills Theory. *Phys. Rev. Lett.*, 109:241602, 2012.
- [111] Zvi Bern, Scott Davies, and Josh Nohle. Double-Copy Constructions and Unitarity Cuts. 2015.